CIRCADIAN CLOCK REGULATION OF TRANSLATION INITIATION IN

NEUROSPORA CRASSA THROUGH PHOSPHORYLATION OF A HIGHLY

CONSERVED INITIATION FACTOR EIF2α

A Dissertation

by

SHANTA KARKI

Submitted to the Office of Graduate and Professional Studies of
Texas A&M University
in partial fulfillment of the requirements for the degree of

DOCTOR OF PHILOSOPHY

Chair of Committee,   Deborah Bell-Pedersen
Committee Members, Matthew Sachs
                     Jerome Menet
                     Dan Ebbole
Head of Department,   Thomas McKnight

December 2019

Major Subject: Microbiology

ABSTRACT

Up to half of the eukaryotic genome is controlled by the endogenous circadian clock at the level of rhythmic transcript abundance. The clock also controls post-transcriptional events, including clock regulation of the levels and phosphorylation state of translation factors that are also thought to promote rhythmic protein synthesis. However, if, and how, the clock controls translation initiation is unknown. I discovered that phosphorylation of eIF2α, a conserved translation initiation factor, is clock-controlled, peaking during the subjective day. The rhythm in phosphorylated eIF2α (P-eIF2α) requires rhythmic activation of the eIF2α kinase CPC-3, the homolog of yeast and mammalian GCN2. Binding of uncharged tRNA to GCN2, such as what occurs during histidine starvation, is required to activate the kinase. Consistent with rhythmic activation of *N. crassa* CPC-3 by binding of uncharged tRNA, starvation of wild type cells for histidine, or a CPC-3 mutation that constitutively activates CPC-3 in the absence of bound uncharged tRNA, abolished rhythmic P-eIF2α levels. Further, translational activator GCN1 cycles and is required for eIF2α phosphorylation by CPC-3. The rhythm in P-eIF2α accumulation led to reduced translation during the day in an *in vitro* cell-free translation system and is required for cycling levels of the mannosyl transferase protein, but not the core clock protein FRQ, *in vivo,* suggesting clock regulation of translation of specific mRNAs. To identify the mechanism of translational regulation of specific mRNAs through rhythmic eIF2α phosphorylation, ribosome profiling in parallel with RNA-seq was carried out. 913 genes showed rhythmic changes in translational efficiency (TE) in WT cells, of which 554 were dependent on CPC-3. Of those 554 genes, 426 have rhythmic TE but arrhythmic mRNA, suggesting these genes are translationally regulated through rhythmic eIF2α

phosphorylation. Of these 426 genes, 113 day-peaking genes contain T-rich motifs, 189 night-peaking genes contain A-rich motifs and 19% have putative uORFs in the 5' UTR. These elements suggest possible mechanisms for how specific mRNAs are controlled by cycling P-eIF2α levels. Finally, loss of rhythmic control of P-eIF2α levels led to reduced growth rates, supporting the idea that partitioning translation to the night, when energy resources are high, provides a growth advantage to the organism. Together, these data reveal a fundamental mechanism by which the clock regulates rhythmic protein production.

DEDICATION

I would like to dedicate my dissertation to my family, especially my Mom, Mom Kumari

Karki and my Dad, Dak Bahadur Karki for their continuous love, support, encouragement,

and above all for believing in me.

ACKNOWLEDGEMENTS

CONTRIBUTORS AND FUNDING SOURCES

TABLE OF CONTENTS

LIST OF FIGURES

LIST OF TABLES

CHAPTER I

INTRODUCTION

The circadian clock

The circadian clock is an endogenous time keeping mechanism present in phylogenetically diverse organisms, ranging from cyanobacteria to mammals. The circadian clock provides organisms with the ability to anticipate and prepare for daily environmental changes, and to maintain internal temporal order [1-3]. The core time-keeping mechanism, or oscillator, is synchronized to the 24 h environmental cycle through input pathways, and signals time-of-day information through output pathways from the oscillator to ultimately regulate rhythms in gene expression, metabolism, physiology, and behavior [4, 5]. The core circadian oscillator in all eukaryotic organisms consists of positive and negative elements that form an auto-regulatory feedback loop, which takes about 24 h to complete [6, 7]. The circadian clock exhibits 3 main properties:

1. In constant environmental conditions, the clock will run with an endogenous free-running rhythm with a period of around 24 h.

2. The clock can be entrained to exactly 24 h by environmental input signals, including light and temperature.

3. The clock is temperature-compensated, whereby the period stays nearly constant over a range of physiological temperatures for the organism.

Neurospora as a model organism to study the circadian clock

N. crassa is a haploid filamentous fungus that displays an easily observed circadian rhythm in the development of asexual spores called macroconidia (or more commonly conidia). The underlying molecular mechanism of the circadian clock is well-conserved from *N. crassa* to mammals, and the availability of an extensive knockout library collection makes it an excellent model organism to study the circadian clock [8-10].

In *N. crassa*, the core FRQ/WHITE COLLAR oscillator (FWO) consists of a transcriptional, translational feedback loop involving the positive elements WHITE COLLAR-1 (WC-1) and WHITE COLLAR-2 (WC-2), which heterodimerize to form the WCC, and FREQUENCY (FRQ) and FREQUENCY INTERACTING RNA HELICASE (FRH), which function as the negative element [11]. During the subjective morning, WCC binds to the promoter of *frq* and activates its transcription [12, 13]. As FRQ protein levels increase throughout the day, FRQ dimerizes with FRH forming the negative FRQ/FRH complex (FFC) [14, 15]. The FFC binds to, and promotes, the phosphorylation of WCC by CKI and CKII kinases. Phosphorylated WCC is unstable and unable to activate *frq* transcription [16, 17]. As FRQ accumulates, it is progressively phosphorylated, ubiquitinylated, and then degraded via the F-box/WD-40 repeat-containing protein-1 (FWD-1) pathway [18, 19]. Once FRQ protein is fully degraded, the WCC is reactivated by phosphatases, and together with new synthesis of the WCC, the molecular cycle restarts the next morning [17, 18, 20]. The FWO is responsible for driving rhythms in accumulation of ~40% of the transcriptome [21] and more than 40% of the proteome [22].

Post transcriptional regulation by the circadian clock

Recent studies have provided ample evidence for post-transcriptional regulation of rhythmicity, including circadian regulation of mRNA capping, splicing, polyadenylation, and de-adenylation [23-27]. In support of post-transcriptional regulation by the clock, quantitative proteomic analysis in *N. crassa* and mouse liver have shown that 20-50% of rhythmically accumulating proteins are expressed from non-cycling mRNAs [28-30]. This may be due to either rhythms in protein turnover, or rhythms in mRNA translation. Translation can be regulated by RNA binding proteins, miRNAs, and/or through regulation of translational components, including initiation factors, elongation factors, ribosomes, or tRNAs [31]. Consistent with clock control of mRNA translation, the levels and/or activity of different translation initiation factors, including eIF4E, eIF4G, and eIF4B, cycle with a ~24 h rhythm [32, 33]. In addition, the clock regulates the levels of several ribosomal proteins, including, RPL5, RPL23, RPL32, and RPLP0 [32], which may lead to rhythms in ribosome activity. In *N. crassa,* rhythmic accumulation of GST-3 (Glutathione S-transferase) protein is regulated by clock control of the activity of elongation factor eEF-2 [34]. During the subjective day, eEF-2 is phosphorylated by RCK-2 kinase, which is activated through clock control of the p38 MAPK pathway [35]. In *Gonyaulax,* Luciferin Binding Protein (LBP), and in *Drosophila* Eip74EF are translationally regulated through RNA-binding proteins interacting at the 3' untranslated region of the mRNA. Together, these data reveal that clock regulation of translation occurs by different mechanisms. However, how the clock controls translation initiation factors, and the downstream effect of this regulation on genome wide scale is not known.

Regulation of translation initiation

Translation begins with recruitment of the methionyl-initiator tRNA by GTP-bound eIF2α called the ternary complex to the 40s ribosomal subunit [36]. This leads to formation of the 43S preinitiation complex (PIC) (**Figure 1.1**). PIC binds the 7-methyl guanine cap of mRNA, and this is assisted by the eIF4F complex. The eIF4F complex is composed of eIF4E, eIF4G, and eIF4A, which scans the mRNA until reaching a start codon, typically an AUG codon, in the proper context. At this point, GTP bound to eIF2α is hydrolyzed, and initiation factors are released from the 40S ribosomal subunit. The 60S ribosomal subunit binds to the 40S subunit forming the 80S initiation complex.
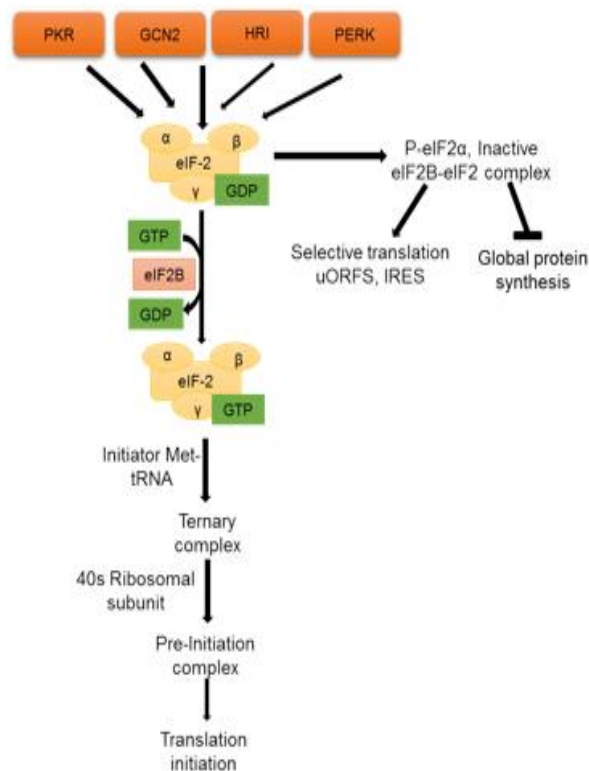
Figure 1.1. eIF2α integrates diverse
stimuli to regulate translation.

To start the next round of translation, GDP-eIF2α exchanges GDP for GTP through the guanine nucleotide exchange factor (GEF) eIF2B [37]. A central mechanism for control of translation initiation involves phosphorylation of the α subunit of Eukaryotic Initiation Factor 2 (eIF2α), which represses the initiation phase of translation of most mRNAs [38, 39]. In mammals, 4 different kinases can phosphorylate eIF2α in response to different stressors [40-42]. These include PKR-like ER kinase (PERK), General control non-depressible-2 (GCN2), Heme-regulated inhibitor (HRI) and Protein kinase double-stranded RNA dependent kinase (PKR). Among the eIF2α kinases, GCN2 is the only one that is conserved from fungi to mammals [43]. In *N. crassa,* the serine/threonine kinase CPC-3 (NCU01187) is a homolog of GCN2 [44].

In *S. cerevisiae* and mammalian cells, GCN2 senses nutrient deprivation, and is activated by the resulting increase in uncharged tRNAs levels [45]. In addition, in *S. cerevisiae,* GCN2 activity requires the effector protein General Control Non-Depressible-1 (GCN1) [46]. Two additional proteins GCN20, and Impact factor (IMF) can also augment GCN2 activity [47-49]. Activated GCN2 phosphorylates Ser51 of eIF2α, which forms a competitive inhibitor of eIF2B [50, 51]. This leads to a reduction in ternary complex formation and a general reduction in translation initiation. However, some mRNAs with specific motifs, such as those with upstream open reading frames (uORFs), 5' TOP or 5' PRTE elements, encoding proteins involved in the stress response pathway are upregulated [52, 53]. Some examples of genes with uORFs that are translationally upregulated in response to nutrient starvation include the transcriptional factors *S. cerevisiae* GCN4, mammalian ATF4, and *N. crassa* CPC-1 [41, 54, 55]. These bZIP

transcription factors activate stress-response pathway genes involved in amino acid metabolism. This response is called the General Amino Acid Control (GAAC)/Amino Acid Response (AAR) pathway. Genes with Internal Ribosome Entry Sites (IRES) [56] are also translationally upregulated when eIF2α is phosphorylated via a cap-independent pathway [57]. As a result of its broad impact on translation, eIF2α activity is correlated with behavior, memory consolidation, and nervous system development [58, 59], and plays a critical role in stress-induced tumorigenesis and neurodegenerative disorders [60-62]. Furthermore, time-dependent translation of *mPer1* mRNA, encoding the core negative oscillator component PER1, in NIH3T3 mouse fibroblasts requires an uORF [63]. In addition, ribosome profiling in mouse liver revealed the presence of uORFs in transcripts of the core clock components *Clock* and *Nr1d1* [64]. In contrast, alternative splicing of uORFs in *N. crassa frq* mRNA leads to formation of a long and a short FRQ isoform, which are important for temperature entrainment [65, 66].

Objective

Translation is highly energy utilizing process, and is therefore, tightly regulated in cells through different signaling pathways [38]. Evidence for clock regulation of the levels and/or phosphorylation state of translation initiation factors, elongation factor (eEF-2), and ribosomal proteins support a role for the clock in regulating mRNA translation. However, the mechanism of clock regulation of initiation factors, as well as the downstream effect of this regulation, is not known. Translation initiation is a rate-limiting step in protein synthesis, and given the critical role of eIF2α in cap-dependent translation, I tested the following hypotheses:

1. **Circadian clock control of translation initiation is through clock control of eIF2α phosphorylation (Chapter II)**

   I hypothesized that the circadian clock regulates translation initiation by regulating eIF2α activity through CPC-3 kinase. To test this hypothesis, I examined rhythmic accumulation of P-eIF2α over a circadian time course in WT, Δ*frq* and Δ*cpc-3* cells, and discovered that the circadian clock regulates daily rhythms in the accumulation of P-eIF2α levels, and that CPC-3 kinase is required for eIF2α phosphorylation. The kinase CPC-3 itself is clock-controlled. However, P-eIF2α rhythms are not dependent on rhythmic CPC-3 abundance, but rather on rhythmic activation of CPC-3. A manuscript describing these results will be submitted for publication.

2. **Investigation of mechanisms of CPC-3 activation (Chapter III)**

   I discovered that rhythmic activation of CPC-3 is necessary for rhythmic accumulation of P-eIF2α. CPC-3 is activated by histidine starvation (Chapter II), supporting activation by uncharged tRNA, similar to GCN2 [67]. As uncharged tRNA levels depend on amino acids concentration, it suggests the possibility of rhythmic CPC-3 activation through rhythmic amino acids abundance. However, free amino acids levels were not rhythmic under conditions on which P-eIF2α levels cycle. Interestingly, I found valyl-tRNA sythetase mutant (*un-3*) defective in charging cognate tRNA with valine, lead to higher and arrhythmic P-eIF2α levels suggesting possible role of aminoacyl-tRNA synthetases in regulating CPC-3 activity through rhythmic change in charged vs uncharged tRNA levels. In addition to uncharged tRNAs, *S. cerevisiae* GCN2 is negatively regulated by S577

phosphorylation. Further, the role of different GCN2 effector proteins, including GCN1, IMF, and CPC-2 in rhythmic accumulation of P-eIF2α through CPC-3 activation in *N. crassa* was not known. Therefore, to determine the mechanism of clock-controlled CPC-3 activity, I examined the role of GCN2 effectors and S577 phosphorylation on rhythmic accumulation of P-eIF2α levels. When cells were grown under conditions of sufficient nutrients, I found that GCN1, but not IMF and CPC-2, is required for eIF2α phosphorylation. GCN2 S577 site is not conserved in CPC-3. However, S583 and S585 sites located in close proximity to S577 in CPC-3 were tested for a role in maintaining rhythmic levels of P-eIF2α. I found that these sites are not required for CPC-3 activity as P-eIF2α levels were rhythmic in a *cpc-3S583A,S585A* mutant. In addition, GCN1 levels were discovered to be clock-controlled. Taken together, these data led to the hypothesis that rhythmic CPC-3 activity is due to rhythmic accumulation of uncharged tRNAs through aminoacyl-tRNA synthetase activity, and/or through rhythmic GCN1 levels. Experiments are in progress to distinguish these possibilities.

3. **Genome-wide investigation of the effect of rhythmic eIF2α phosphorylation on mRNA translation (Chapter IV)**

Daily rhythmic accumulation of P-eIF2α is not required for rhythmic FRQ protein accumulation, but is necessary for maintaining ALG11::LUC rhythms (**Chapter II**). These data indicated that not all mRNAs are translationally controlled by rhythmic accumulation of eIF2α phosphorylation, and instead supported the hypothesis that specific mRNAs are regulated by clock control of eIF2α phosphorylation. This

hypothesis was confirmed using ribosome profiling in parallel with RNA-seq in WT, Δ*frq*, and Δ*cpc-3* cells. 554 genes that are translationally regulated by the clock through rhythmic P-eIF2α levels were identified out of 913 rhythmically translated mRNAs. These genes are enriched for metabolic pathways, including amino acid and carbohydrate metabolism, suggesting coordinated regulation of translation and metabolism by the clock.

CHAPTER II

CIRCADIAN CLOCK CONTROL OF EIF2α PHOSPHORYLATION DRIVES

RHYTHMIC TRANSLATION INITIATION

Introduction

Circadian clocks regulate physiology and behavior through the rhythmic control of gene expression to optimize the timing of resource allocation for improved fitness [68]. Remarkably, up to 50% of the eukaryotic genome is under control of the clock at the level of rhythmic mRNA abundance [21, 25, 69-73]. In addition, mounting evidence supports circadian post-transcriptional regulation, including clock control of mRNA capping, splicing, polyadenylation, and de-adenylation [23-27]. Furthermore, rhythmic proteomic analysis revealed that up to 50% of rhythmic proteins arise from non-cycling mRNAs [22, 28-30], indicating that cycling protein accumulation is driven by temporal protein degradation and/or mRNA translation. In support of clock control of translation, the levels and modification of several translation initiation factors accumulate rhythmically in *Neurospora crassa* [22] and mammals [32, 33], and the activity of translation elongation factor eEF-2 is controlled by the *N. crassa* clock through rhythmic activation of the p38 MAPK pathway and the downstream eEF-2 kinase RCK-2 [35]. However, the mechanisms and extent of clock regulation of translation initiation are unknown.

One of the first steps in translation initiation is binding of eIF2 to GTP and the methionyl-initiator tRNA to form the ternary complex [39, 74]. The ternary complex associates with the 40S ribosomal subunit to form the 43S preinitiation complex (PIC), which binds to the

mRNA cap to form the 48S PIC. The PIC scans the mRNA as an open complex, and upon choosing a start codon, typically an AUG in a preferred context, becomes a closed complex with the start codon paired to the initiator Met-tRNA$_{iMet}$ anticodon [75, 76]. In the process, eIF2-GDP is released. The 60S ribosomal subunit then joins the 40S subunit to form a functional 80S ribosome for protein synthesis. eIF2-GDP is recycled to eIF2-GTP by the guanine nucleotide exchange factor eIF2B to enable reconstitution of the ternary complex for another round of translation [39].

A central mechanism for translational control is phosphorylation of the α subunit of eIF2 [38, 39]. Among different kinases that phosphorylates eIF2, GCN2 is conserved in fungi and mammals [44, 52, 77]. GCN2 is activated by amino acid starvation, and other stresses, that lead to the accumulation of uncharged tRNAs [78]. Uncharged tRNA binds to the histidyl-tRNA synthetase (HisRS) domain and the C-terminal domain (CTD) of GCN2 to activate the kinase domain [26, 45, 77, 79]. In yeast and mammalian cells, GCN1, which makes contact with Rps10 in the ribosome A site, is required for GCN2 to detect uncharged uncharged tRNA, necessary for GCN2 activation [80]. Active GCN2 phosphorylates a conserved serine of eIF2α in fungi and mammals, which inhibits GDP/GTP exchange by eIF2B. [38]. This reduces translation of many mRNAs, while selectively enhancing the translation of mRNAs that encode proteins required to cope with the stress, including genes encoding key amino acid biosynthetic enzymes [81]. Because phosphorylated eIF2α (P-eIF2α) is a competitive inhibitor of eIF2B, and because eIF2α is present in excess of eIF2B, small changes in the levels of P-eIF2α in cells are enough to substantially alter protein synthesis [41, 82].

Starvation for all or any single amino acid, as well as too much of any one amino acid, leads to an amino acid imbalance, activation of GCN2, and synthesis of all 20 amino acids to relieve the imbalance [83-86]. This general amino acid control (GAAC) [41], originally called cross-pathway control in *N. crassa* [86], leads to the activation of GCN2 kinase, phosphorylation of eIF2α, and translation of the bZIP transcription factors CPC-1 in *N. crassa*, and Gcn4 in yeast [41, 52]. Both *cpc-1* and GCN4 contain upstream open reading frames (uORF) in the 5' mRNA leader sequence that control translation of the main ORF in response to amino acid limitation. GCN4 contains 4 uORFs, and translation of uORF1 functions as a positive regulatory element to facilitate re initiation of translation at the start of either uORF4 or GCN4 [41, 49]. Translation of uORF4 strongly inhibits the translation of GCN4, whereas uORF2 and uORF3 appear to have only minor roles. When P-eIF2α accumulates in response to amino acid imbalance, ribosomes scan past uORF4, leading to increased re-initiation at the GCN4 start codon and synthesis of Gcn4p. *N. crassa cpc-1*, and the mammalian homolog, ATF4, contain 2 uORFs that function analogously to uORF1 and uORF4 in *S. cerevisiae* GCN4 [54, 87].

The critical role for eIF2α in translation initiation led us to examine if the circadian clock regulates translation initiation by regulating the phosphorylation state and activity of eIF2α. We show that ~30% of available *N. crassa* eIF2α is phosphorylated during the subjective day under control of the circadian clock. CPC-3 rhythmic activity, which was altered by amino acid levels, was necessary for rhythmic accumulation of P-eIF2α. This daytime peak in P-eIF2α levels corresponded to reduced translation in cell-free translation assays prepared from those cells. Furthermore, the core clock component

12

FRQ accumulated rhythmically in Δcpc-3 cells, whereas ALG-11 protein rhythms were dependent on CPC-3 and rhythmic P-eIF2α levels *in vivo*. These data demonstrated that clock regulation of P-eIF2α levels by CPC-3 drives rhythmic translation of specific mRNAs, rather than controlling global rhythmic translation, specifying a novel mechanism for clock control of select mRNA translation by potentially conserved mechanisms.

Results

eIF2α phosphorylation is clock-controlled

To determine if the circadian clock regulates translation initiation, rhythms in phosphorylation of eIF2α (NCU08277) were investigated. Protein extracts were isolated from *N. crassa* cells grown in constant dark (DD) and harvested every 4h over 2 days (a circadian time course). The protein extracts were used to assay the levels of total and phosphorylated eIF2α with anti-mammalian eIF2α antibodies directed against conserved epitopes (**Figures 2.1A, 2.1B, 2.2**). eIF2α is essential; therefore, the specificity of the antibodies could not be confirmed using a deletion of eIF2α. Instead, antibody directed against total eIF2α was confirmed to cross-react with *N. crassa* eIF2α expressed and purified from bacteria with a band corresponding to the appropriate molecular weight (36 kDa) (**Figure 2.1**). The specificity of the phospho-specific eIF2α antibody (P- eIF2α antibody) was confirmed by the signal being dependent on CPC-3 kinase (NCU01187), and by stimulation of the signal during histidine starvation using 3-amino-1,2,4-triazole (3-AT) treatment (see **Figure 2.5A**).

In WT cells, P-eIF2α levels (**Figure 2.2A**), but not total eIF2α levels (**Figure 2.2B**), cycled with a daily rhythm, reaching peak levels in the subjective late morning (DD16 and DD40). The levels of P-eIF2α and total eIF2α fluctuated in clock mutant Δfrq cells, but rhythmicity of P-eIF2α accumulation was abolished (**Figure 2.2C**). These data demonstrated that the rhythm in P-eIF2α accumulation is controlled by the circadian clock.
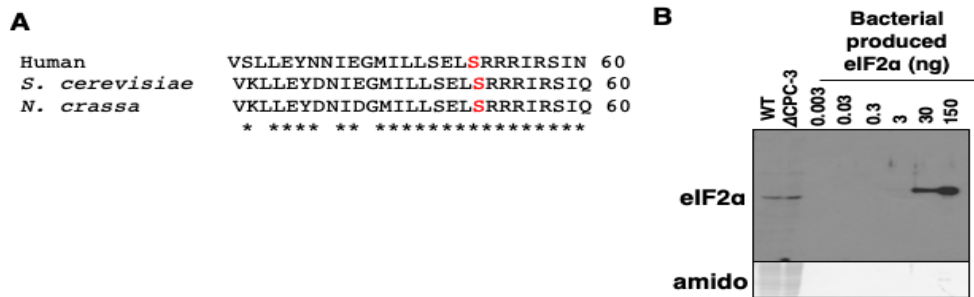
Figure 2.1. eIF2α is highly conserved. (A) Conservation of the inhibitory serine phosphorylation site at amino acid 52 (highlighted in red) between human, S. cerevisiae, and *N. crassa* eIF2α that is recognized by the P-eIF2α antibody. Stars below the sequence denote identity in all 3 proteins. (B) Western blot of purified eIF2α from E. coli probed with total eIF2α antibody. Different concentrations of bacterial produced eIF2α are shown, along with WT and Δcpc-3 controls.
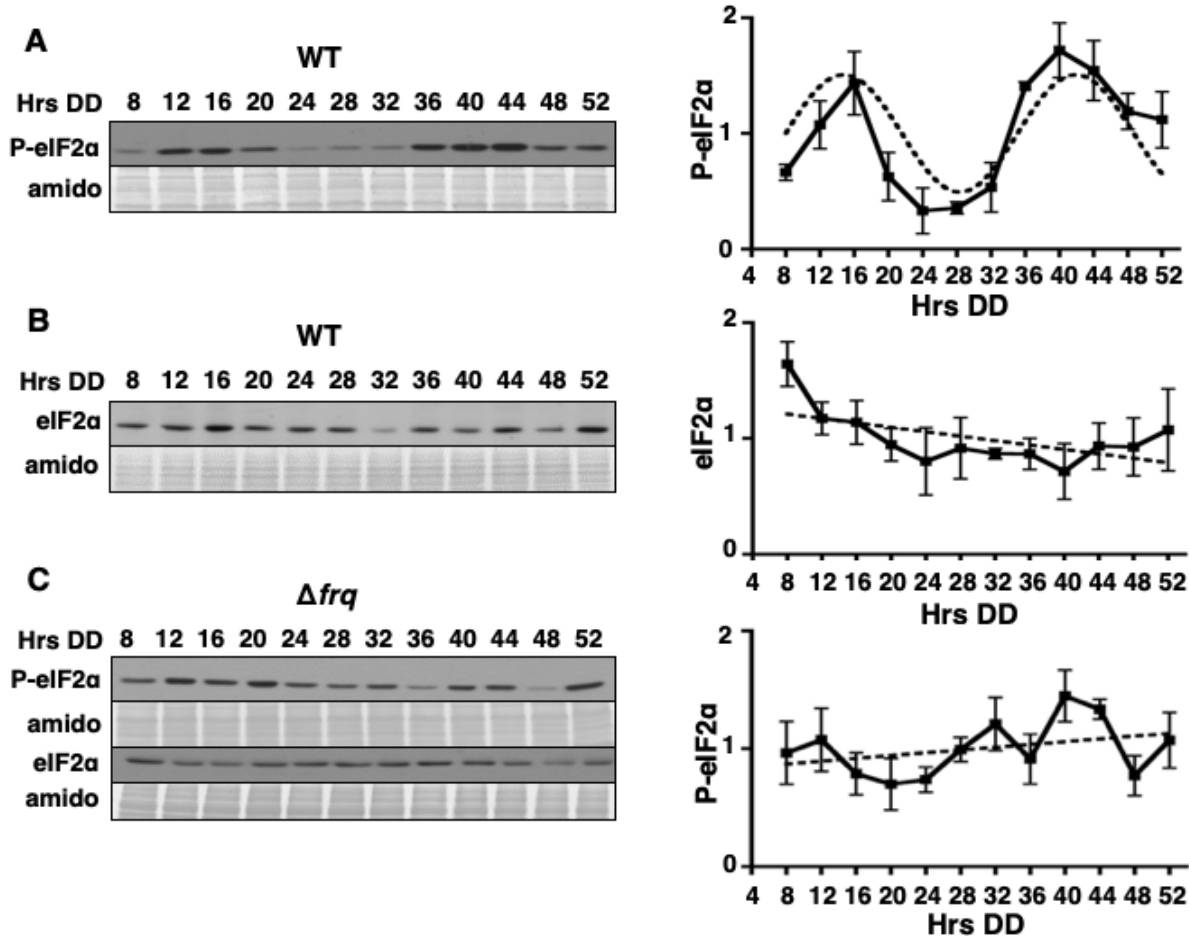
Figure 2.2. The circadian clock regulates the activity of eIF2α. Representative western blots of protein extracts isolated from WT (A, B) or Δfrq (C) strains grown in DD and harvested every 4 h (Hrs DD) over 2 days and probed with anti phospho-specific eIF2α antibody (A, C) or total eIF2α antibody (B,C). The same protein extracts were used in A and B. Amido stained protein is shown as a loading control. Plots of the data (mean ± SEM, n=3) on the left show the average P-eIF2α (A, C) or eIF2α (B) signal normalized to total protein (solid black line). Rhythmicity of P-eIF2α in WT cells (A) was determined using F-tests of fit of the data to a sine wave (dotted black line, $P<0.001$), while eIF2α in WT cells (B), both eIF2α and P-eIF2α, in Δfrq (C) were arrhythmic as indicated by a better fit of the data to a line (dotted black lines).

CPC-3 is required for phosphorylation of eIF2α

To determine if CPC-3 kinase is required for phosphorylation of eIF2α in *N. crassa*, the levels and phosphorylation status of eIF2α were examined in $\Delta cpc\text{-}3$ cells grown in a circadian time course in DD (**Figures 2.3**). No P-eIF2α was detected in $\Delta cpc\text{-}3$ cells in DD (**Figure 2.3A**), whereas eIF2α was detected at all time points (**Figure 2.3B**). Furthermore, complementation of $\Delta cpc\text{-}3$ cells with a wild type copy of *cpc-3* rescued P-eIF2α to a level similar to that observed in WT cells in DD (**Figure 2.3C**). These data supported that CPC-3 kinase is necessary for eIF2α phosphorylation when cells are grown in DD.

Because eIF2α is a general translation initiation factor that may be critical for expression of components of the molecular circadian oscillator, we examined if $\Delta cpc\text{-}3$ cells retain a functional clock by assaying FRQ protein rhythms from the same extracts used to examine P-eIF2α levels (**Figure 2.3A**). FRQ protein levels were rhythmic in both WT and $\Delta cpc\text{-}3$ cells (**Figures 2.3D, A-1**). In addition, $\Delta cpc\text{-}3$ had no effect on the overt circadian rhythm of development in strains carrying the *ras_bd* mutation, which slows growth rate and clarifies the rhythm in asexual spore development [88]. However, the growth rate in *ras_bd*, $\Delta cpc\text{-}3$ was slow compared to *ras_bd* cells (**Figure 2.3E**). Thus, CPC-3 is necessary for phosphorylation of eIF2α, and for normal growth rate in DD. However, neither CPC-3 nor rhythmic P-eIF2α levels are required for a functional circadian oscillator.
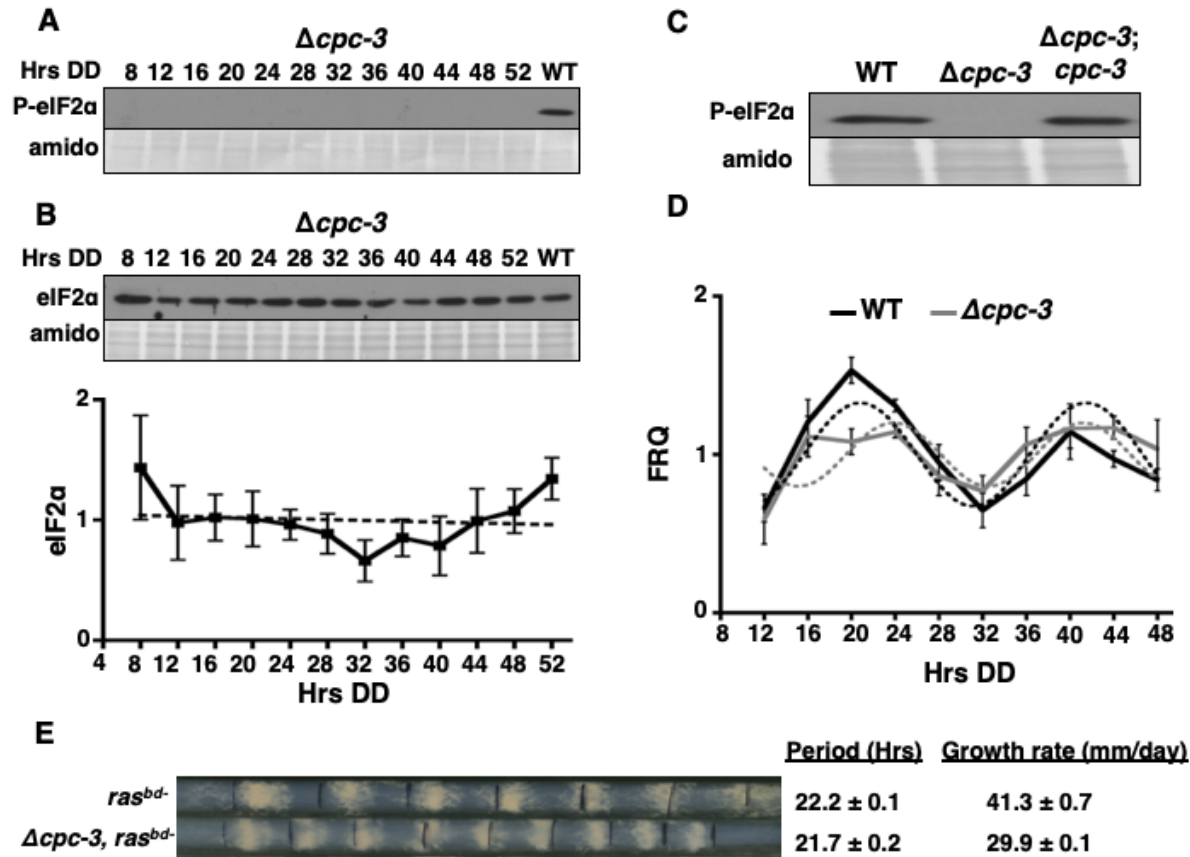
Figure 2.3. CPC-3 is required for phosphorylation of eIF2α and normal growth rate, but not for a functional clock. (A) Western blot of protein extracted from Δcpc-3 cells grown in DD and harvested every 4 h (Hrs DD) over 2 days and probed with P-eIF2α antibody (A), or total eIF2α antibody (B). (C) Western blot of protein extracted from WT, Δcpc-3 and Δcpc-3 complemented cells (Δcpc-3; cpc-3) grown in DD for 40 hrs and probed with P-eIF2α antibody. Amido stained protein is shown as loading controls in A-C. The data in B are plotted below. Total eIF2α levels were arrhythmic as determined using F-tests of fit of the data to a line (dotted black line). (D) FRQ protein was analyzed by western blot in WT and Δcpc-3 cells (**Figure A-1**), and FRQ protein levels are plotted. FRQ rhythmicity in both strains was determined using F-tests of fit of the data to a sine wave (dotted black line, $P<0.001$). (E) Race tube assay of the indicated strains. Period and growth rates of the strains are indicated on the right.

Rhythmic phosphorylation of eIF2α is not dependent on rhythmic CPC-3 levels

Phosphorylation of eIF2α is rhythmic and requires CPC-3 in DD. Rhythmic control of eIF2α phosphorylation might be due to clock control of the levels and/or activity of CPC-3 kinase. To first establish if the clock controls the levels of *cpc-3* mRNA and protein, WT and Δ*frq* cells were transformed with either a *cpc-3* promoter::luciferase transcriptional fusion (*Pcpc-3::luc*), or a CPC-3::V5 translational fusion. *Pcpc-3::luc* and CPC-3::V5 accumulated rhythmically in WT, but not in Δ*frq*, cells grown in DD (**Figures 2.4A & B, A-2A, A-2B**). The peak in CPC-3::V5 levels occurred during the subjective day (DD12-16 and DD 40), similar to the peak in P-eIF2α levels **(Figure 2.2A),** and consistent with the data from a proteomics study demonstrating that CPC-3 protein levels cycled under control of the clock [22]. Clock control of CPC-3 protein levels supported the possibility that rhythmic accumulation of CPC-3 is necessary for rhythmic P-eIF2α accumulation. To test this possibility, CPC-3 was constitutively expressed from a copper regulatable *Ptcu-1* promoter [89], and in the presence of *Ptcu-1* inducer bathocuproinedisulfonic acid (BCS), constitutive expression of CPC-3::V5 protein was observed in cells grown in DD over a circadian time course (**Figures 2.4C & A-2A, 2B**). However, constitutive expression of CPC-3 protein did not alter rhythmic P-eIF2α levels (**Figures 2.4D & A-2C, 2D).** These data indicated that rhythmic accumulation of CPC-3 protein is not sufficient to explain the rhythms in P-eIF2α levels. Instead, these data raised the possibility that the activity of CPC-3 is clock-controlled, and that it is the control of CPC-3 activity, not level, that accounts for the rhythm in P-eIF2α levels.
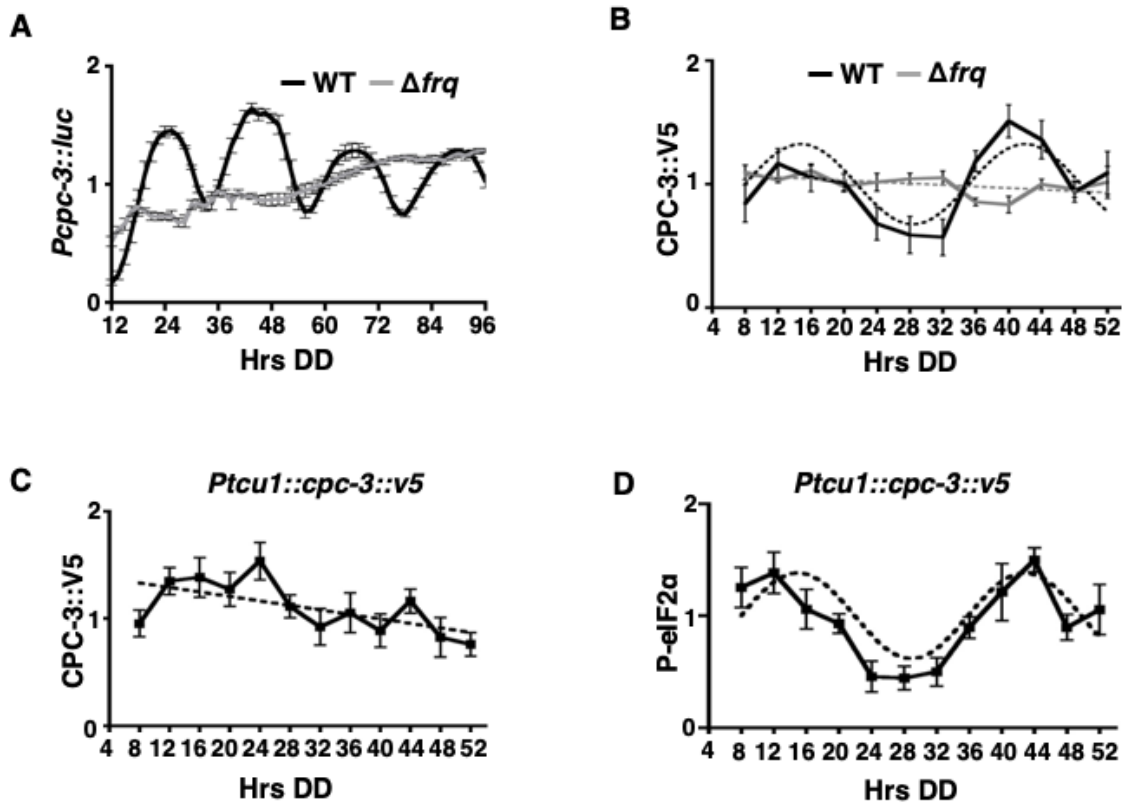
Figure 2.4. CPC-3 mRNA and protein levels are clock-controlled, and the rhythmic abundance of CPC-3 is not required for rhythmic P-eIF2α levels. (A) Bioluminescence from a *Pcpc-3::luc* transcriptional fusion construct (n = 10) expressed in WT (black line) or Δfrq (gray line) cells and recorded in DD every 90 min over 4 d (Hrs DD). (B) Plot of CPC-3::V5 protein from WT and Δfrq cells grown in DD and harvested every 4 h (Hrs DD) over 2 days. The western blots are shown in Figure A-2A, 2B. Rhythmicity of CPC-3::V5 cells in WT was determined using F-tests of fit of the data to a sine wave (P<0.05), whereas the data for Δfrq was better fit to a line. Plot of CPC-3::V5 (C) and P-eIF2α protein levels from *Ptcu1::cpc-3::v5* cells grown in DD with BCS, and harvested every 4h over two days. The western blot is shown in Figure A-2C, 2D. Rhythmicity of P-eIF2α was determined by F-tests of fit of the data to a sine wave (black dotted line, P<0.005) and CPC-3::V5 was best fit to a line (black dotted line).

Constitutive activation of CPC-3 abolishes rhythmic P-eIF2α levels

In *S. cerevisiae,* GCN2 kinase is activated upon binding of uncharged tRNA to the regulatory domains [67, 77, 90]. In addition, activation of GCN2 by uncharged tRNA requires the trans-acting positive effector protein GCN1 [91]. The regulatory domains of *S. cerevisiae* GCN2 are conserved in *N. crassa* CPC-3 [44]; therefore, we hypothesized that CPC-3 is similarly activated by uncharged tRNA and GCN1 (NCU05803). To first establish if CPC-3 is activated by amino acid starvation, 3-Amino-1,2,4-triazole (3-AT), a competitive inhibitor of imidazoleglycerol-phosphate dehydratase enzyme necessary for histidine production, was added to *N. crassa* cultures 8 h prior to harvest at the peak (DD40) and trough (DD28) of P-eIF2α levels (see **Figure 2.2A**). As a result of clock control, the levels of P-eIF2α were 2-fold higher in untreated WT cells at DD40 compared to DD28 **(Figure 2.5A)**. However, in 3-AT-treated cells, the time-of-day difference in P-eIF2α levels was abolished, and the overall levels of P-eIF2α were ~3-fold higher than the peak at DD40 in WT cells. As expected, no significant change in total eIF2α levels was observed in 3-AT-treated versus untreated cells at either time point. These data demonstrated that up to 30% of eIF2α is phosphorylated by the clock during the day (DD40) as compared to maximum levels of P-eIF2α during amino acid starvation. Consistent with the requirement for binding of uncharged tRNA for activation, CPC-3 required GCN1 for activation of the kinase domain to phosphorylate eIF2α, but deletion of GCN1 had no effect on total eIF2α levels **(Figures 2.5B)**. These data are consistent with the idea that, similar to *S. cerevisiae* GCN-2, *N. crassa* CPC-3 requires uncharged tRNA and GCN1 for activation. Therefore, we predicted that the corresponding mutations known to constitutively activate GCN-2 in *S. cerevisiae* would similarly constitutively

activate *N. crassa* CPC-3, and provide the tool needed to examine if rhythmic CPC-3 activity is required for cycling P-eIF2α levels.

In *S. cerevisiae* the F835L mutation leads to constitutive activation of GCN2, independent of uncharged tRNA binding, dimerization, association with ribosomes, and association with GCN1 [92]. The homologous mutation generated in *N. crassa* CPC-3, *cpc-3c*, led to a >3-fold increase in P-eIF2α levels, but had no significant effect on total eIF2α levels compared to WT cells grown for 28 h in DD **(Figure 2.5C)**. To validate that the *cpc-3c* mutation bypasses the requirement for activation by binding of uncharged tRNA, we showed that P-eIF2α levels were similar to WT levels in Δ*gcn1; cpc-3c* cells (**Figure 2.5B)***. These data supported that in *cpc-3c* mutant cells, CPC-3 is constitutively active, and this activity is independent of the requirement for GCN1 and uncharged tRNA.

Next, to determine if P-eIF2α rhythmicity requires rhythmic activation of CPC-3, we examined P-eIF2α levels in *cpc-3c* strains in a circadian time course in DD. If clock control of the activity of CPC-3 is necessary for P-eIF2α accumulation rhythms, then the levels of P-eIF2α should be high and arrhythmic in *cpc-3c* cells. Indeed, in the *cpc-3c* mutant, the levels of P-eIF2α were high compared to WT (**Figure 2.5B**) and arrhythmic **(Figures 2.5D),** with no corresponding change in the levels of total eIF2α (**Figures 2.5C & A-3A**). Furthermore, the clock functioned normally in the mutant, as demonstrated by robust FRQ::LUC protein rhythms in *cpc-3c* cells (**Figure A-3B**). Constitutive activity of CPC-3, and the resulting loss of rhythmic accumulation of P-eIF2α, also led to a reduction in linear
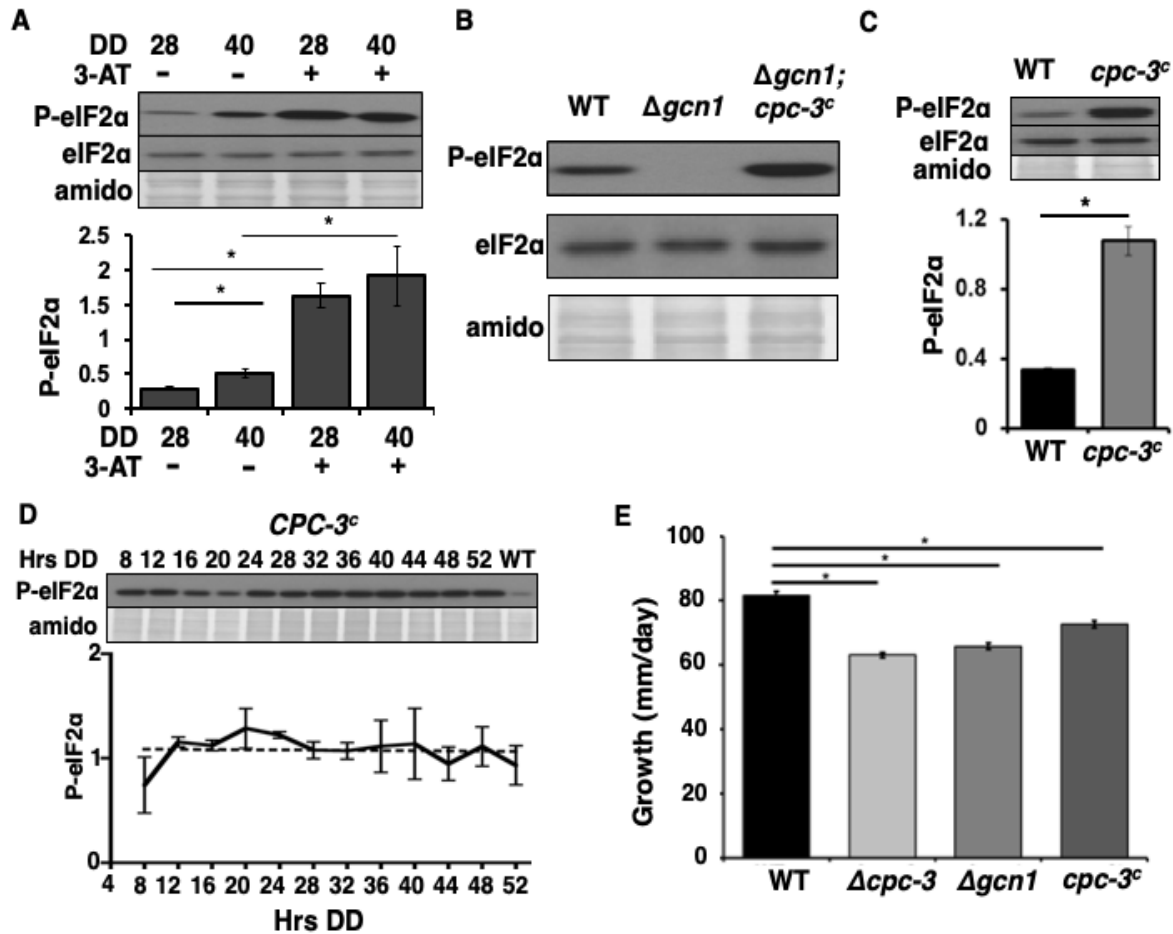
Figure 2.5. Rhythmic activation of CPC-3 is required for rhythmic P-eIF2α levels.
(A) Western blots of protein from WT cells treated (+) or not (-) with 3-AT and harvested in the subjective day (DD40) or night (DD28). (B & C) Western blot of protein from the indicated cells harvested in the subjective day (DD28). The blots were probed with P-eIF2α antibody or total eIF2α antibody. Amido stained protein is shown below as a loading control. The graphs in A and C show the average signal normalized to total protein loaded; (mean ± SEM, n=3; *p< 0.004, student T-test). (D) Western blot of protein isolated from *cpc-3c* cells, and including a WT sample harvested at DD40, grown in DD and harvested at the indicated times (Hrs DD) and probed with P-eIF2α antibody. The data are plotted below. P-eIF2α levels were arrhythmic as indicated by a better fit of the data to a line (dotted black lines).

growth rate compared to WT cells (**Figure 2.5E**). Thus, CPC-3 activity is regulated by the clock, and this regulation is necessary for the rhythmic accumulation of P-eIF2α and normal growth. These data indicated that rhythmic accumulation of CPC-3 protein is not sufficient to explain the rhythms in P-eIF2α levels. Instead, these data raised the possibility that the activity of CPC-3 is clock-controlled, and that it is the control of CPC-3 activity, not level, that accounts for the rhythm in P-eIF2α levels.

Clock control of P-eIF2α activity is required for rhythmic translation *in vitro* and *in vivo*

Phosphorylation of eIF2α leads to an overall decrease in protein synthesis [38], and the clock regulates rhythms in the levels of P-eIF2α in *N. crassa*. Thus, we predicted that translation of some mRNAs would be reduced during the subjective day when the levels of P-eIF2α are high, and that translation would be increased during the subjective night when the levels of P-eIF2α are low. To begin to test this prediction, we carried out *in vitro* translation assays using cell-free extracts isolated from WT, Δ*frq*, and Δ*cpc-3* cells harvested at the peak (DD40) and trough (DD28) of rhythmic P-eIF2α levels and capped polyadenylated mRNA encoding firefly luciferase (LUC). Translation was monitored by quantitating LUC activity **(Figure 2.6A)**. As predicted, LUC translation was higher when P-eIF2α levels were low during the subjective evening (DD28), and translation was reduced at the peak of P-eIF2α levels in the subjective day (DD40). In Δ*frq* cells, LUC translation was similar to WT DD28 at both times of the day, supporting that the clock is
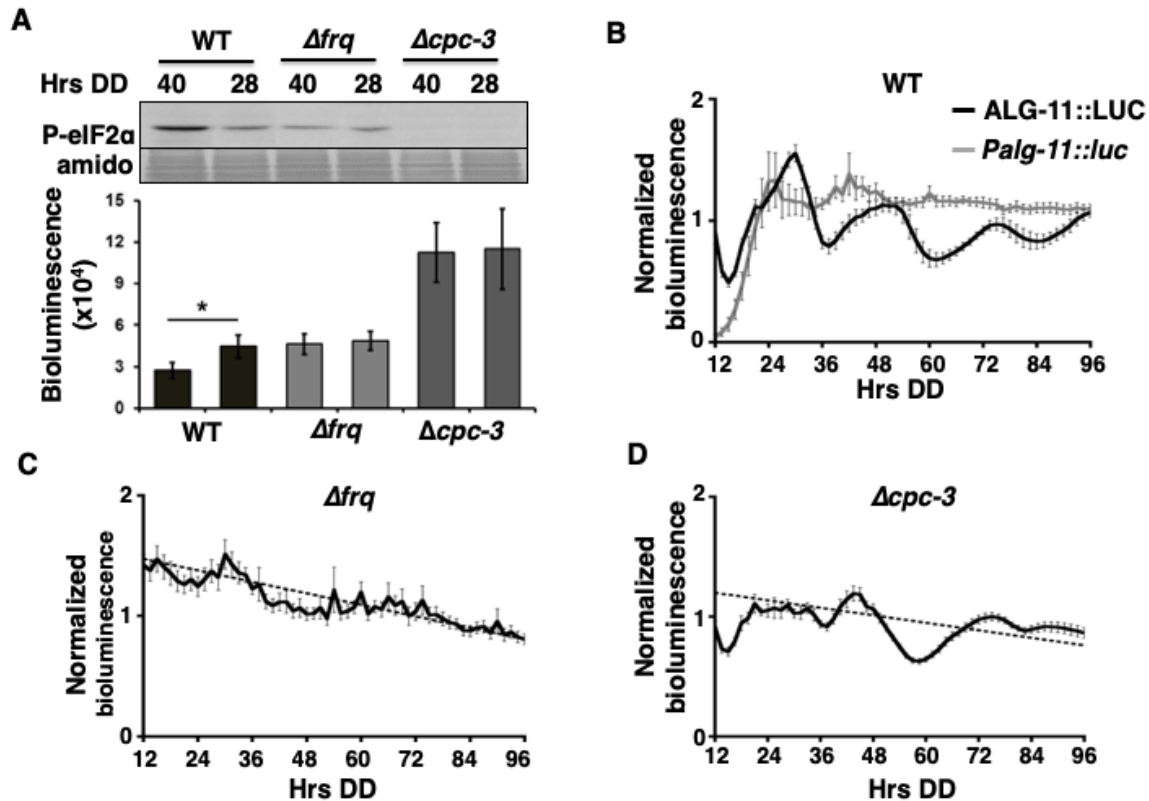
Figure 2.6. Clock control of P-eIF2α activity is required for rhythmic translation *in vitro* and *in vivo*. (A) *In vitro* translation of *luc* mRNA using *N. crassa* cell-free extracts from WT, Δ*frq* and Δ*cpc-3* cells harvested in the subjective day (DD40) or night (DD28). Western blots (top) of the indicated strains were probed with P-eIF2α antibody. Amido stained protein is shown below as a loading control. The plot below shows the average bioluminescence signal from translation of *luc* mRNA (*p<0.05, n=3). (B) Luciferase activity from ALG-11::LUC translational (black line) and *Palg-11::luc* transcriptional (gray line) fusions in WT cells, and (C) ALG-11::LUC in Δ*frq* and (D) Δ*cpc-3* cells grown in DD and recorded every 90 min over 4 d (Hrs DD). The average bioluminescence signal is plotted (mean ± SEM, n=12). ALG-11::LUC in Δ*frq* and Δ*cpc-3* cells was arrhythmic as indicated by a better fit of the data to a line (dotted black lines). (E) Linear growth rates for the indicated strains are plotted (mean ± SEM, n=6, *p<0.001)

necessary for increased P-eIF2α during the day. In Δ*cpc-3* extracts, LUC translation was significantly higher at both times of day, reflecting the absence of phosphorylated eIF2α under these growth conditions **(see Figure 2.2A)**. These data supported that clock control of the levels of P-eIF2α provides a mechanism to regulate rhythmic translation initiation.

To examine a role for rhythmic P-eIF2α accumulation on mRNA translation *in vivo*, we examined rhythmicity of *alg-11* (NCU06779) mRNA and ALG-11 protein levels in WT, Δ*frq*, and Δ*cpc-3* cells. ALG-11, a mannosyl transferase involved in N-linked glycosylation of proteins, was chosen based on its conserved role in posttranslational modifications important in cell wall stability, signaling, and endoplasmic reticulum protein quality control [93]. In addition, our preliminary RNA-seq and ribosome profiling data suggested that ALG-11 might be regulated at the translational level by the clock. In WT cells, an ALG-11::LUC translational reporter fusion was rhythmic in DD, peaking during subjective night when P-eIF2α levels are low, whereas an *alg-11* promoter *luc* fusion (P*alg-11::luc)* was arrhythmic **(Figure 2.6B)**. Consistent with translation regulation by the clock and rhythmic eIF2α activity, ALG-11::LUC was arrhythmic in Δ*frq* and Δ*cpc-3* cells **(Figure 2.6C&D)**. These data demonstrated that ALG-11 protein rhythms, which arise from constant mRNA levels, require a functional clock and rhythmic eIF2α activity.

Discussion

Translation initiation is a tightly regulated process that requires several translation initiation factors. One of the main targets of translational control is eIF2α. Here we established that the *N. crassa* clock regulates the activity of eIF2α (**Figure 2.2**), with

inhibitory P-eIF2α levels peaking during the subjective day and active eIF2α levels peaking during the subjective night. The nighttime activity of eIF2α parallels the peak activity of eEF-2 [35], suggesting coordinate control of mRNA translation initiation and elongation at night. Consistent with this idea, translation peaked at night *in vitro* when P-eIF2α (**Figure 2.6**) and PeEF-2 [35] levels are low. Similarly, ALG-11 protein levels, which requires CPC-3 for rhythmic translation, peaked at night (**Figure 2.6**). Furthermore, mass spectroscopy analyses of rhythmic protein accumulation revealed an ~2-fold increase in rhythmic protein accumulation at night compared to the day [21], whereas the peak in rhythmic mRNA levels was biphasic, with most transcripts peaking during the late night to early morning [21, 22, 94, 95]. Interestingly, clock-controlled genes involved in catabolism generally peak during the day to provide energy for anabolic functions that occur at night [21, 95]. As protein synthesis is energetically costly, it makes sense for the organism to synchronize most translation to the night when energy resources are at their maximum to support growth. Indeed, disruption of rhythmic P-eIF2α levels led to a significant reduction in growth rate (**Figure 2.5E**). Conversely, some proteins accumulate to high levels during the day under control of the clock. A daytime peak in protein levels may be, in part, due to only up to half of available eIF2α and eEF-2 reaching peak phosphorylation levels under control of the clock in constant environmental conditions (**Figure 2.5** and [35]), allowing some mRNAs to escape the daytime inhibition of translation. Moreover, phosphorylation of eIF2α selectively enhances translation of some target mRNAs, particularly those with upstream open reading frames in the leader sequence [54, 96, 97]. Similarly, in mice, some neuronal mRNAs involved in memory processing have increased translation when eEF-2 is hyper-phosphorylated [98], and in

Aplysia neurons, eEF-2 phosphorylation promotes the translation of some messages, while repressing others [99]. Taken together, these data support that certain mRNAs are more sensitive to increased daytime P-eIF2α and P-eEF-2 levels, and therefore peak in translation at night when energy levels are predicted to be high, whereas others are less sensitive, or are specifically activated, and peak in levels during the day, possibly to deal with increased environmental stress during the daylight hours. While P-eIF2α rhythms are necessary for the rhythmic accumulation of ALG-11 (**Figure 2.6**), they are not required for rhythmic FRQ protein accumulation and a functional clock (**Figure 2.3D&E**), supporting that some, but not all, rhythmic proteins are derived from rhythmic translation. Ribosome profiling experiments coupled with RNA-seq are currently underway to reveal the extent and phase of rhythmic control of mRNA translation, and the potential mechanisms of specificity driven by rhythmic P-eIF2α and P-eEF-2 levels.

Rhythmic CPC-3 activity (**Figure 2.5D**), but not cycling CPC-3 levels (**Figure 2.4C&D**), are necessary for the daytime peak in P-eIF2α levels. Activation of GCN2 requires binding of uncharged tRNA to the HisRS domain and the CTD, leading to a conformational change, activation of GCN2 protein kinase domain, and phosphorylation of eIF2α [39, 45, 79, 100]. Because the HisRS domain is conserved in all GCN2 homologs [45], we speculated that CPC-3 in *N. crassa* is similarly activated by rhythmic binding of uncharged tRNA, which would be driven by rhythmic amino acid abundance. In support of this idea, we showed that CPC-3 requires GCN1 (**Figure 2.5B**), which delivers uncharged tRNA from the A-site of the ribosome to GCN2 for activation [91, 101, 102]. In addition, histidine starvation, induced by the addition of 3-AT to *N. crassa* cells, abolished the time of day

difference in P-eIF2α levels (**Figure 2.5A**). Amino acid levels accumulate rhythmically in the mouse brain under control of the clock [103], and in *N. crassa*, genes involved in amino acid biosynthesis are clock-controlled [21, 22, 95]. Taken together, these data support that clock control of amino acid levels leads to rhythms in uncharged tRNAs that, in turn, activate CPC-3 during the day. To further test this idea, experiments are currently underway to examine possible rhythms in amino acid levels in *N. crassa.* Lastly, in *S. cerevisiae*, protein phosphatases Sit4 and Glc7 remove the phosphate from P-eIF2α [104, 105]. We are currently testing if the homologous phosphatases in *N. crassa* are active at night to remove the phosphate from P-eIF2α to augment nighttime translation initiation.

The finding that rhythms in *cpc-3* mRNA and CPC-3 protein accumulation are not required for rhythms in P-eIF2α levels (**Figure 2.4**) suggests the possibility that CPC-3 protein may have other functions in the cell. In support of this idea, in yeast cells, eEF1A binds to the C-terminal domain of GCN2 to inhibit its activity; however, the physiological significance of this interaction is not known [106]. Furthermore, in yeast cells, a downstream effector of GCN2 is TORC1, also involved in amino acid sensing. In response to amino acid starvation GCN2 binds to TORC1 and phosphorylates and inactivates KOG1, the regulatory subunit of TORC1 [107]. Although additional targets of CPC-3 have not been identified in *N. crassa*, the conserved eEF1A and KOG1 proteins provide good starting points for further investigation.

Based on these and published data, our current working model is that at dawn, cellular amino acid levels are low as a result of generally increased protein synthesis at night. This, along with rhythms in amino acid biosynthetic pathways, would lead to increased uncharged tRNA levels, activation of CPC-3, increased P-eIF2α levels, and reduced translation initiation. In addition, increased uncharged tRNA levels would be expected to slow translation elongation rates in the context of high P-eEF-2 levels. As a result, during the day, mRNA translation would be generally low, and protein catabolism would rise. This would lead to increased cellular amino acid levels, reduced deacetylated tRNA levels, low CPC-3 activity and inhibitory P-eIF2α levels, and enhanced mRNA translation at night. In addition, links between translation factors and ribosome activity are known. In yeast, The GCN2 CTD domain is required for association with translating ribosomes, and this interaction is necessary for GCN2 kinase activity [102, 108]. Furthermore, in mice, GCN2 activation has been tied to stalled ribosomes [109], indicating that functional connections exist between translation elongation, eEF-2, and GCN-2 activity during nutrient deprivation. Clock control of the activity of conserved initiation and elongation factors adds a further level of regulation to allow integration of nighttime anabolic and daytime catabolic cellular pathways with protein translation to effectively utilize available energy resources, and to contend with predictable daily stress.

Materials and methods

Strains and growth conditions

Vegetative growth conditions and crossing protocols were as previously described [110]. All strains containing the *hph* construct were maintained on Vogel's minimal media [110], supplemented with 200 µg/mL of hygromycin B (#80055-286, VWR, Radner, PA). Strains containing the *bar* cassette were maintained on Vogel's minimal media lacking NH_4NO_3 and supplemented with 0.5% proline and 200 µg/mL of BASTA (Liberty 280 SL Herbicide, Bayer, NC). Race tube assays to monitor developmental rhythms in strains carrying the *ras_{bd}* mutation, and linear growth rates, were done using 1X Vogels salt, 0.1% glucose, 0.17% arginine and 50 µg/mL biotin media as previously described [89]. *N. crassa* wild-type (WT) FGSC#4200 (*mat a*, 74-OR23-IV) or FGSC#2489 (*mat A*, 74-OR23-IV), FGSC#10697 (*mat a*, Δ*cpc-3::hph*), FGSC#14200 (*mat a*, Δ*gcn1::hph*), FGSC#14201 (*mat A*, Δ*gcn1::hph*) were obtained from the Fungal Genetics Stock Center (FGSC, Kansas State University). DBP1228 (Δ*frq::bar*) was previously generated [111]. The primers used to generate and validate strains are listed in Table 2.1. To assay *cpc*-3 mRNA rhythms, a *Pcpc-3::luc* transcriptional fusion was generated by first amplifying a 1.5 kb promoter fragment upstream of the CPC-3 coding region using primers LUCF1 and LUCR1 containing *Not*1 and *Asc*1 restriction sites. The resulting 1.5 kb fragment was cloned into pRMP53 [112], linearized with *Nde*1, transformed into WT cells (FGSC#4200) and transformants were assayed for luciferase activity. *Pcpc-3::luc* transformants were crossed with WT (FGSC#2489) and Δ*frq::bar* (DBP1228) strains to generate *Pcpc-3::luc* (DBP2439) and *Pcpc-3::luc, Δfrq::bar* (DBP2442) homokaryons. *cpc-3::v5::hph* was generated by 3-way PCR with 1.4 kb of the *cpc-3* ORF (primers V5F1 and V5R1), 1.8 kb

10X glycine linker-V5-hygromycin-B resistance gene (*hph*) (primers V5F2 and V5R2), and 1 kb of the 3' end of *cpc-3* (primers VF3 and V5R3). PCR was used to verify endogenous integration of the construct into the *cpc-3* locus using V5F4 and V5R4 primers, and expression of CPC-3::V5 was validated by western blot using anti-V5 antibody (R960-25, Invitrogen, Carlsbad CA). A *cpc-3::v5::hph* homokaryon (DBP2717) was generated by transforming WT with *cpc-3::v5::hph*, followed by crossing with WT (FGSC#2489). For overexpression of CPC-3::V5, a *bar::Ptcu-1::cpc-3::v5::hph* strain was generated by transforming a 3-way PCR product containing 1.5 kb of the 5' *cpc-3* ORF (primers tcu1F1 and tcuR1), *bar::Ptcu-1* from plasmid DBP450 (primers tcu1F2 and tcuR2) [113], and 1 kb of 3' end of *cpc-3* (primers tcu1F3 and tcuR3) into the DBP2717 strain. Following validation of integration by PCR (primers tcu1F4 and tcuR4), a *bar::Ptcu-1::cpc-3::v5::hph* homokaryon (DBP2742) was obtained by microconidia filtration [114]. To generate the constitutive active *cpc-3c* mutation, phenylalanine at codon 835 (TTC) and serine 837 (TCT) of CPC-3 was changed to leucine (CTG), and serine (TCT), respectively, to create a *Bcl*I restriction enzyme site. The mutant 3.8 kb fragment was generated by 2-way PCR using primers *cpc-3c*F1, *cpc-3c*R1, *cpc-3c*F2 and *cpc-3c*R2, verified by sequencing, and then co-transformed with the hyg_R pDBP301 plasmid into *Δmus-52::bar* (FGSC#9719). A transformant containing *cpc-3c* was crossed to WT (FGSC#4200) and *Δgcn1* (FGSC#14201) to obtain DBP3290 (*cpc-3c)* and DBP3292 (*Δgcn1; cpc-3c*) homokaryons, respectively. Progeny from the crosses were screened by PCR using primers *cpc-3c*F3 and *cpc-3c*R3, followed by restriction digestion with *Bcl*I. The ALG-11::LUC translational fusion was generated by 3-way PCR (alg-11F2 and alg-11R2, and alg-11F4 and alg-11R4 primers) using the *N. crassa* codon-optimized luciferase gene (primers alg-11F3 and alg-

11R3) [112], and co-transformed with either hyg$_R$ pDBP301 into WT (FGSC#2489) and

Δ*frq* (DBP1320) strains, or with BASTA$_R$ pBARGEM7-2 [115] into Δ*cpc-3* cells

(FGSC#10697). Hygromycin or basta-resistant transformants were screened for

luciferase activity and homologous insertion into the *alg-11* gene (primers alg-11F5 and

alg-11R5). To generate the P*alg-11::luc* transcriptional fusion, a 1.3 kb promoter region

of *alg-11* was amplified with primers alg-11F1 and alg-11R1 containing *Xma*I restriction

sites. The PCR product was digested with *Xma*I and cloned into plasmid pRMP57

containing the codon-optimized luciferase gene [112]. The resulting plasmid was

linearized by digestion with *Pci*I, co-transformed with hyg$_R$ pDBP301 into WT

(FGSC2489) cells, and hygromycin-resistant transformants were screened for luciferase

activity. To assay FRQ::LUC protein rhythms, strains FGSC#14201, FGSC#10697, or

DPB3290, were crossed to strains containing a FRQ::LUC translational fusion linked to

bar [116]. Hygromycin and basta-resistant progeny were screened for luciferase activity

to generate *frq::luc, Δgcn1* (DBP3321), *frq::luc, Δcpc-3* (DBP2789), and *frq::luc, cpc-3$_c$*

(DBP3315) strains. *cpc-3$_c$* was validated by PCR using cpc-3$_c$F3 and cpc-3$_c$R3 primers

followed by restriction digestion with *Bcl*I.

Circadian time course experiments for western blots were accomplished according to

published methods [117]. Briefly, mycelial mats were grown in Vogel's minimal media,

2% glucose, 0.5% arginine, pH 6.0 with shaking in constant light (LL) for 24 h at 30°C.

The cultures were then transferred to DD at 25°C to synchronize the clock in all cells to

dusk and harvested at the indicated times (Hrs DD). Harvested tissue was immediately

frozen in liquid N$_2$. For constitutive expression of *bar::P$_{tcu-1}$::cpc-3::v5::hph*, cells were

grown in Vogel's medium containing 30μm of the copper chelator bathocuproinedisulfonic acid (BCS, B1125; Sigma-Aldrich St. Louis, MO) to induce the *tcu-1* promoter [89].

Complementation of Δ*cpc-3*

Complementation of Δ*cpc-3* was done to validate that CPC-3 was required for P-eIF2α rhythms. A wild type copy of *cpc-3* was amplified from the genome by PCR (primers cpc-3F1and cpc-3R1) using Phusion Hot Start High-Fidelity DNA polymerase (Thermo Fisher, Waltham MA). The primer pair amplified 1.5 kb upstream of the *cpc-3* coding region, the 5.8 kb *cpc-3* ORF, and 1 kb downstream of the *cpc-3* coding region. The PCR product was co-transformed with a basta-resistant plasmid (DBP425) into Δ*cpc-3* (FGSC#10697). Transformants were selected for basta resistance and validated for having a WT copy of *cpc-3* by PCR using primers cpc-3F2 and cpc-3R2.

3-Amino-1,2,4-triazole (3-AT) treatment

To determine if CPC-3 is activated by amino acid starvation, germinating conidia were treated with 3-AT (Sigma-Aldrich). Conidia ($1X10^5$) from WT and Δ*cpc-3* strains were inoculated in 500 ml Vogel's minimal media containing 2% glucose. Conidia were germinated in LL 25_oC for 4 h, and then transferred to DD 25_oC. A final concentration of 9 mM 3-AT was added to the cultures 8 h before harvesting at the indicated time points for western blotting.

Protein extraction and western blotting

Protein was extracted as previously described [118] with the following modification: the extraction buffer contained 100 mM Tris pH 7.0, 1% SDS, 10 mM NaF, 1 mM PMSF, 1 mM sodium ortho-vanadate, 1 mM β-glycerophosphate, 1X aprotinin (#A1153, Sigma-Aldrich), 1X leupeptin hemisulfate salt (#L2884, Sigma-Aldrich), and 1X pepstatin A (#P5318, Sigma-Aldrich). Protein concentration was determined by the Bradford assay (#500-0112, Bio-Rad Laboratories, Hercules, CA). Protein samples (50 μg) were separated on 8% SDS/PAGE gels and blotted to an Immobilon-P nitrocellulose membrane (#IPVH00010, Millipore, Billerica, MA) according to standard methods.

The levels of P-eIF2α were detected using rabbit monoclonal Anti-EIF2S1 antibody (phosphoS51, #32157 Abcam, Cambridge UK) diluted 1:5000 in 5% Bovine Serum Albumin (BSA), 1X TBS, 0.1% Tween, and anti-rabbit IgG HRP secondary antibody (#170-6515, Bio-Rad) diluted 1:10000. Total eIF2α levels were detected using rabbit polyclonal anti-EIF2S1 antibody (#47508, Abcam) diluted 1:5000, and anti-rabbit IgG HRP secondary antibody (#170-6515, Bio-Rad) diluted 1:10000. CPC-3::V5 was detected using mouse monoclonal anti-V5 antibody (#R960-25 Invitrogen) diluted 1:5000 in 5% milk, 1XTBST, 0.1% Tween, and anti-mouse IgG HRP (#170-6515 BioRad) secondary antibody diluted 1:10000. FRQ protein was detected using mouse monoclonal anti-FRQ antibody (from clone 3G11-1B10-E2, a gift from Michael Brunner's lab, University of Heidelberg) diluted 1:200 in 7.5% milk,1XTBS, 0.1% Tween and anti-mouse IgG-HRP (#170-6515 BioRad) secondary antibody diluted at 1:10000. All proteins except FRQ were detected using chemi-luminescence SuperSignal West Pico Substrate (#34077, Thermo

Scientific). FRQ was detected using SuperSignal West Femto Maximum Sensitivity Substrate (#34085, Thermo Scientific). Densitometry was performed using NIH ImageJ software [119] and normalized to protein loading using amido black-stained protein.

Purification of eIF2α

To validate the specificity of total eIF2α antibody, eIF2α was first amplified from *N. crassa* cDNA with primers eIF2F1 and eIF2R1 containing restriction sites for *Nde*1 and *Not*1. The PCR product and pET30b vector (Invitrogen) were digested with *Nde*1 and *Not*1 prior to ligation to create pDBP607. pDBP607 was transformed to *E. coli* BL21 cells and screened for kanamycin resistance. Cells were grown overnight in Luria Broth (LB), supplemented with 30 μg/ml kanamycin for selection, with shaking at 37$_{o}$C. For purification of eIF2α, cells were grown in 400 ml LB at 37$_{o}$C with shaking at 250 rpm until an OD of 0.82 was reached. For induction, a final concentration of 1mm IPTG was added 3 h before harvesting by centrifugation. Total eIF2α was purified with a final concentration of 1 mM following published methods [120]. After purification, the protein was visualized by western blot using total eIF2α antibody.

Luciferase assays

To examine bioluminescence rhythms arising from strains containing luciferase fusions, 1×10^{6} conidia were inoculated into 96 well microtiter plates containing 150 μl of 1X Vogel's salts, 0.01% glucose, 0.03% arginine, 0.1M quinic acid, 1.5% agar, and 25 μM firefly luciferin (LUNCA-300; Gold Biotechnology, St. Louis, MO), pH 6. After inoculation of conidia (1×10^{5} conidia), the microtiter plate was incubated at 30$_{o}$C in LL for 24 h and

transferred to DD 25$_o$C to obtain bioluminescence recordings using EnVision Xcite Multilabel Reader (PerkinElmer, Life Sciences, Boston, MA), with recordings taken every 90 min over 4–5 days. Raw luciferase activity data were analyzed for period, phase, and amplitude using BioDARE (Biological Data Repository) (http://www.biodare.ed.ac.uk) [121]. Raw reads were normalized to the mean to graph the data.

Statistical analysis

Rhythmic data was fit to a sine wave or a line as previously described [117]. P-values represent the probability that the sine wave best fits the data. The student T-test was used to determine significance in changes in the levels of P-eIF2α when compared between DD28 and DD40, and after induction with 3-AT. Error bars in all graphs represent the SEM from at least 3 independent experiments.

Table 2.1: Primers used for chapter II

Primer name	Used for	Primer sequence$_a$	Restriction site
LUCF1	*Pcpc-3::luc*	5' CTAT<u>GCGGCCGC</u>TGTTGGGCTCGA3'	*Not*I
LUCR1	*Pcpc-3::luc*	5' ATGT<u>GGCGCGCC</u>TATCTTCACAGCAGG3'	*Asc*I
V5F1	*cpc-3::v5::hph*	5' GCTGCGGTCCTCAGTAAGCTC3'	
V5R1	*cpc-3::v5::hph*	5'GCCGCCTCCGCCAGCCGACAAGTCGTAATAGATGC3'	
V5F2	*cpc-3::v5::hph*	5'GACTTGTCGGCTGGCGGAGGCGGCGGAGG3'	

Table 2.1 continued

Primer name	Used for	Primer sequence	Restriction site
V5R2	*cpc-3::v5::hph*	5'CTGCCGACCCGATCACGTAGAATCGAGACCGAGGAGAGG3'	
VF3	*cpc-3::v5::hph*	5'CTCGATTCTACGTGATCGGGTCGGCAGGGT3'	
V5R3	*cpc-3::v5::hph*	5'GCAGCCGAGCTGAGCGAG3'	
V5F4	Validation of endogenous integration of *cpc-3::v5::hph*	5'AGAAGAAGCCTGCCCAACAACA3'	
V5R4	Validation of endogenous integration of *cpc-3::v5::hph*	5'CTGCCGACCCGATCACGTAGAATCGAGACCGAGGAGAGG3'	
tcu1F1	*Ptcu1::cpc-3::v5::hph*	5'CTGAGGCTCCTGCAATGGCC3'	
tcu1R1	*Ptcu1::cpc-3::v5::hph*	5'TTAGGTCGACCCCTGCAGTAGGTCCCACTT3'	
tcu1F2	*Ptcu1::cpc-3::v5::hph*	5'TACTGCAGGGGTCGACCTAAATCTCGGTG3'	
tcu1R2	*Ptcu1::cpc-3::v5::hph*	5'ATCGTCAACCACTACATCGAGA3'	
tcu1F3	*Ptcu1::cpc-3::v5::hph*	5'GGAGACGTACACGGTCGACT3'	
tcu1R3	*Ptcu1::cpc-3::v5::hph*	5'TCCACGCCATGGTTGGGGATGTGTGTGCGA3'	
tcu1F4	Validation of endogenous integration of *Ptcu1::cpc-3*	5'ATCCCCAACCATGGCGTGGAAGAAACCTGC3'	
tcu1R4	Validation of endogenous integration of *Ptcu1::cpc-3*	5'AGCGGCTTCCTCCAGGATATC3'	
cpc-3$_c$F1	*cpc-3$_c$*	5'CTGGAAGCACTTGCATTCCTACAC3'	
cpc-3$_c$R1	*cpc-3$_c$*	5'AGAACTGATCAGGATATTCTCGGGCTTGAGGTC3'	*Bcl*I
cpc-3$_c$F2	*cpc-3$_c$*	5'TATCCTGATCAGTTCTGGACCTGACGGCCT3'	*Bcl*I
cpc-3$_c$R2	*cpc-3$_c$*	5'CACCTCCCCGTCCTGAAATTAT3'	
cpc-3$_c$F3	Validation of endogenous integration of mutated fragment	5'CACCGATTCTTCTGAGCCGAC3'	

Table 2.1 continued

Primer name	Used for	Primer sequence	Restriction site
cpc-3$_c$R3	Validation of endogenous integration of mutated fragment	5'AGGAGTATCGTCAAAGGAGGGA 3'	
	cpc-3 complementation	5'CTGAGGCTCCTGCAATGGCC3'	
cpc-3R1	*cpc-3* complementation	5' GCAGCCGAGCTGAGCGAG3'	
cpc-3F2	Validation of cpc-3 WT copy	5'AGAAGAAGCCTGCCCAACAACA3'	
cpc-3R2	Validation of cpc-3 WT copy	5'CACCTCCCCGTCCTGAAATTAT3'	
alg-11F1	*Palg-11::luc*	5ATCGACTAGTCGTCGGCGACGG GCGTGGTA 3'	*Spe*I
alg-11R1	*Palg-11::luc*	5'CGATCCCGGGACCGGGAAGCGT TATTTATG3'	PciI
alg-11F2	ALG-11::LUC	5'GGGAACCGATGAGGCTGGACTA 3'	
alg-11R2	ALG-11::LUC	5'TGGCGTCCTCCTGTCTGCTCTTG GGCTTTT3'	
alg-11F3	ALG-11::LUC	5'GAGCAGACAGGAGGACGCCAAG AACATCA3'	
alg-11R3	ALG-11::LUC	5'GATGGCGCAATTACACGGCGAT CTTGCCGC3'	
alg-11F4	ALG-11::LUC	5'CGCCGTGTAATTGCGCCATCTAC TGCTCTS3'	
alg-11R4	ALG-11::LUC	5'CGGCTTGGCCTCAGCCTGAGCC 3'	
alg-11F5	Validation of endogenous integration of ALG-11::LUC	5'CAGAATGGGCTTGAGCAGGG3'	
alg-11R5	Validation of endogenous integration of ALG-11::LUC	5'GAAGCTCCTGCTTGGTCTCG3'	
eIF2F1	For cloning eIF2α for purification	5'ACGAGTCATATGATGTCGCTCTC AAACTGC3'	*Nde*I

Table 2.1 continued

Primer name	Used for	Primer sequence	Restriction site
	For cloning eIF2α for purification	5'ATAATC<u>GCGGCCGCG</u>ACGGTCT CGGGGATA3'	*NotI*

_aRestriction sites in primer sequences are underlined

CHAPTER III

INVESTIGATION OF MECHANISMS OF RHYTHMIC CPC-3 ACTIVATION

Introduction

A central mechanism for translation initiation control in eukaryotes involves phosphorylation of the α subunit of eukaryotic Initiation Factor 2 (eIF2α). When eIF2α is phosphorylated, cap-dependent translation initiation is repressed [38, 39]. In fungi and mammals, eIF2α is phosphorylated by GCN2, which is activated by binding of uncharged tRNA during nutrient deprivation, or other stress [40-42, 78]. In *Neurospora crassa*, the circadian clock regulates daily rhythms in the accumulation of phosphorylated eIF2α (P-eIF2α), when cells are grown in constant environmental conditions. However, the mechanism for GCN2 activation by the clock is not known yet.

The homolog of the serine/threonine kinase GCN2 in *N. crassa* is CPC-3 (NCU01187) (**Figure 3.1.A**). Extensive sequence and functional similarity between CPC-3 and the well-studied *S. cerevisiae* GCN2 protein suggested that investigating homologous *N. crassa* components known to activate GCN2 in yeast might provide insight into how the circadian clock rhythmically activates CPC-3. On the basis of known mechanism of GCN2 activation, CPC-3 could be rhythmically activated by several possible mechanisms; rhythmic amino acid levels, amino acyl tRNA synthetases with accompanied rhythms in uncharged tRNA uncharged tRNA, S577 phosphorylation, and effector proteins.

GCN2 is directly activated by binding of uncharged tRNA which depends on change in amino acid levels and/or aminoacyl tRNA synthetases (aaRSs) [45]. Several studies have

reported rhythms in amino acid levels [103, 122, 123]. For instance, arginine, aspartic acid, glycine, histidine, lysine and proline are reported to peak during the day in mouse SCN [103]. This suggested rhythmic amino acids abundance could be the potential driver for rhythmic CPC-3 activation in *N. crassa*. Binding of uncharged tRNA to the histidyl tRNA synthetase domain of GCN2 leads to a conformational change, dimerization, and autophosphorylation of Threonine 882 and 887 (T882, T887) in the kinase domain, which is critical for GCN2 kinase activity [67, 90, 92, 124-126]. In addition to uncharged tRNAs, GCN2 activity is negatively regulated by phosphorylation of Serine 577 (S577) through the Target Of Rapamycin (TOR) pathway. When TOR is active, the negative regulator TAP42 binds to the type 2A-related phosphatase SIT4 and inhibits its activity. This leads to higher levels of S577 phosphorylation which reduces GCN2 activity by decreasing uncharged tRNA binding affinity and maintains low levels of phosphorylated eIF2α [127]. Alternatively, when the TOR pathway is inhibited by amino acid starvation or rapamycin treatment, SIT4 phosphatase is active leading to low levels of S577 phosphorylation and high GCN2 activity which results in high levels of phosphorylated eIF2α [128]. In addition, GCN2 requires the positive effector GCN1 for activation. GCN1 binds to N-terminal RWD domain (RING finger-containing proteins, WD-repeat-containing proteins) of GCN2, and is thought to transfer uncharged tRNA to GCN2 from the A site of the ribosome during stress (**Figure 3.1B**). Furthermore, GCN20, a member of the ATP-binding cassette (ABC) superfamily, binds ribosomes and GCN1 to stabilize interactions between GCN1 and ribosomes [46-48, 91]. In addition to GCN1/GCN20, the Yeast Impact Homolog (YHI)/IMPACT protein functions as a negative regulator of *S. cerevisiae* and mammalian GCN2. IMPACT has a RWD domain, a binding site for GCN1 similar to GCN2, and

represses GCN2 activity by competing for binding with GCN1 [49]. In both mammals and yeast, knock down of IMPACT did not alter P-eIF2α levels. However, overexpression of IMPACT led to low P-eIF2α levels. These data support that IMPACT competes with GCN2 for GCN1 binding and represses GCN2 function, leading to reduced P-eIF2α levels [129]. *N. crassa* CPC-2, like CPC-3, is required for cross pathway control and cell survival during nutrient limitation [130, 131]. In *S. pombe*, CPC-2 is required for autophosphorylation of GCN2 and subsequent eIF2α phosphorylation, suggesting an important role for CPC-2 in GCN2 activation [132].

To determine the mechanism of clock control of *N. crassa* CPC-3 activity, I examined three possible mechanism of rhythmic CPC-3 activation: rhythmicity in amino acid levels which could activate CPC-3 through cycling uncharged tRNA levels, preliminary experiment examining role of tRNA synthetase, S577 phosphorylation, and the role of effector proteins on rhythmic accumulation of P-eIF2α levels. Rhythmic proteomic and ribo-seq data suggested that GCN1 (NCU05803), CPC-2 (NCU05810) and IMF (NCU09542) (Chapter IV) are clock-controlled [22]. Therefore, in this study, I tested the hypothesis that these effector proteins contribute to rhythmic control of CPC-3 activity. I discovered that GCN1 is required for eIF2α phosphorylation; however, deletion of IMF and CPC-2 and S583A, S585A mutations did not alter the levels or rhythms in P-eIF2α accumulation. Furthermore, no rhythmicity in amino acid abundance was detected under conditions where P-eIF2α levels cycle. On examining P-eIF2α levels in a valyl-tRNA synthetase mutant (*un-3*), I found the levels were higher at both times of day (DD28 and DD40) and abolished time of day difference in the mutant indicating important role of

aaRSs in rhythmic CPC-3 activation. Based on these findings and rhythmicity of GCN1, I hypothesize that GCN1 rhythmicity and asRSs drive rhythmic activation of CPC-3.
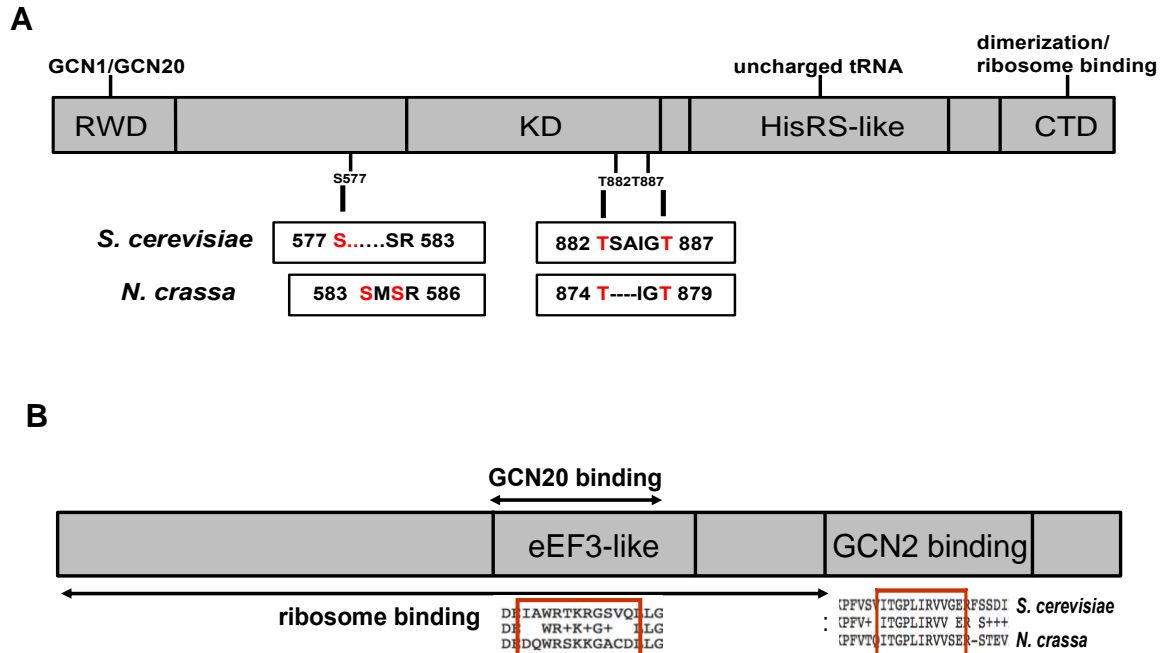
Figure 3.1. Conserved domains of CPC-3 and GCN1. (A) Schematic representation of *S. cerevisiae* GCN2 domains depicting conserved RWD, KD and HisRS-like domains T883 and T887 autophosphorylation sites, and the S577 regulatory phosphorylation site are conserved in *N. crassa.* CPC-3. (B) Schematic representation of GCN1 domains and alignment of key regulatory regions of *S. cerevisiae* and *N. crassa* GCN1, including sequences required to bind ribosomes and GCN2 (red boxed area) [43] (adapted from: Castilho et al., 2014).

Results

Investigation of rhythmic abundance of free amino acids and possible role of aminoacyl-tRNA synthetases in CPC-3 activation

CPC-3 is activated by amino acid starvation, as shown by high P-eIF2α levels (Chapter II) following histidine starvation by the histidine analogue 3-AT (3-amino-triazole) indicating it is a direct sensor of changes in amino acid levels. Previous studies in the mouse SCN and human plasma revealed rhythmic accumulation of amino acid levels [103, 123]. Given the evidence of amino acid rhythmicity in other model systems and CPC-3 activation by histidine starvation, I hypothesized that CPC-3 is rhythmically activated through rhythmic accumulation of amino acids. To test this hypothesis, a circadian time course was performed in WT and Δfrq cells. The samples were harvested using vacuum filtration followed by flash freezing in liquid nitrogen and were processed for HPLC analyses. The amino acid profile looked similar to previously published studies in *N. crassa,* with alanine and glutamine being the most abundant amino acids (**Figure B-1, B-2**) [133]. However, there was no apparent circadian rhythm in amino acid abundance (**Figure 3.2**). This result ruled out the possibility of rhythmic CPC-3 activation by rhythmic changes in amino acid levels under normal physiological conditions.

The possible mechanism of rhythmic CPC-3 activation could be through rhythmic levels of charged vs uncharged tRNAs by rhythmic aminoacyl-tRNA synthetases. Previously published data (RNA-seq, proteomics and preliminary ribosome profiling data) (**Chapter IV**) provide evidence for rhythmic accumulation of different amino-acyl tRNA synthetases (**Table 3.1**) [21, 134]. These tRNA synthetases could rhythmically aminoacylate cognate

tRNAs leading to rhythmic change in charged vs uncharged tRNA levels and hence, rhythmic activation of CPC-3. Therefore, to examine the role of aminoacyl-tRNA synthetase in rhythmic activation of CPC-3, preliminary experiments were carried out by examining P-eIF2α levels in valyl-tRNA synthetase mutant (NCU01965, *un-3*), with decreased valyl-tRNA synthetase activity. Valyl-tRNA synthetase is rhythmic in 2 h RNA-seq time course data **(Figure 3.3A)** peaking during subjective night which corelates with low CPC-3 activity and low P-eIF2α levels. In *un-3,* the expectation was higher P-eIF2α levels due to lower activity of valyl-tRNA synthetase leading to higher accumulation of valyl uncharged tRNAs and eventually high activation of CPC-3. Indeed, in *un-3* mutant, P-eIF2α levels were higher and time of day difference was abolished indicating potential role of aaRS in activating CPC-3 through rhythmic tRNA charging (**Figure 3.3B**). To examine if rhythmic P-eIF2α levels are abolished in *un-3* mutant, P-eIF2α levels were examined in a circadian time course in DD. As expected, P-eIF2α levels were higher and arrhythmic **(Figure 3.3C)** in *un-3*, with no corresponding change in total eIF2α levels **(Figure 3.3D)**. To examine clock-control of valyl-tRNA synthetase, work is under progress to create translational VALYL::LUC reporter in WT and Δfrq cells. If found valyl-tRNA synthetase is clock-controlled, the role of rhythmic valyl-tRNA synthetase levels in rhythmic accumulation of P-eIF2α will be tested by expressing it under copper responsive promoter (*Ptcu1*) [89]. Furthermore, the clock functioned normally in *un-3*, as shown in **Figure 3.3D & F**.
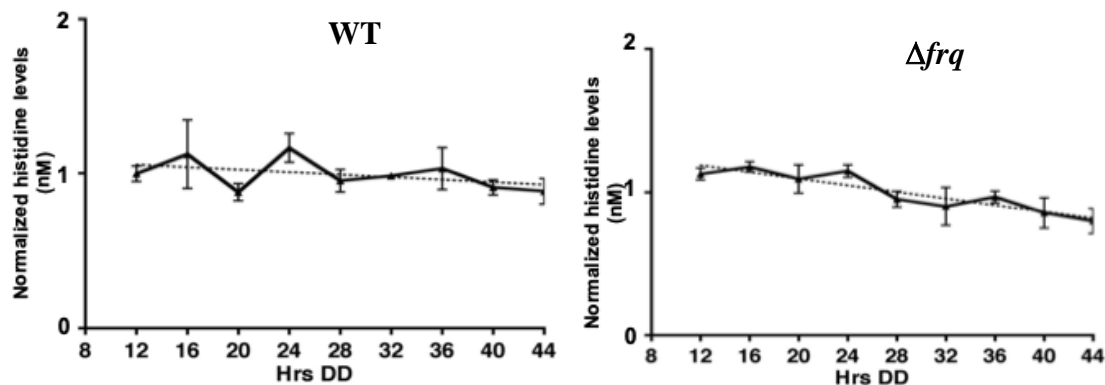
Figure 3.2. No rhythmicity in free amino acid levels. Quantification of free amino acid analysis by HPLC showed no rhythmicity in amino acid abundance. The plots represent histidine levels (nm/10ul) quantified from WT and Δ*frq* cells grown in a circadian time course for 2 days (Hrs DD). The levels were arrhythmic as indicated by a better fit of the data to a line (dotted black line, mean ± SEM, n=3). Similar results were obtained for all amino acids detected. See appendix B.

Table 3.1: Rhythmic aminoacyl-tRNA synthetase with their peak time of expression

Gene ID	Aminoacyl-tRNA synthetase (aaRSs)	Peak Time
NCU00915	Aspartyl	Late night
NCU03030	Tyrosyl	Midday
NCU04449	Prolyl	Late night
NCU06722	Tryptophanyl	Late night
NCU01512	Phenylalanyl	Early morning
NCU06914	Histidyl	Dawn
NCU07926	Glutamyl	Late night
NCU01443	Seryl	Dawn
NCU03759	Methionine	Early morning
NCU01965	Valyl	Late night
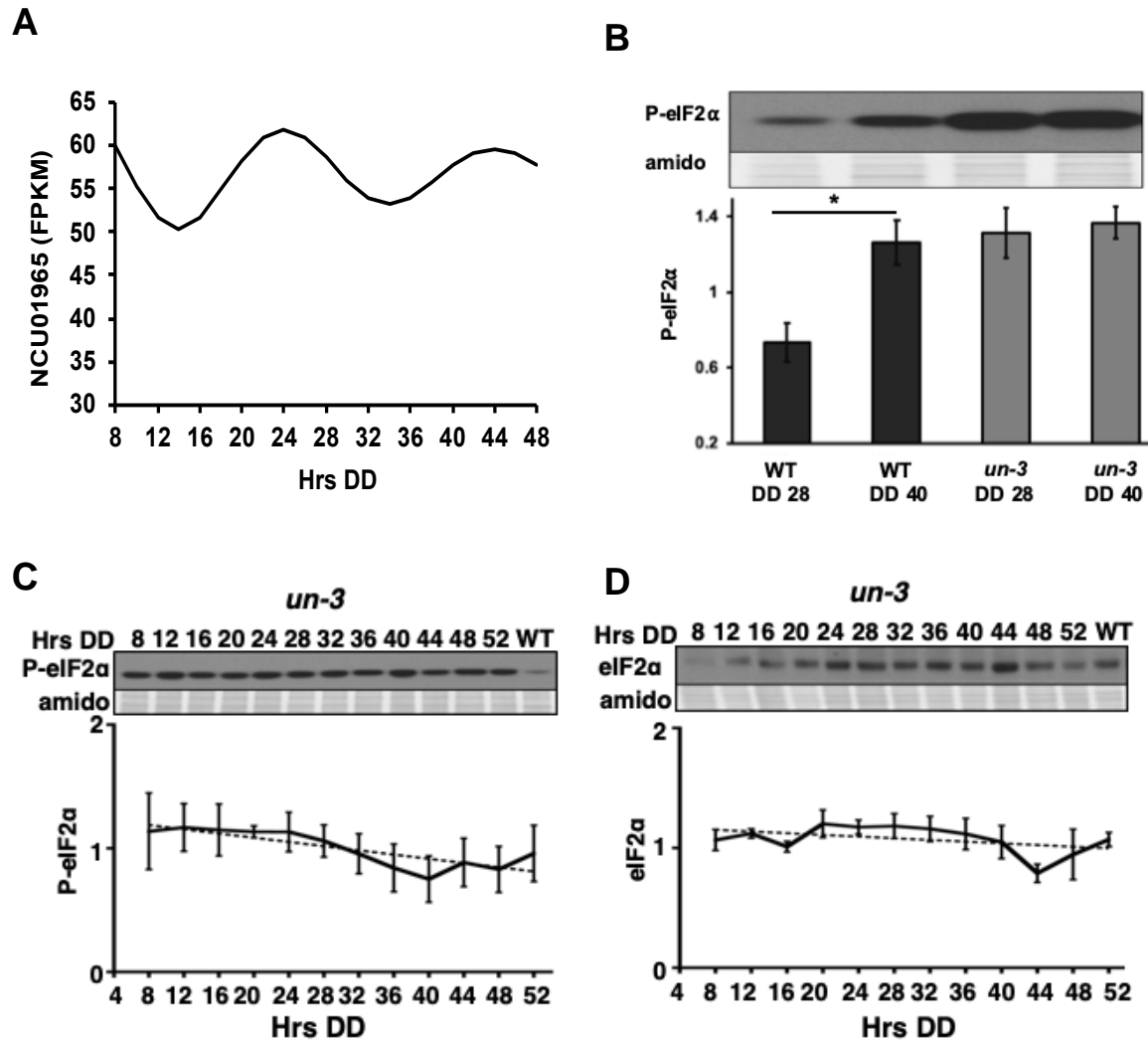
Figure 3.3. Valyl-tRNA synthetase mutant (*un-3*) activates CPC-3 leading to higher and arrhythmic P-eIF2α levels. (A) Plot of FPKM values of valyl-tRNA synthetase (NCU01965) from 2 h time course RNA-seq data. (B) Western blot of protein from the indicated cells harvested in the subjective day (DD40) and night (DD28). The blots were probed with P-eIF2α antibody. Amido stained protein is shown below as a loading control. The graph shows the average signal normalized to total protein loaded; (mean ± SEM, n=3; *p< 0.05, student T-test). Representative western blots of protein extracts isolated from *un-3* strains grown in DD and harvested every 4 h (Hrs DD) over 2 days and probed with anti phospho-specific eIF2α antibody (C) or total eIF2α antibody (D). Both P-eIF2α and total eIF2α, were arrhythmic in *un-3* strain as indicated by a better fit of the data to a line (dotted black lines)

47
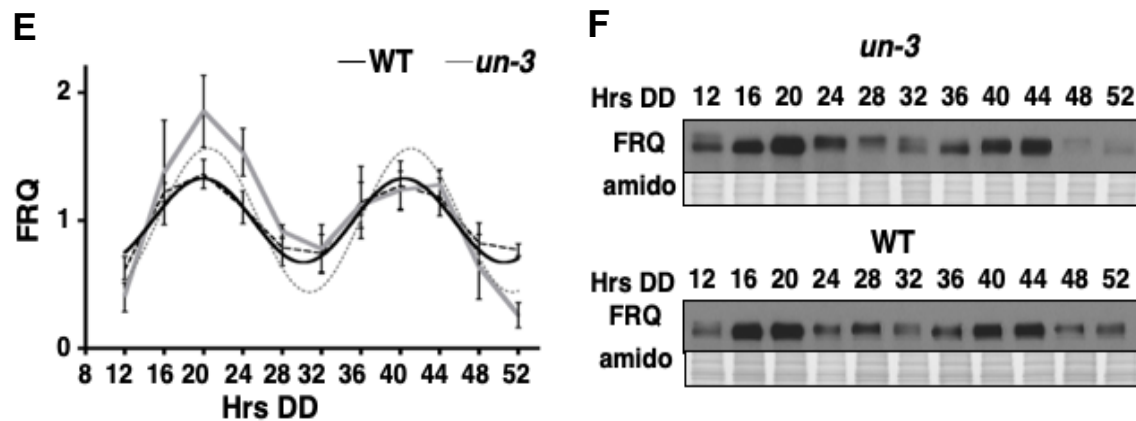
Figure 3.3 continued (E, F) FRQ protein was analyzed by western blot in WT and *un-3* cells and FRQ protein levels are plotted. FRQ rhythmicity in both strains was determined using F-tests of fit of the data to a sine wave (dotted black line, P<0.001). Amido stained protein is shown as a loading control. Plots of the data (mean ± SEM, n=4) show the average FRQ (D) signal normalized to total protein (solid black line).

CPC-3 S583 and S585 residues are not required for rhythmic P-eIF2α accumulation

In *S. cerevisiae*, GCN2 S577 is phosphorylated by an unknown kinase. SIT4 phosphatase, a component of TOR pathway, dephosphorylates S577 leading to GCN2 activation [128]. Mutation of S577 to alanine (S577A) increased GCN2 activity in the absence of amino acid starvation, suggesting that S577 phosphorylation inhibits GCN2 function [127]. S577 is not conserved in CPC-3, but two serine residues S583 and S585 are located near the same region (**Figure 3.1A**). To determine if S583 and S585 are important for CPC-3 function, both residues were mutated to alanine (S583A, S585A) by site-directed mutagenesis. If phosphorylation of S583 and/or 585 inhibits CPC-3 activity, I would expect to observe high P-eIF2α levels. Therefore, P-eIF2α levels were examined

in the mutant strain following growth in constant dark (DD) for 28 h. Similar to *S. cerevisiae*, P-eIF2α levels were higher in *cpc-3S583A, S585A* compared to the levels in WT (**Figure 3.4A**), suggesting a role for S583, and/or S585 phosphorylation in modulating CPC-3 activity. Next, to determine if S583 and/or S585 are necessary for rhythmic P-eIF2α accumulation, P-eIF2α levels in *cpc-3S583A, S585A* were compared to WT cells in a circadian time course experiment (**Figure 3.4B)**. Although P-eIF2α levels were higher in the mutant compared to WT at DD28 and DD40, rhythmicity was not abolished. Therefore, S583 and S585 phosphorylation are not necessary for rhythmic CPC-3 activation when cells are grown in DD.
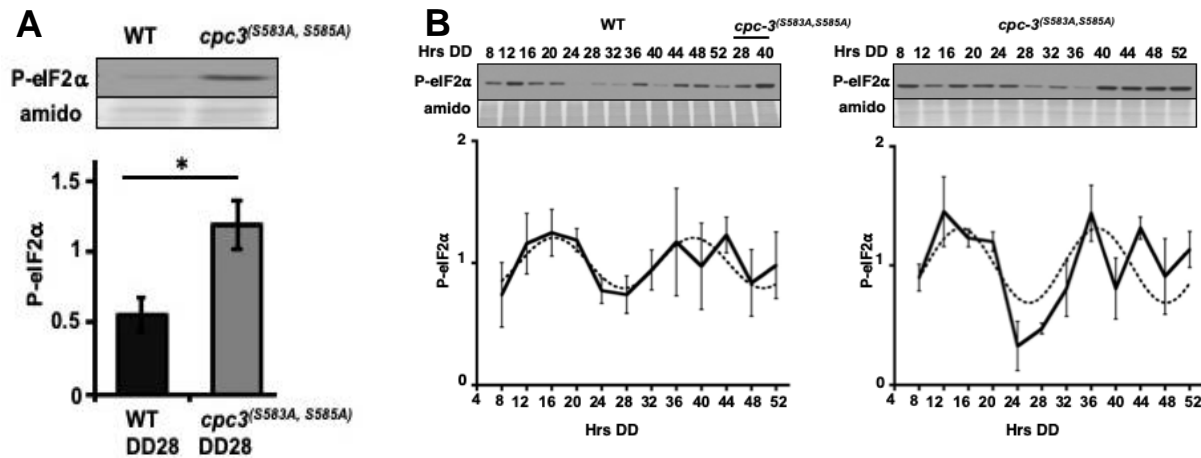
Figure 3.4. S583 and S585 are not required for rhythmic eIF2α phosphorylation. (A) Western blot of protein extracted from *cpc-3S583A, S585A* cells grown in DD for 28h and probed with anti-P-eIF2α antibody. The graph shows the average signal normalized to total protein loaded (mean ± SEM, n=3; *p<0.05, student T-test) (B) Western blot of protein extracted from *cpc-3S583A, S585A* and WT cells grown in DD and harvested every 4h over 2 days (Hrs DD) and probed with anti-P-eIF2α antibody. Rhythmicity test was

determined using F-tests of fit of the data to a sine wave (dotted black line, mean $\pm$ SEM, n=3; p<0.001).

GCN1 is required for eIF2α phosphorylation

To determine if GCN1 is required for eIF2α phosphorylation in *N. crassa*, the levels and phosphorylation status of eIF2α were examined in Δ*gcn1* cells (NCU05803) grown in a circadian time course in DD (**Figure 3.5A**). No P-eIF2α was detected in Δ*gcn1* cells in DD (**Figure 3.4A**), whereas total eIF2α levels were detected in all time points (**Figure 3.4A**) Thus, GCN1 is required for eIF2α phosphorylation, similar to the requirement of GCN1 for GCN2 activation in yeast and mammalian cells (**Chapter 2**) [46]. These data suggested clock control GCN1 levels may be required to rhythmically activate CPC-3 during the subjective day. To confirm that GCN1 is clock-controlled, a GCN1::LUC translational fusion was generated (**Figure 3.4B**). GCN1::LUC levels cycled in WT cells, with a period of 22.6$\pm$0.5 h. The peak in GCN1::LUC occurred during the subjective night, opposite to the daytime peak in CPC-3 and P-eIF2α levels. However, it is possible that GCN1 binds to ribosomes during the late night and transfers uncharged tRNA to CPC-3 During subjective day. GCN1::LUC is currently being crossed to Δ*frq* cells to validate that GCN1 rhythms require a functional clock. GCN1 is not necessary for a functional clock as demonstrated by FRQ::LUC translational fusion as well as FRQ proteins rhythmicity in WT and Δ*gcn1* cells (**Figure 3.4C, A-3**). Similar to Δ*cpc-3* **(CHAPTER II),** Δ*gcn1* grows slowly **(Figure 3.4D)** suggesting important role of GCN1 in growth and development and supports the idea that clock control of P-eIF2α levels provide a growth advantage to *N. crassa* cells.
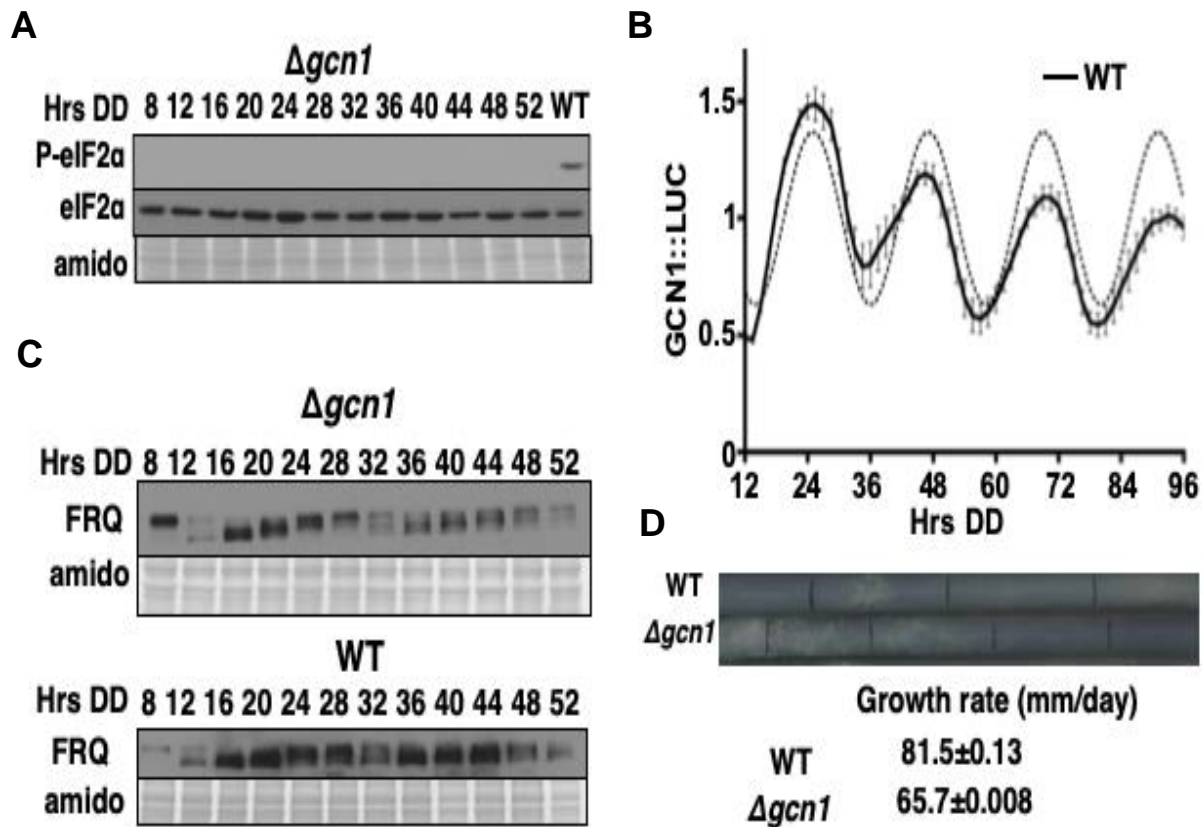
Figure 3.5. GCN1 is required for eIF2α phosphorylation through CPC-3 but not for functional clock. (A) Western blot of protein extracted from Δ*gcn1* cells grown in DD and harvested every 4 h (Hrs DD) over 2 days and probed with phospho-specific eIF2α antibody (top) total eIF2α antibody (bottom). (B) Bioluminescence from a GCN1::LUC translational fusion construct (mean ± SEM, n=7) expressed in WT cells and recorded in DD every 90 min over 4 d (Hrs DD). Rhythmicity test was determined using F-tests of fit of the data to a sine wave (dotted black line, p<0.0001). (C) FRQ protein was analyzed by western blot in Δ*gcn-1* and WT cells. Amido stained protein is shown as loading controls (N=2). (D) Race tube assay of WT *and* Δ*gcn1* grown in DD and marked (black lines) every 24 hrs.

IMF is not required for rhythmic eIF2α phosphorylation

To determine if IMF is required for rhythmic P-eIF2α accumulation in *N. crassa*, P-eIF2α levels were examined in Δ*imf* cells (NCU09542) grown in a circadian time course in DD. There was no change in levels or rhythmicity of P-eIF2α in Δ*imf* cells compared to WT cells **(Figure 3.6A)**. These data are consistent with data showing that deletion of *S. cerevisae* YiH1(the *imf* homolog) had no effect on P-eIF2α levels under physiological growth conditions.

CPC-2 is not required for P- eIF2α rhythmicity

In *N. crassa,* CPC-2 (NCU05810) has been shown to be involved in cross pathway control similar to CPC-3 [130, 131]. In *S. pombe*, CPC-2 regulates GCN2 activity [132]. These data suggested that CPC-2 may be involved in CPC-3 activation in *N. crassa*. To examine if CPC-2 regulates rhythmic CPC-3 activity and downstream cycling P-eIF2α levels, P-eIF2α levels were examined in Δ*cpc-2* cells grown in a circadian time course in DD (**Figure 3.6B**). While the amplitude of P-eIF2α rhythms was dampened in the 1_{st} cycle, P-eIF2α levels were rhythmic when examined over two days, suggesting that CPC-2 is not required for rhythmic accumulation of P-eIF2α.
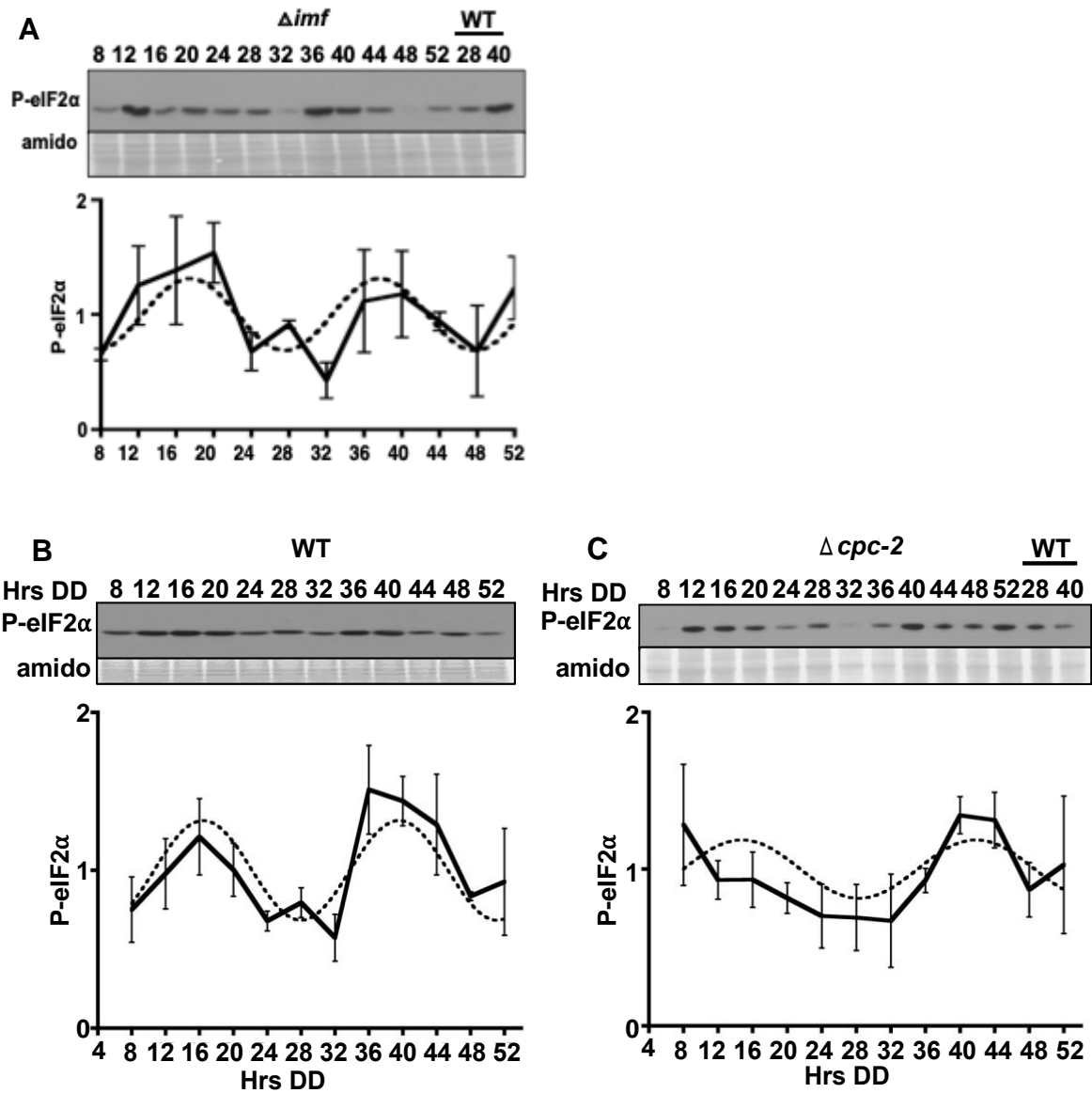
Figure 3.6. IMF and CPC-2 are not required for rhythmic eIF2α phosphorylation. Western blot of protein extracted from (A) Δ*imf* (B) WT and (C) Δ*cpc-2* cells grown in DD and harvested every 4 h (Hrs DD) over 2 days and probed with phospho-specific eIF2α antibody. Amido-stained protein is shown as a loading control. The data are plotted below. Rhythmicity of P-eIF2α was determined by F-tests of fit of the data to a sine wave (black dotted line, mean ± SEM, n=3, p<0.001).

Discussion

I discovered clock control of eIF2α phosphorylation is dependent on rhythmic activation of CPC-3; however, how CPC-3 is rhythmically activated is not known. To understand the mechanism of CPC-3 activation, I examined the rhythmic abundance of amino acids, the potential role of homologs of GCN2 effector proteins GCN1, CPC-2 and IMF on CPC-3 in *N. crassa* and the role of inhibitory phosphorylation of S583 and S585 in the CPC-3 coding sequence.

No rhythms in amino acid abundance were found. In *S. cerevisiae* as well as *N. crassa.*, amino acids such as arginine, histidine, tryptophan, tyrosine, asparagine, leucine, isoleucine are stored in vacuole with the help of vacuolar transporters [135, 136]. Therefore, it is possible that free amino acids extracted might not reflect the overall amino acids abundance in the cell.

Mutation of CPC-3 S583A and S585A led to increased P-eIF2α levels but did not alter rhythmic accumulation of P-eIF2α. In *S. cerevisiae*, GCN2$_{S577A}$ activates GCN2 by increasing its affinity for uncharged tRNA [127]. Similarly, increased P-eIF2α levels in the CPC-3 mutant may be due to increased affinity for uncharged tRNA, whereas rhythmic P-eIF2α accumulation may result from rhythmic accumulation of uncharged tRNAs. Mass spec analysis of CPC-3 by Zhaolan Ding showed that conserved T882 and T887 were phosphorylated when cells were harvested at DD28. However, S583 and S585 sites were not identified. Current experiments are underway by Jana Gomez to mutate the T874 and T879 sites, and then examine possible effects on CPC-3 activity by assessing changes

in P-eIF2α levels or rhythmicity. If there is an effect for any of the phosphorylation-site CPC-3 mutants on P-eIF2α levels or rhythmicity, the identity of kinases and phosphatases will be pursued. One potential regulator of CPC-3 activity is the component of TOR pathway. Several studies have reported crosstalk between the TOR pathway and GCN2 through SIT4 phosphatase [128]. However, the mechanism of this regulation in yeast cells is not known. The homolog of SIT4 in *N. crassa* is PPEI (NCU03436). To examine if PPEI plays any role in P-eIF2α rhythmicity, Zhaolan Ding examined P-eIF2α levels and rhythmicity in $\Delta ppeI$ cells grown in circadian time course in DD. P-eIF2α levels were higher and arrhythmic in $\Delta ppeI$ cells suggesting possible role of PPEI in regulating CPC-3 activity. Based on these data, the working hypothesis is PPEI phosphatase regulates CPC-3 activity by dephosphorylating T874, T879 site leading to rhythmic activation of CPC-3. Alternatively, PPEI can rhythmically de-phosphorylate eIF2α leading to rhythmic P-eIF2α accumulation. These hypotheses are currently being tested.

I found GCN1 is required for CPC-3 activity, CPC-2 and IMF are dispensable for rhythmic P-eIF2α levels, under the growth conditions examined. In addition, preliminary data indicates that GCN1 levels are rhythmic. These data suggested the possibility that rhythmic CPC-3 activity is controlled by rhythm in uncharged tRNA levels, and/or GCN1 levels. Based on observations in yeast cells [91], GCN1 is predicted to interact with CPC-3 at the ribosomes and activates CPC-3 by transferring uncharged tRNA. Thus, rhythms in GCN1 may be sufficient to drive rhythmic CPC-3 activity. In support of this idea, preliminary mass spectroscopy data from enriched ribosome preparations identified CPC-3 as a ribosome-associated protein (Kathrina Castillo and Stephen Caster, unpublished

data). Future experiments to test this possibility will require generating a strain that constitutively expresses GCN1. However, I was surprised to find GCN1 peaks in the late night, rather than during the day when CPC-3 and P-eIF2α levels peak. If indeed GCN1 rhythms are required for CPC-3 activity rhythms, these data support a model in which GCN1 binds to ribosomes in the late night in preparation for transfer of uncharged tRNA to CPC-3 in the early morning and subsequent activation of CPC-3. Future experiments need to be done to test this model, including examining the interaction between GCN1, CPC-3, and ribosomes at different times of day, as well as determining if there is a rhythm in uncharged tRNA levels, and if so, if this is required for rhythmic CPC-3 activity.

CPC-2, which also binds ribosomes [137], is a part of the cross pathway control involved in amino acid starvation response pathway [130]. I found that CPC-2 is not required for rhythmic P-eIF2α levels under the growth conditions used in these experiments. The homolog of CPC-2 in mammalian cells is RACK1 (Receptor for Activated C Kinase), which binds with the small ribosomal subunit and modulates different signaling pathways by interacting with signaling molecules, including Protein Kinase C, eIF6, and mRNA binding proteins [137]. It was suggested that RACK1 regulates the translation of specific mRNAs by integrating signaling pathways with translation [137]. Thus, additional experiments are needed to fully characterize the role of CPC-2 in circadian regulation of translation. Finally, several other possible regulators of GCN2 are known, including GCN20, HSP90/80, Gir2, Reg1, Rgb1 [43]. Homologs for each of these proteins exist in *N. crassa*, and these need to be examined for a possible role in controlling rhythmic CPC-3 activity.

In summary these data suggest that CPC-2, IMF and S853, S585 phosphorylation are not required for rhythmic accumulation of P-eIF2α levels. GCN1 is required for eIF2α phosphorylation and valyl-tRNA synthetase mutant (*un-3*) led to high P-eIF2α levels and abolished time of day difference. These evidences suggest potential role of GCN1 and aminoacyl-tRNA synthetases in rhythmic CPC-3 activation.

Materials and methods

Strains and growth

Vegetative growth conditions and crossing protocols were as previously described [110]. All strains containing the *hph* construct were maintained on Vogel's minimal media [110], supplemented with 200 µg/ml of hygromycin B (#80055-286, VWR, Radner, PA). Strains containing the *bar* cassette were maintained on Vogel's minimal media lacking NH$_4$NO$_3$ and supplemented with 0.5% proline and 200 µg/mL of BASTA (Liberty 280 SL Herbicide, Bayer, NC). Race tube assays were carried out using 1× Vogels salts, 0.1% glucose, 0.17% arginine and 50 µg/mL biotin media as previously described [89]. *N. crassa* wild-type (WT) FGSC#4200 (*mat a*, 74-OR23-IV) or FGSC#2489 (*mat A*, 74-OR23-IV), FGSC#10697 (*mat a*, Δ*cpc-3::hph*), FGSC#81 (mat a, *un-3*), FGSC#14200 (*mat a*, Δ*gcn1::hph*), FGSC#14201 (*mat A*, Δ*gcn1::hph*), FGSC#5810 (Δ*cpc-2::hph*), FGSC#21066 (Δ*imf::hph*) were obtained from the Fungal Genetics Stock Center (FGSC), Kansas State University. The deletions were validated using the primers listed in Table 3.2. The GCN1::LUC translational fusion was generated by 3-way PCR with 1.5 kb *gcn1* ORF (*GCN1* F2 and R2 primers), 1.65kb of *N. crassa* codon-optimized luciferase gene [112] (*GCN1* F3 and R3 primers), 1.0kb of 3' *gcn1* (*gcn1* F4 and R4), and co-transformed

into WT cells (FGSC#4200) with plasmid for pBARGEM7-2 [115] for BASTA selection. The *gcn-1* gene was targeted for replacement by the GCN1::LUC construct via homologous recombination. Basta-resistant transformants were picked, screened for luciferase activity, and endogenous integration of GCN1::LUC was validated using *gcn-1* F5 and R5 primers. To generate the *cpc-3 (S583A, S585A)* mutation, serine 583 and 585 of CPC-3, PCR was used to change the serine to alanine and to create a *KasI* restriction enzyme site. A 4.9kb fragment containing serine mutations was generated by stitching together 1.7kb and 3.17kb of the *cpc-3* ORF with the mutations in overlapping regions at the 3' and 5' ends of the primers, respectively, with primers SF1, SR1, SF2 and SR2. A PCR fragment with the mutation was verified by sequencing, and then co-transformed with plasmid pBARGEM7-2 [115] for BASTA selection into DBP 2717 (CPC-3::V5) cells. Transformants with mutations were validated by restriction digestion of a PCR product from SF3 and SR2 primers with *KasI*. A homokaryon was obtained by microconidia filtration [114].

Circadian time course experiments for western blots were accomplished according to published methods [117]. Briefly, mycelial mats were grown in Vogel's minimal media, 2% glucose, 0.5% arginine, pH 6.0 with shaking in constant light (LL) for 24 h at 30°C. The cultures were then transferred to DD at 25°C to synchronize the clock in all cells to dusk. Tissue was immediately frozen in liquid N_2.

Protein extraction and western blotting

Protein was extracted as previously described [118] with the following modification: the extraction buffer contained 100 mM Tris pH 7.0, 1% SDS, 10 mM NaF, 1 mM PMSF, 1 mM sodium ortho-vanadate, 1 mM β-glycerophosphate, 1X aprotinin (#A1153, SigmaAldrich, St. Louis, MO), 1X leupeptin hemisulfate salt (#L2884, Sigma-Aldrich), and 1X pepstatin A (#P5318, Sigma-Aldrich). Protein concentration was determined using the Bradford assay (#500-0112, Bio-Rad Laboratories, Hercules, CA). Protein samples (50 μg) were separated on 8% SDS/PAGE gels and blotted to an Immobilon-P nitrocellulose membrane (#IPVH00010, Millipore, Billerica, MA) according to standard methods.

The levels of P-eIF2α were detected using rabbit monoclonal anti-EIF2S1 (phospho S51) antibody (Abcam, City State, #32157) diluted 1:5000 in 5% Bovine Serum Albumin (BSA), 1X TBS, 0.1% Tween and anti-rabbit IgG HRP secondary antibody (#170-6515, Bio-Rad, C[118]ity, State) diluted at 1:10000. Total eIF2α levels were detected using rabbit polyclonal anti-EIF2S1 antibody (Abcam #47508) and anti-rabbit IgG HRP secondary antibody diluted at 1:10000. CPC-3::V5 was detected using mouse monoclonal anti-V5 antibody (Invitrogen, #R960-25) diluted 1:5000 in 5% milk, 1XTBST, 0.1% Tween, and anti-mouse IgG HRP (BioRad laboratories,#170-6515) secondary antibody diluted 1:10000. FRQ protein was detected using mouse monoclonal anti-FRQ antibody (from clone 3G11-1B10-E2, a gift from M. Brunner's lab) in 7.5% milk,1XTBS, 0.1% Tween at 1:200 concentration and anti-mouse IgG-HRP (BioRad laboratories, #170-6515) secondary antibody diluted at 1:10000. All proteins, except FRQ, were detected using

chemi-luminescence SuperSignal® West Pico Substrate (#34077, Thermo Scientific,Rockford,IL). FRQ was detected using Supersignal™ West Femto Maximum Sensitivity Substrate (#34085, Thermo Scientific, Rockford,IL). Densitometry was performed using NIH ImageJ software [119] and normalized to protein loading using amido-stained protein.

Luciferase assays

To examine bioluminescence rhythms arising from strains containing *luc*, 1×10^6 conidia were inoculated into 96 well microtiter plates containing 150 µl of 1X Vogel's salts, 0.01% glucose, 0.03% arginine, 0.1M quinic acid, 1.5% agar, and 25 µM firefly luciferin (LUNCA-300;Gold Biotechnology,ST Lousi, MO); pH 6. After inoculation, the microtiter plate was incubated at 30_oC in LL for 24h and transferred to DD 25_oC to obtain bioluminescence recordings using the multi-mode detection EnVision Instrument (PerkinElmer, Life Sciences, Boston, MA). Recordings were taken every 90 min over 4–5 days. Raw luciferase activity data were analyzed for period, phase, and amplitude using BioDARE (Biological Data Repository) (http://www.biodare.ed.ac.uk) [121]. Raw reads were normalized to the mean to graph the data.

Free amino acid quantification

For examining free amino acid levels, circadian time courses were performed in WT and Δ*frq* cells grown in liquid Vogel's 2% glucose medium. The cells were washed with cold water, harvested using vacuum filtration followed by flash freezing in liquid nitrogen, and were crushed into a thin powder using a mortar and pestle. Crushed cells 0.35gm were

boiled in 600μl of distilled water for 20 mins, followed by centrifugation for 15 mins at 14000 rpm. Supernatant 500μl was transferred to VIVASPIN 500 column concentrator (Sartorius Stedim Lab Ltd, Stonehouse, GL10 3UT, UK) with a molecular weight cutoff of 5000 Da followed by centrifuged at 4° for 45 mins at 14000 rpm. The samples were analyzed for free amino acid levels using HPLC in the Protein Chemistry Lab Facility, TAMU. 10μl of the sample was used for quantification.

Statistical analysis

Rhythmic data was fit either to a sine wave or a line as previously described [117]. P-values represent the probability that the sine wave best fits the data. Error bars in all graphs represent the SEM from at least 3 independent experiments, unless otherwise indicated.

Table 3.2: List of primers used for chapter III

Primer name	Used for	Primer sequence	Restriction site
GCN1F1	GCN1 KO validation	5' CAGTTCTACGCTACGTCGTTC 3'	
GCN1R1	FGCN1 KO validation	5' TCCTTGTCAGCTGCCTCGGTC 3'	
GCN1F2	GCN1::LUC construct	5' GATACTCTCCGCGAGGAGCTT 3'	
GCN1R2	GCN1::LUC construct	5' GGCGTCCTCCATATCAAACATCT CCCCCCC3'	

Table 3.2 continued

Primer name	Used for	Primer sequence	Restriction site
GCN1F3	GCN1::LUC construct	5' GAGATGTTTGATATGGAGGACG CCAAGAACATC 3'	
GCN1R3	GCN1::LUC construct	5' CTTCTCCCCCAATTACACGGCGA TCTTGCCGCC3'	
GCN1 F4	GCN1::LUC construct	5' ATCGCCGTGTAATTGGGGGAGA AGAAGAAGATG 3'	
TGCN1R4	GCN1::LUC construct	5' GAAGGTCCTACTGAGCCCACGT 3'	
GCN1 F5	Validation of GCN1::LUC at 5' integration	5' GCGAAGATGCTTTGCCGGACC 3'	
GCN1 R5	Validation of GCN1::LUC at 5' integration	5' TCAGAGCTTGGACTTGCCGCCC TTCT3'	
GCN1 F6	Validation of GCN1::LUC at 3' integration	5' ATGGAGGACGCCAAGAACATCA AGA3'	
GCN1 R6	Validation of GCN1::LUC at 3' integration	5' AGCGATGCCTGCCATTGGCGA 3'	
IMF F1	IMF KO validation	5' CGTCATTGGAGGTGACGAATG3'	
IMF R1	IMF KO validation	5' CAGCGCGAACCTCGG 3'	
CPC-2 F1	CPC-2 KO validation	5' CGATACAAAGCAGTTCCGAGAA 3'	
CPC-2 R1	CPC-2 KO validation	5' AGCCCCAACCCCCAGAA 3'	
SF1	Mutation of S583,585A	5' AGAAGAAGCCTGCCCAACAACA3 '	

Table 3.2 continued

Primer name	Used for	Primer sequence	Restriction site
SR1	Mutation of S583,585A	5' TCCGCG<u>GCCGGCGCC</u>GTCGTG CCTCATCCTCTGCGG 3'	*KasI*
SF2	Mutation of S583,585A	5' CACGAC<u>GGCGCCGGC</u>GGACCC ATGTCTTCCAGA 3'	*KasI*
SR2	Mutation of S583,585A	5' CACCTCCCCGTCCTGAAATTAT3'	
SF3	Validation of S583,585A mutation	5' GCAGCCGAGCTGAGCGAG3'	

aRestriction sites in primer sequences are underlined

CHAPTER IV

THE CIRCADIAN CLOCK REGULATES mRNA TRANSLATION OF SPECIFIC GENES THROUGH RHYTHMIC EIF2α PHOSPHORYLATION

Introduction

Circadian oscillators control rhythmic gene expression that underlies the overt rhythms in behavior and physiology. Initially, studies of rhythmic gene expression focused on understanding the extent and mechanisms of clock regulation of transcript abundance. However, new technology, including quantitative proteomics and metabolite labeling provide the ability to investigate clock regulation of protein and metabolite levels in cells. Importantly, quantitative proteomics studies in mammals and *N. crassa* revealed low correlation between rhythmic mRNA and protein abundance, supporting the importance of post-transcriptional regulation on rhythmic gene expression [22, 29, 30]. Among several possible post-transcriptional mechanisms controlled by the clock, including circadian regulation of mRNA capping, splicing, polyadenylation, and de-adenylation, clock control of mRNA translation is not fully understood [23-27]. In mammals, phosphorylated forms of initiation factors eIF4E, eIF4EBP, eIF4B cycle with a daily rhythm, but how the clock controls initiation, and the effect of clock-controlled phosphorylation of these factors on rhythmic translation is not known [27, 33]. In *N. crassa*, the circadian clock regulates translation elongation by controlling rhythmic activity of elongation factor eEF-2 through the p38 mitogen-activated protein kinase (MAPK) and the downstream effector eEF-2 kinase RCK-2 [34].

64

My studies identified additional evidence for clock regulation of translation through clock control of phosphorylation and inactivation of the highly conserved translation initiation factor eIF2α. I discovered that about 30% of eIF2α is phosphorylated during the subjective day under constant environmental conditions, and that this requires rhythmic activation of the eIF2α kinase CPC-3. Importantly, increased levels of P-eIF2α during the day leads to reduced daytime translation of some, but not all, mRNAs *in vivo*. Yet, the extent of rhythmic control of mRNA translation, and the potential mechanisms of specificity, driven by rhythmic P-eIF2α were not known.

To determine the genome-wide impact of rhythmic P-eIF2α accumulation on translation initiation by the clock in *N. crassa*, we carried out ribosome profiling (ribo-seq) in parallel with RNA-sequencing (RNA-seq) from WT, clock mutant Δ*frq,* and Δ*cpc-3* cells. We identified 554 genes that require rhythmic P-eIF2α accumulation for rhythmic translation. These genes were enriched for proteins involved in amino acid and carbohydrate metabolism, supporting clock regulation of metabolism through rhythmic P-eIF2α.

Results

Time-resolved ribosome profiling in *Neurospora crassa*

To identify mRNAs that are translationally regulated by the clock through rhythmic P-eIF2α, ribo-seq and RNA-seq were carried out in WT, Δ*frq* and Δ*cpc-3* cells grown in constant darkness (DD) and harvested every 4 h over 48 h. The time points were arranged so that all cells were at the same developmental age at the time of harvest (see Materials and Methods and **Figure 4.1A**). Ribo-seq and RNA-seq libraries for each of the

time points were generated [138] from two biological replicates of WT and Δ*frq* cells, and one biological sample of Δ*cpc-3* cells. FRQ protein accumulated rhythmically in WT and Δ*cpc-3* cells, demonstrating that the clock was functional in the samples (**Figure 4.1B).** Two additional replicate libraries of Δ*cpc*-3, and one of WT and Δ*frq* constructed by Dr. Kathrina Castillo, are currently being sequenced and will be used to complete our analyses of the data.

Ribo-seq and RNA-seq reads were mapped to the FungiDB *N. crassa* genome release 38 using HISAT2 [139]. Ribo-seq reads were enriched for lengths between 28-32 nt, consistent with the expected size of ribosome footprints (**Figure 4.1C**) [138]. As expected, the largest fraction of sequence reads mapped to the protein-coding regions (**Figure 4.1D**). Cufflink was used to estimate the relative abundance, FPKMs (fragments per kilobase of transcript per million mapped reads), of ribo-seq footprints and RNA-seq transcripts.

The circadian clock and CPC-3 are required for rhythmic translation of specific mRNAs Using RNA-seq, we identified 1856 genes (18% of expressed mRNAs) with rhythmically accumulating mRNA levels. To determine the effect of clock control of the activity of eIF2α on rhythmic translation, translation efficiency (TE), the ratio of the abundance of translated mRNA to mRNA levels, was calculated using X-tail [140]. Out of the 10,591 genes annotated in *N. crassa*, WT, Δ*frq* and, Δ*cpc-3* had 7875, 7583, and 7964 genes encoding mRNAs with measurable TE, respectively. TEs across the time series for these mRNAs were used to determine rhythmicity using ECHO (Extended Harmonic Circadian

Oscillation) [141]. ECHO examines the fit of the data to 5 types of oscillations: driven, dampened, harmonic, overexpressed and repressed (the last two are not oscillatory). For a gene to be called rhythmic we used a stringent p-value (adjusted p-value) of < 0.05, and with driven, dampened or harmonic oscillations. 913 mRNAs (12%) had rhythmic TE in WT cells and arrhythmic TE in Δfrq cells. Of these 913 mRNAs with rhythmic translation, 554 were arrhythmic in $\Delta cpc\text{-}3$ cells, indicating that they require cycling CPC-3 and eIF2α activity for rhythmic translation initiation (**Figure 4.2**).

To examine the peak phase distribution of the 554 rhythmically-translated mRNAs that require CPC-3 for rhythmicity, a rose plot was generated using phase values derived from JTK cycle [141, 142]. The mRNAs show a bimodal phase distribution, with peak phases of translation occurring primarily at dawn and dusk (**Figure 4.2B**). Given that inhibitory P-eIF2α levels peak during the day, these data suggested that mRNAs that are translated during the day are less sensitive to high P-eIF2α levels.

Genes encoding mRNAs that are rhythmically translated are enriched for amino acid metabolism

To examine the nature of mRNAs that are rhythmically translated, RNA-seq data was compared to the TE profiles. Three distinct categories were identified: 1) in-phase mRNA and TE, 2) out-of-phase rhythmic mRNA and rhythmic TE, and 3) arrhythmic mRNA and
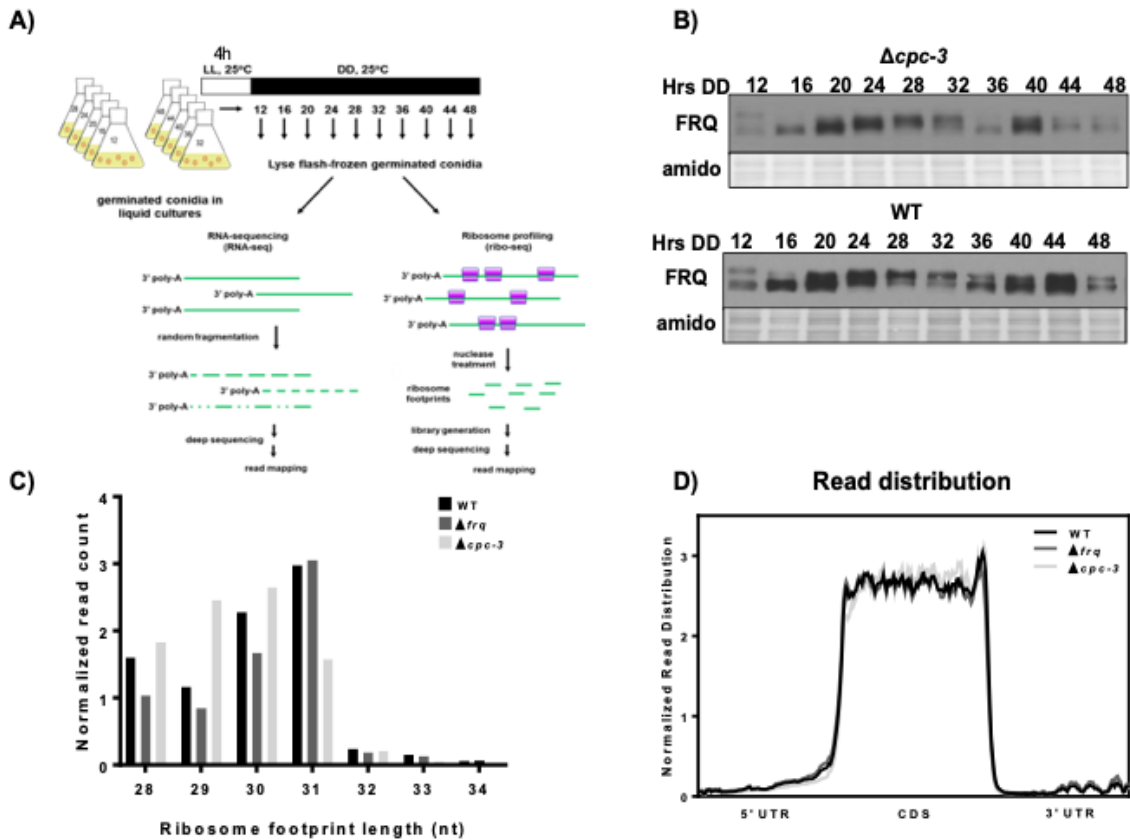
Figure 4.1. Ribosome profiling of *N. crassa* germinated conidia A) Overview of the experimental design of the circadian time course. Samples were grown in the light, and then shifted to dark every 4 hours and harvested at the end of 48 hours. The samples were then prepared for RNA-seq and Ribosome profiling (Ribo-seq). B) FRQ protein was analyzed by western blot from the same WT and Δ*cpc-3* cells harvested for RNA-seq and Ribo-seq. C) Bar graph showing the distribution of sequence length over all sequences for ribosome profiling of the indicated samples. D) Read distribution within 5′ UTRs, coding DNA sequence (CDS), and 3′ UTRs for Ribo-seq in WT (black) and Δ*cpc-3* (grey) showing that most of the reads mapped to CDS.
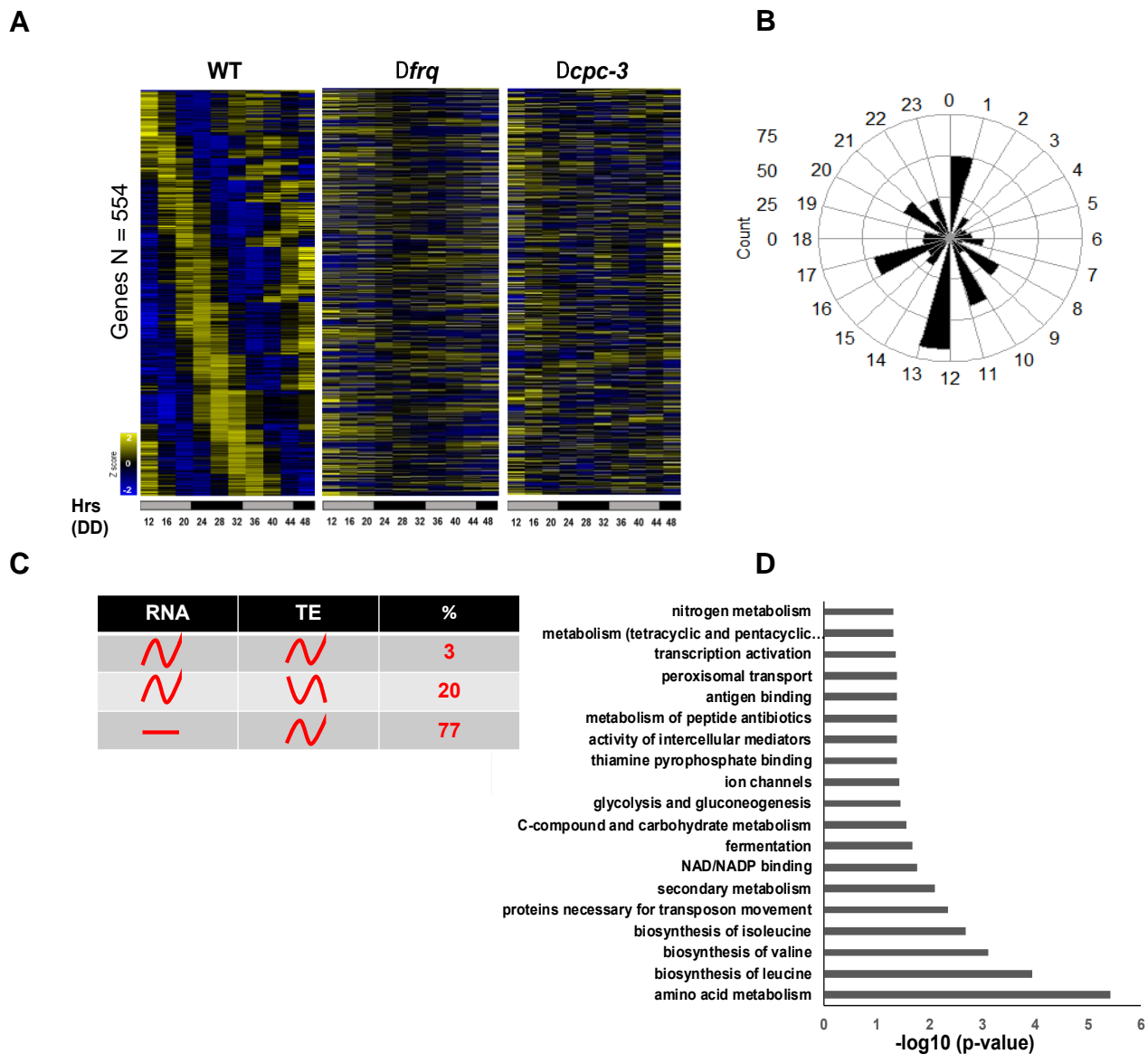
Figure 4.2. The clock, through its control of rhythmic CPC-3 activity, regulates translation of a subset mRNAs. A) Heat maps of 554 mRNAs with rhythmic translational efficiency (TE) in WT cells, and arrhythmic TE in Δ*frq* and Δ*cpc-3* cells. The mRNAs are sorted by the peak phase of translation. TE values are normalized for each heatmap by calculating the z-score [(TE - mean TE)/Std.Dev]. B) Rose plot showing the peak phase distribution of the 554 mRNAs identified in panel A. C) The percent of the 554 mRNAs categorized on the basis of rhythmic mRNA and TE data D) Fun-Cat analysis of genes with arrhythmic mRNA, rhythmic TE in WT cells, and arrhythmic TE in Δ*cpc-3* cells. The categories shown are enriched in the genome (p<0.05).

rhythmic TE (**Figure 4.2C**). To better understand rhythmic translation, we focused further analyses on the genes that synthesize arrhythmic mRNA levels but have rhythmic TE that requires CPC-3. Of the 554 genes with CPC-3-depenent rhythmic TE, 426 genes (77%) were derived from arrhythmic mRNA.

Functional analysis of the 426 genes using Fun Cat [143] revealed enrichment for different metabolic processes, including amino acid metabolism, glycolysis and gluconeogenesis (carbohydrate metabolism), and secondary metabolism (**Figure 4.2D**). To determine the function of these genes in amino acid metabolism, KEGG pathway mapping analysis was performed. Significant enrichment for components of several amino acid biosynthetic pathways was observed (**Figure 4.3A**). TE plots of mRNA expressed from genes NCU01412 (*pro-3*), NCU01652 (*met-21*), NCU04303 (*asn-1*), NCU04579 (*ilv-1*) required for proline, methionine, asparagine, and isoleucine synthesis, respectively, are shown (**Figure 4.3B**). The peak phase of translation for each of these mRNAs occurs during the subjective night, corresponding to the time of day when P-eIF2α are low (Chapter 2), and suggests translation of these mRNAs is sensitive to high levels of P-eIF2α. In addition to amino acid metabolism, KEGG revealed enrichment for genes involved in the Tricarboxylic Acid cycle (TCA cycle) (**Figure 4.3D**). Rhythmic TE profiles for mRNAs encoding proteins in the TCA cycle NCU02438 (*tca-19*), NCU09810 (*suc-4*), NCU01227 (*tca-8*) are shown (**Figure 4.3C**). The intermediates of glycolysis, the TCA cycle, and the pentose-phosphate pathway are used as precursors for amino acid synthesis [144]. While I previously showed that the levels of free amino acid do not cycle

in abundance in Chapter III, these data support the idea that the clock coordinates increased amino acid production with increased translation during the night.
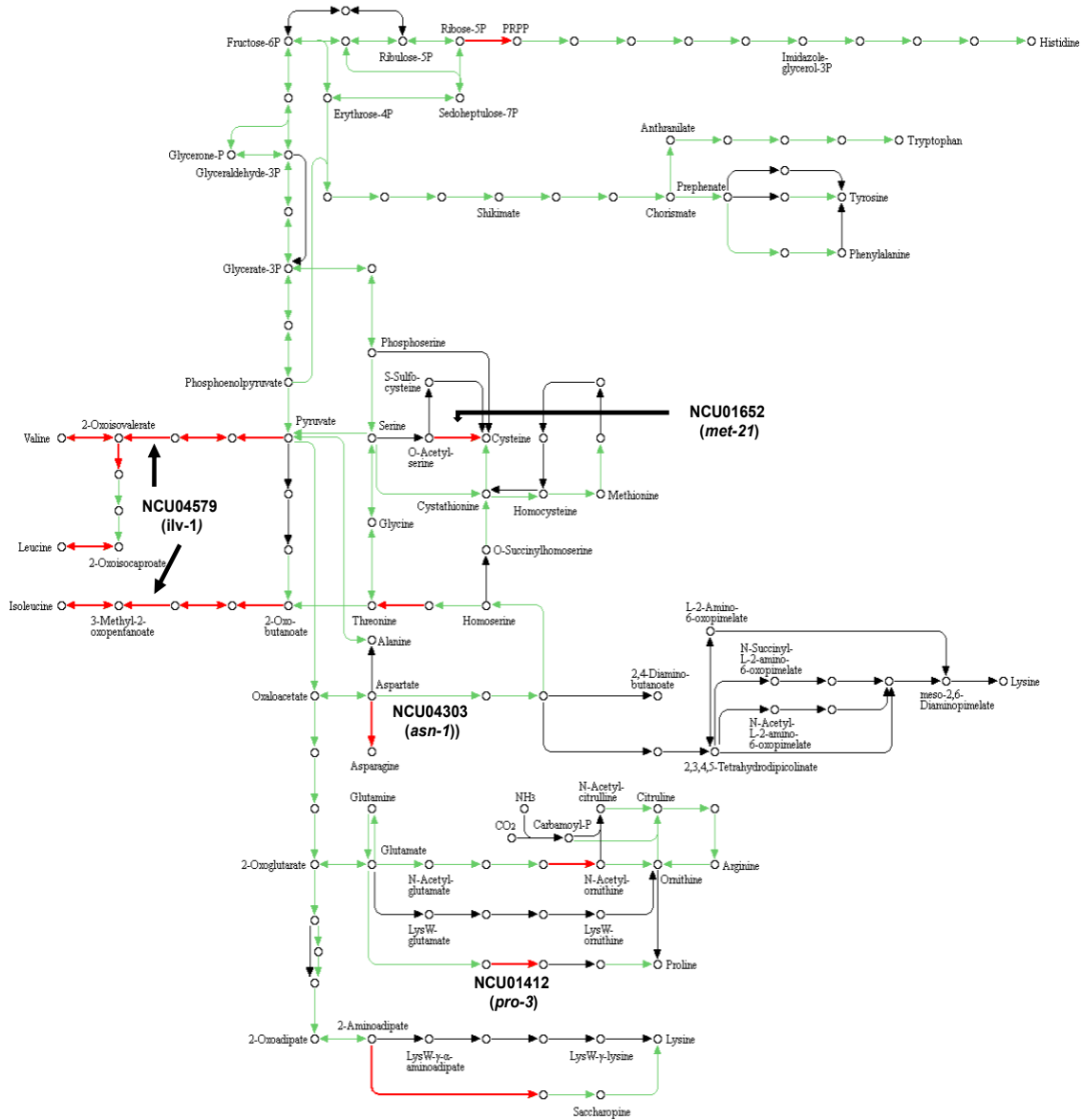
Figure 4.3. Rhythmically translated mRNAs are enriched in amino acid metabolism. A) KEGG pathway analysis of rhythmically translated genes involved in amino acid biosynthetic pathways (red lines).
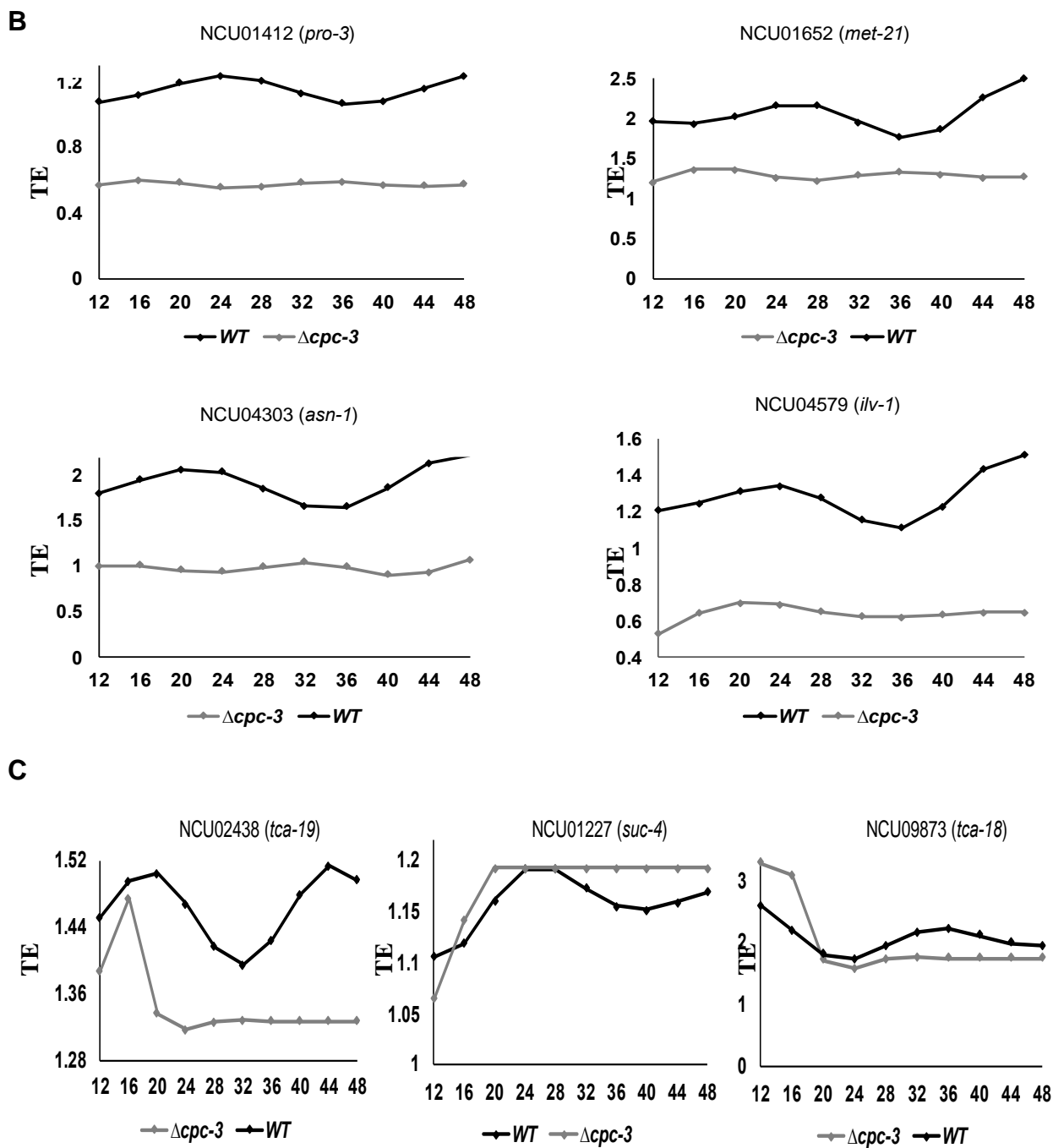
Figure 4.3 continued B) TE values calculated from X-tail of genes involved in amino acid biosynthetic pathways are plotted. C) TE values calculated from X-tail of genes involved in the TCA cycle are plotted (p<0.05).

D
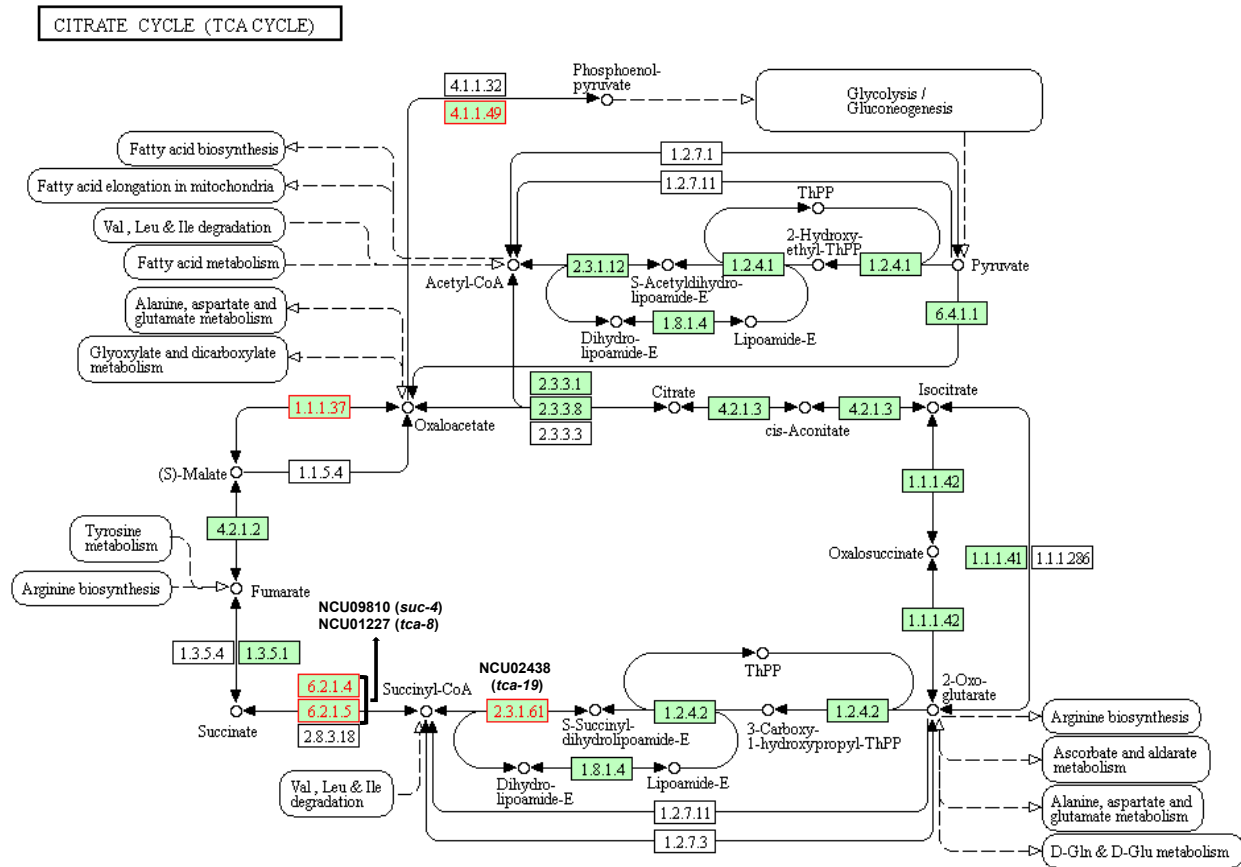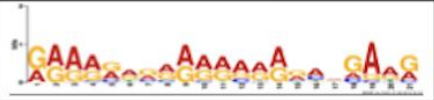
Figure 4.3 continued D) KEGG pathway analysis of rhythmically translated genes involved in the TCA cycle (shown in red).

Identification of sequence motifs in rhythmically translated mRNAs

Conserved motifs or structured 5' UTR sequences have been identified in mRNAs that are more sensitive or resistant to a change in the activity of initiation factors [53, 145]. For example, mTOR sensitive mRNAs are enriched with 5' terminal oligopyrimidine (5' TOP) and/or a 5' pyrimidine rich translational element (5' PRTE motif) [53]. TOP motif consists of 5-15 pyrimidines located close to 5' cap structure and are highly enriched in genes

encoding translational components such as ribosomal proteins, elongation factor (eEF-2) [146]. Genes with these motifs are translationally regulated either positively or negatively by different RNA binding proteins such as La-related protein 1 (LARP1) and micro-RNA [147, 148]. LARP1 binds to TOP motif and represses the translation of respective genes in response to TOR inhibition [148]. Further, there is evidence of clock-controlled translational regulation of genes with TOP motifs through TOR pathway [149]. Of 426 genes controlled at the translational level by CPC-3, 193 genes peaked during day suggesting they are resistant to high P-eIF2α levels and 233 peaked during night suggesting they are sensitive to high P-eIF2α during day. To investigate what makes these genes sensitive/resistant to changes in P-eIF2α, we examined if mRNAs under P-eIF2α/CPC-3 translation regulation have conserved motifs by carrying out MEME analysis [150] on the 426 clock- and CPC-3-dependent rhythmically translated mRNAs. Using 500bp in the 5' UTR region as input, a statistically significant T-rich motif was identified on 113-day peaking genes and A-rich motif on 189-night peaking genes (p<0.05) (**Figure 4.4A**). For example, a T-rich motif was identified in the 5' UTR of NCU06679 (*alg11*) gene which was shown to be translationally clock-controlled through CPC-3/ P-eIF2α (see **Chapter II, Figure 2.6**) (**Figure 4.4B**). In addition, about 13% (1330 genes) of *N. crassa* mRNAs have a potential upstream ORF (uORF) identified by RiboCode, which when translated can reduce expression from the main ORF (Michael Werry, Dr. Matthew Sach, unpublished data) [151]. On comparing those 1330 genes with the 426 genes dependent on CPC-3/P-eIF2α for translation, 81 have predicted uORFs. Future experiments will determine a possible functional role for these motifs and predicted uORFs in circadian translational regulation.

A)

Day-peaking genes		Night-peaking genes	
Sequence	No. of genes	Sequence	No. of genes
	113/193		189/233

E-value = 2.4e-145   E-value = 2.7e -0.77

B)

NCU06779 – *alg11*
α-1,2-mannosyltransferase

CGTTTAGCCGTTACTCCCTTTCTGTTTTC

ATG
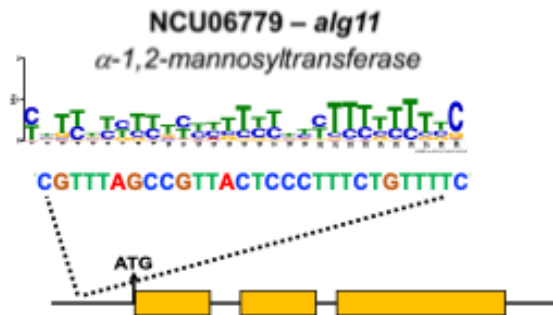
Figure 4.4. Predicted MEME motif present in CPC-3 controlled genes. A) Predicted MEME motif present in the 5' UTR of mRNAs that are rhythmically translated under control of CPC-3. B) The predicted motif lies within the 5' UTR of *alg11* mRNA.

Discussion

Several studies revealed rhythms in protein abundance arising from arrhythmic mRNAs, providing evidence to support clock control of posttranscriptional events, including mRNA translation [22, 29, 30]. In *N. crassa,* the clock regulates the activity of eIF2α (Chapter 2) and eEF-2 [35], both of which are conserved in eukaryotes, and may support widespread rhythms in mRNA translation and protein abundance. To determine the extent of clock

control of mRNA translation initation in *N. crassa,* circadian ribo-seq and RNA-seq was performed in WT, clock mutant Δ*frq*, and eIF2α kinase mutant Δ*cpc-3* cells.

Comparing our rhythmic RNA-seq dataset with published data, we found that ~18% of expressed mRNA cycles in WT cells and not in clock mutant Δ*frq*, compared to 40% of expressed mRNAs in other rhythmic RNA-seq data sets, with very small number of overlapping mRNAs (17 genes) [21, 134]. These differences likely reflect different culture conditions used, which may lead to differences in mRNA expression levels. Our study used translationally active germinating conidia to enhance our ribo-seq analyses [152], and a 4 h time resolution, versus published studies that used mycelia with a 2 h resolution [21, 134], and in one study Bird's media [21]. It is recommended in genome wide time-series analyses to use 2 h time resolution sampling to increase the number of rhythmic genes [153, 154]. However, due to cost limitations, it wasn't feasible to perform 2 h time resolution in our study. In addition to differences in the culture conditions used, differences in rhythmicity analysis using different programs such as ARSER and JTK cycle in the published data vs ECHO in our data analysis could also give different results [21, 134]. Experiments are currently underway to compare translation regulation by the clock between germinating conidia and mycelia. These data, from 3 biological replicates, along with the current study, will provide sufficient replicates for improved statistical analyses and will form the basis of a manuscript that will be submitted for publication.

About ~12% of the sampled *N. crassa* mRNAs (913 mRNAs) had rhythmic TE in WT cells, compared to 1274 proteins that were identified as clock-controlled in a circadian

proteomics study [22]. These data suggested that protein rhythms can arise from rhythmically accumulating mRNA and constitutive translation, rhythms in protein turnover, and /or other post-transcriptional mechanisms. More than half of the mRNAs (554 mRNAs) with rhythmic TE were arrhythmic in Δ*cpc-3* cells, supporting that rhythmic translation initiation plays a central role in rhythmic protein accumulation. The remaining mRNAs with rhythmic translation in Δ*cpc-3* cells may be controlled by rhythmic eEF-2 activity, which peaks at night, or other translation factors. Ribo-seq experiments in a deletion of the eEF-2 kinase RCK-2 are currently in progress to test this idea, and to determine if common sets of mRNAs require both rhythmic initiation and elongation for cycling protein accumulation.

A rhythmic proteome study in *N. crassa* reported that 521 proteins were rhythmic with corresponding arrhythmic mRNA [22]. This study examined the role of ubiquitin ligases that could confer to rhythmicity through protein turnover and found that protein turnover did not significantly impact protein rhythmicity. Therefore, they concluded that protein rhythms that arise from non-cycling mRNAs are the result of translational regulation. In support of this idea, they found that several proteins involved in translation cycle in abundance, including ribosomal proteins, and translation initiation and elongation factors. [32, 33]. Similarly, rhythms in the abundance of initiation factors including eIF4E, eIF4G, eIF4B, and ribosomal proteins RPL5, RPL23, RPL32, RPLP0 have been reported in higher eukaryotes [32].

We discovered that at least 30% of eIF2α is phosphorylated and inactivated during the subjective day, under control of the circadian clock, and this is sufficient to reduce *luc* mRNA translation in cell-free translation extracts (Chapter 2). Based on these and other data, we hypothesized that P-eIF2α-driven rhythmic translation would peak at night for most mRNAs, when P-eIF2α levels are low. Instead, we discovered a bimodal phase distribution for TE rhythms that require CPC-3 for rhythmicity, with translation of most mRNAs peaking either at the dawn to dusk or dusk to dawn transition. Based on our findings, mRNAs, that are translated at night may be more sensitive to increased P-eIF2α levels and vice versa. Using MEME, a consensus sequence present in the 5' UTR of mRNAs that are preferentially translated day or was identified. If and how these sequences influence translation needs further experimentation. Genes with different motifs are regulated differently in response to change in levels or activity of different initiation factors. For instance, mRNAs with Translation Initiator Short 5' UTR motifs (TISU) (SAASATGGCGGC consensus sequence) are more sensitive to change in levels of translation initiation factor eIF1 and are actively translated during stress via non-canonical scanning initiation [155]. A study in mice, showed that clock-controlled translationally regulated mRNAs were enriched with 5' TOP and TISU motifs [149]. Genes with TOP motif peaked during night in response to TORC1 activity [149] which is similar to our data of day-peaking mRNAs with T-rich motif when CPC-3 is active suggesting similar mechanism of regulation.

The structure of mRNA in the 5' end can influence translation, including Internal Ribosome Entry Sites (IRES) that promotes internal initiation [156, 157]. However,

identifying IRES elements is challenging due to a lack of sequence specificity [158]. About 13% of *N. crassa* 5' UTR's have upstream ORFs (uORFs) which were identified by using Ribocode [151] (Micheal Werry, Dr. Matthew Sachs, unpublished data). Comparing 426 genes that are translationally regulated by CPC-3 with the predicted uORFs list, 81 had predicted uORFs. In the future we will examine the role of translation of the uORFs in select mRNAs by determining how mutations/deletions of the uORF alter rhythmic translation of the main ORF *in vitro* and *in vivo*.

In addition to rhythmic translation initiation and elongation, rhythmic RNA binding proteins may drive rhythmic translation. For example, the Iron Binding Protein binds to mRNAs with Iron-Responsive Elements (IRE motif- YRCACCCR) to regulate translation of mRNAs involved in iron metabolism. Binding of the iron binding protein to target mRNA impedes association of the pre-initiation complex and mRNA [159]. On performing motif scanning analysis FIMO using MEME suite on 426 CPC-3 regulated genes, 13 of them showed significant enrichment for IRE motif (p<0.001) [160]. Among those, one of the interesting genes with IRE motif is phosphoenol pyruvate carboxykinase, NCU09873 (PEPCK). PEPCK is highly conserved enzyme involved in gluconeogenesis [161, 162]. Crosstalk between clock, gluconeogenesis and iron metabolism has been well documented [163]. In *S. cerevisiae,* crosstalk between iron and amino acid homeostasis through GCN2-eIF2α has been shown [164]. It will be interesting to follow upon if clock regulation of eIF2α through CPC-3 is one of the signaling pathway linking circadian clock, iron homeostasis and gluconeogenesis. Furthermore, in U2OS cell lines, the rhythmically accumulating Lymphocyte specific protein 1 (LSP1) RNA-binding protein targets mRNAs

to P-bodies [165]. This could lead to rhythmic sequestration of mRNAs. These possibilities for alternative mechanisms for rhythmic mRNA translation provide opportunities for investigation in the future.

mRNA translation is energetically costly to cells; therefore, it makes sense for organisms to temporally organize translation to times of day when energy levels are high, and stress is low. As such, this work provides a major step towards understanding the mechanisms by which mRNAs are selected for translation under control by the clock, including those that peak in translation during the day when inhibitory levels of P-eIF2α and P-eEF2 peak, versus those that peak at night. Because translation mechanisms are highly conserved, and up to half of rhythmic proteins arise from arrhythmic mRNAs in fungi and mammals [29, 30], our studies in *N. crassa* will likely provide critical information on how the clock controls mRNA translation in higher eukaryotes.

Materials and methods

Strains and growth conditions

Vegetative growth conditions were as previously described [110]. All strains containing the *hph* construct were maintained on Vogel's minimal media [110], supplemented with 200 µg/mL of hygromycin B (#80055-286, VWR, Radner, PA). Strains containing the *bar* cassette were maintained on Vogel's minimal media lacking NH_4NO_3 and supplemented with 0.5% proline and 200 µg/mL of BASTA (Liberty 280 SL Herbicide, Bayer, NC). *N. crassa* wild-type (WT) FGSC#4200 (*mat a*, 74-OR23-IV) or FGSC#2489 (*mat A*, 74-OR23-IV), and FGSC#10697 (*mat a*, Δ*cpc-3::hph*) were obtained from the Fungal

Genetics Stock Center (FGSC, Kansas State University). DBP 1320 (*Δfrq::bar*) was previously generated [111]. For RNA-seq and ribo-seq, conidia were grown on slants containing 1X Vogel's salts and 2% glucose (V2G) incubated at 30°C in constant light (LL). Conidia were resuspended in V2G, counted using hematocytometer and $1X10^5$ conidia/ml was inoculated into 500ml of liquid V2G media. The cultures were grown in LL at 25°C with shaking at 110 rpm and shifted to DD 25°C every four hours for their respective time points and were harvested after 48 h of growth. The cells were harvested by vacuum filtration, washed with Milli-Q ice cold water and flash frozen in liquid nitrogen.

Protein extraction and western blotting

For western blot, protein was extracted as previously described [118] with the following modification: the extraction buffer contained 100 mM Tris pH 7.0, 1% SDS, 10 mM NaF, 1 mM PMSF, 1 mM sodium ortho-vanadate, 1 mM β-glycerophosphate, 1X aprotinin (#A1153, SigmaAldrich, St. Louis, MO), 1X leupeptin hemisulfate salt (#L2884, Sigma-Aldrich), and 1X pepstatin A (#P5318, Sigma-Aldrich). Protein concentration was determined using the Bradford assay (#500-0112, Bio-Rad Laboratories, Hercules, CA). Protein samples (50 μg) were separated on 8% SDS/PAGE gels and blotted to an Immobilon-P nitrocellulose membrane (#IPVH00010, Millipore, Billerica, MA) according to standard methods. FRQ protein was detected using mouse monoclonal anti-FRQ antibody (from clone 3G11-1B10-E2, a gift from M. Brunner's lab) in 7.5% milk,1XTBS, 0.1% Tween at 1:200 concentration and anti-mouse IgG-HRP (BioRad laboratories, #170-6515) secondary antibody diluted at 1:10000. FRQ was detected using Supersignal™ West Femto Maximum Sensitivity Substrate (#34085, Thermo Scientific,

Rockford, IL). Densitometry was performed using NIH ImageJ software [119] and normalized to protein loading using amido-stained protein.

RNA-seq

Total RNA was isolated from frozen mycelia, and poly(A) mRNA was purified from 125 µg of total RNA as previously described (134, 147) using oligo d(T)25 magnetic beads (#S1419S, New England Biolabs, Ipswich, MA). Isolated mRNA was enriched using Epicentre Terminator^{TM} 5'-phosphate-dependent exonuclease (#TER51020, Illumina (Epicentre), Madison, WI). cDNA and RNA-seq libraries were prepared as previously described (134, 147).

Ribosome profiling

Lysis beads were made using 20 mM Tris-Cl (pH 7.5), 150 mM NaCl, 5 mM MgCl2, 1 mM DTT, 1% Triton X-100, 25 U/mL Turbo DNase (#AM2238, Thermo Fisher Scientific Inc., Waltham, MA), and 100 µg/mL cycloheximide in advance using liquid nitrogen and stored at -80°. Frozen mycelia (2gm) and lysis beads (1:1 ratio) were pulverized using a SPEX CertiPrep 6850 freezer/mill (#6850, SPEX Sample Prep, Metuchen, NJ) using a 10 min pre-cooling cycle, followed by 3 X 2 min grind cycles, with 1 min cooling between each cycle. Lysed samples were collected in ice-chilled polycarbonate tubes, thawed on ice for 45 mins, and centrifuged at 4° for 15 mins at 16,000 rpm using a JA-200 rotor. 2ml supernatant was collected in a sterile tube and A260 was measured using a Varian Cary 50 UV-Vis Spectrophotometer (Agilent Technologies, Santa Clara, CA). For processing, 50 A260 units of sample was mixed with lysis buffer (20 mM Tris-Cl (pH 7.5), 150 mM

NaCl, 5 mM MgCl2, 1 mM DTT, 1% Triton X-100, 25 U/mL Turbo DNase, 100 µg/mL cycloheximide) to bring the total volume to 300ul. Samples were then treated with 1.875 RNAse I (#AM2294, Thermo Fisher Scientific Inc., Waltham, MA) for 45 min at RT with gentle mixing. The extract was immediately transferred to a pre-chilled 3.5 mL, 13 X 51 mm, polycarbonate ultracentrifuge tube, 0.9 mL of a 1M sucrose cushion underlay was added, and ribosomes were pelleted by centrifugation at 70,000 rpm at 4° C for 4h. All subsequent steps followed the method of Ingolia et al., 2012, except the rRNA depletion step was not performed. Instead, after heat-inactivation of CircLigase (#CL4111K, Illumina (Epicentre), Madison, WI), 2.0 µL of GlycoBlue^{TM} (#AM9515, Thermo Fisher Scientific Inc., Waltham, MA), 6.0 µL 5 M NaCl, 74 µL of DEPC water, and 150 µL of isopropanol were added to each tube and precipitation was carried out overnight at -80° C. The cDNA generated from ribosome protected RNA was pelleted by centrifugation for 30 min at 20,000 g at 4° C; samples were washed with 70% ethanol and allowed to air-dry for 10 min. The pellet was then resuspended in 5.0 µL of 10 mM Tris (pH 8.0), and PCR amplification/barcode addition was performed as described (149). The concentration of the sequencing libraries was determined and checked for quality on an Agilent 2100 Bioanalyzer using a DNA high-sensitivity chip (Agilent, Santa Clara, CA) per the manufacturer's instructions. Sequencing was carried out on an Illumina HiSeq 3000 (Illumina, Inc., San Diego, CA).

Data analysis

Reads were processed for RNA and Ribo seq reads (**Figure 4.5**). For RNA seq data, FPKM was calculated using cufflink [166]. For ribo-seq data, cut adapt was performed to

remove the linker sequence [167]. Read qualities and length were checked using FastQC [168]. After quality checking, reads were trimmed by Trimmomatic [169] using a 28-34 nt cutoff and were mapped to *N. crassa* assembly 38 using Hisat2 [139]. BAM files from Hisat2 were then processed through HTseq-count [170] to get read counts for each mRNA that maps uniquely to single gene. Read counts were used as input for X-tail to calculate TE [140]. ECHO, a recently developed R-package program was used to determine the rhythmicity [141]. Heatmaps and rose plots were generated from R-studio using phase value from JTK cycle [171].
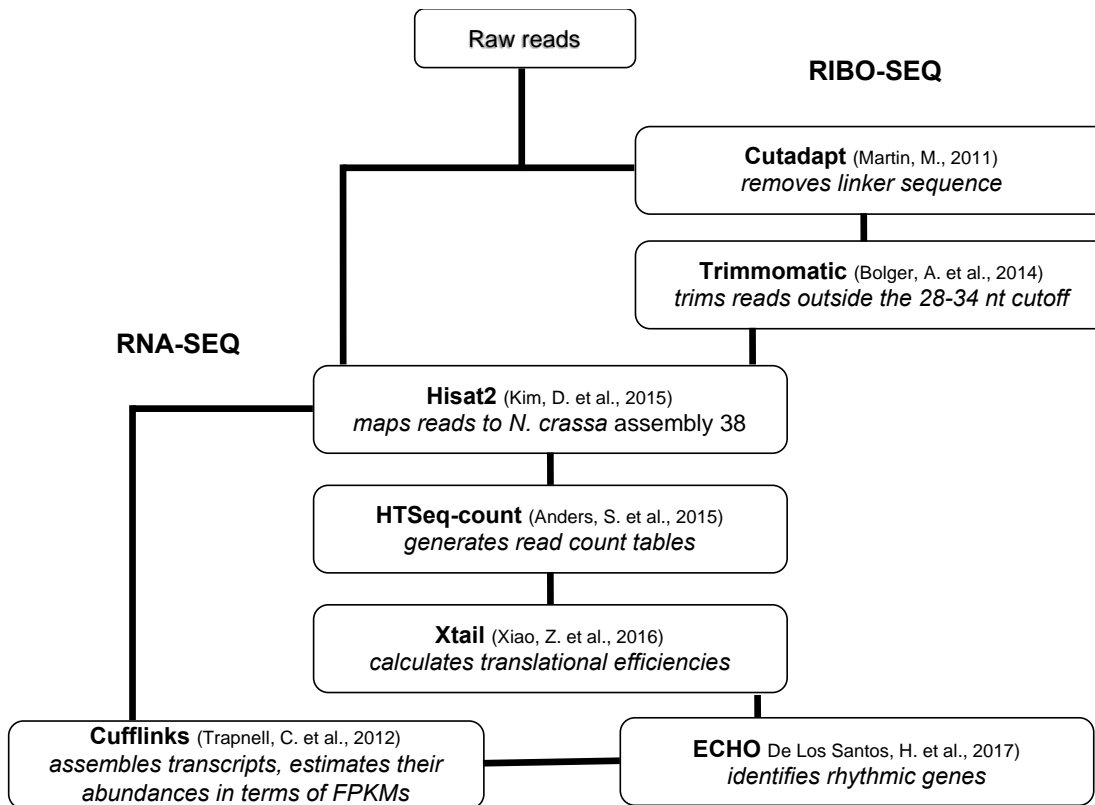
Figure 4.5. Pipeline used for data processing and analysis of RNA-seq and ribo-seq data.

CHAPTER V

SUMMARY AND FUTURE DIRECTIONS

Protein synthesis is the end product of gene expression and needs to be tightly regulated to maintain a healthy organism [31, 38]. The widespread impact of the circadian clock on rhythmic mRNA and protein levels in eukaryotic cells suggested the possibility that the clock may control aspects of mRNA translation. In support of this idea, the levels and/or activity of several translation initiation and elongation factors are clock regulated. However, until this study, clock control of the activity of eIF2α was not known. Both eIF2α and the eIF2α kinase GCN2 are key regulators of cellular homeostasis. Mis-regulation of eIF2α or GCN2 has been associated with cancer and neurodegenerative disorders. Therefore, eIF2α and GCN2 are potential therapeutic targets for treating these diseases [172, 173]. Although a great deal is known about the mechanism of GCN2 activation in *S. cerevisiae*, most studies are carried out under adverse conditions, including nutrient starvation, high salinity, oxidative stress, or UV radiation [43]. As such, these data might not reflect how GCN2 is activated in normal physiological conditions, and the downstream consequences may differ.

My study revealed that the *N. crassa* circadian clock regulates the levels of phosphorylated eIF2α, which serves as a key driver of rhythmic mRNA translation. Phosphorylated eIF2α (P-eIF2α) levels, which peak during subjective day, requires the GCN2 homolog, CPC-3. CPC-3 levels are clock-controlled; however, expressing constant levels of CPC-3 did not alter rhythmic accumulation of P-eIF2α. These data suggested that the clock controls the activity of CPC-3, and that rhythmic CPC-3 activity is necessary

for rhythmic P-eIF2α accumulation. In addition, the CPC-3 effector protein GCN1, accumulates rhythmically, and is necessary for eIF2α phosphorylation when cells are grown in constant darkness DD. However, it is not yet known if rhythmic GCN1 levels or activity are necessary for rhythmic CPC-3 activity and P-eIF2α accumulation. Addition to the role of CPC-3 in rhythmic accumulation of P-eIF2α, PPEI phosphatase is also required to maintain rhythmic P-eIF2α levels (Zhaolan Ding, unpublished data). With all the supporting evidence, we propose a model in which CPC-3 is activated during day by GCN1 and/or by high accumulation of uncharged tRNA leading to high P-eIF2α levels whereas during night low levels of uncharged tRNA, night peaking PPEI phosphatase rhythmically dephosphorylates CPC-3, thereby leading to lower CPC-3 activation and low P-eIF2α levels. Alternatively, PPEI can directly dephosphorylate P-eIF2α leading to low P-eIF2α levels.

Clock-controlled eIF2α activity temporally regulates mRNA translation of a subset of *N. crassa* genes that are enriched for amino acid and carbohydrate metabolic pathways. Of these genes, 193 day-peaking genes contain T-rich motifs, 233 night-peaking genes contain A-rich motifs and 81 have putative uORFs, in 5' UTR. These elements suggest possible mechanisms for how specific mRNAs are controlled by cycling P-eIF2α levels and will be investigated in the future.

Our data supports a testable model for how the clock controls translation initiation in coordination with energy metabolism (**Figure 5.1**). Previous studies showed that the clock partitions metabolism to different times of the day, with energy producing catabolic

87

functions generally occurring during the day, and energy consuming anabolic processes occurring at night [21, 134]. Translation requires large amounts of cellular energy; therefore, it makes sense to partition translation to the nighttime, when energy levels are high. Consistent with this model, we discovered that the levels of inhibitory phosphorylation of eEF-2 and eIF2α peak during day under the control of the clock. This was predicted to lead to decreased translation during the day and increased translation at night when energy levels are high. In accordance with the model, translation was higher during subjective night when P-eIF2α is low and vice versa as shown by *in vitro* translation assay. However, on examining effect of rhythmic P-eIF2α levels on genome wide translational level, there was equal distribution of genes peaking during dawn and dusk phase. This could be partly because only 30-40% of eIF2α and eEF-2 are phosphorylated under control of clock in normal growth conditions which leads to translation inhibition of selective mRNAs during day. Moreover, phosphorylation of eIF2α selectively enhances translation of some target mRNAs, particularly those with upstream open reading frames in the leader sequence and/or TISU element in 5' UTR [54, 149, 155]. Similarly, in mice, some neuronal mRNAs involved in memory processing have increased translation when eEF-2 is hyper-phosphorylated [98], and in Aplysia neurons, eEF-2 phosphorylation promotes the translation of some messages, while repressing others [174]. Taken together, these data support that certain mRNAs are more sensitive to increased daytime P-eIF2α and P-eEF-2 levels, and therefore peak in translation at night when energy levels are predicted to be high, whereas others are less sensitive, or are specifically activated, and peak in levels during the day, possibly in anticipation to environmental stress during the daylight hours. While P-eIF2α rhythms are necessary for the rhythmic accumulation

of ALG-11, they are not required for rhythmic FRQ protein accumulation and a functional clock (**Chapter II**), supporting that some, but not all, rhythmic proteins are derived from rhythmic translation.
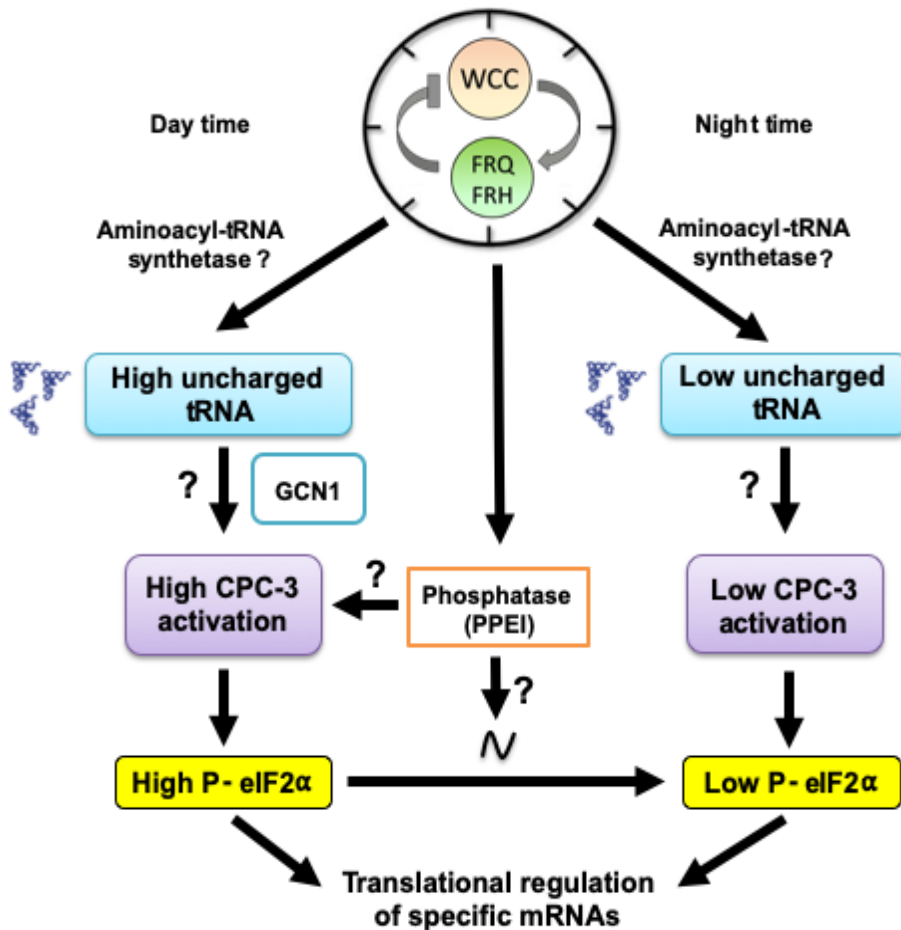
Figure 5.1. Proposed model for clock regulation of translation by regulating eIF2α phosphorylation through CPC-3/PPEI

Rhythmic phosphorylation of eIF2α requires clock control of CPC-3 activity, but the mechanism for this regulation is unknown. In yeast and mammalian cells, GCN2 is activated by binding of uncharged tRNAs [45], and this requires GCN1 to transfer uncharged tRNA to GCN2 [43]. Thus, amino acid levels, uncharged tRNAs and/ or the levels of tRNA synthetases, GCN1 levels and/or activity, are the most likely candidates for playing a role in rhythmic CPC-3 activation and need to be further investigated.

Based on the published data in mouse SCN and human plasma, different amino acids accumulate rhythmically over the course of two days [103, 175]. This indicated the possibility of rhythmic amino acids abundance leading to rhythmic activation of CPC-3 through rhythms in uncharged tRNA levels. However, on measuring free amino acid concentration, there was no evidence of rhythms in levels of free amino acids **(Figure 3.2, B-1,B-2)** over the course of two days, indicating the possible regulation of rhythmic CPC-3 through uncharged tRNA via aminoacyl-tRNA synthetases, and/or GCN1.

Clock control of uncharged tRNAs can be determined using tRNA-seq over a circadian time-course in WT versus clock mutant Δ*frq* cells [176]. Alternatively, acid urea polyacrylamide gel electrophoresis (PAGE) can be used to examine changes in the levels of specific uncharged tRNAs. This method is based on differences in electrophoretic mobility shift of charged tRNA vs uncharged tRNA at acidic pH [177]. Currently, Dr. Kathrina Castillo is using this method to examine changes in level of histidyl-tRNA over a circadian time course. The expectation is uncharged tRNA peaks during subjective day in WT cells, but if clock-controlled, this rhythm would be abolished in Δ*frq* cells. Another

90

possibility is rhythmic tRNA aminoacylation by aminoacyl-tRNA synthetases (ARSs) enzymes, which catalyze attachment of amino acids to their cognate tRNAs, leads to daily rhythms in charged vs uncharged tRNA levels. Preliminary experiments on *un-3* mutant, defective on valyl-tRNA synthetase activity showed high P-eIF2α levels with no time of day difference. This provides supporting evidence for role of ARS on rhythmic CPC-3 activation. I am working on examining P-eIF2α levels over a circadian time course and if found higher arrhythmic P-eIF2α levels, clock regulation of valyl-tRNA synthetase will be examined. In support of this idea, our ribo-seq data as well as published proteomic and RNA-seq data shows rhythmic TE and/or RNA of some tRNA synthetases, including valyl-tRNA synthetase (NCU01965), histidyl-tRNA synthetase (NCU06914), phenylalanyl-tRNA synthetase (NCU01512) and glycyl-tRNA synthetase (NCU00405) [22, 134]. Once clock control of the levels of ARSs are independently validated, their role in rhythmic CPC-3 activation can be examined by repressing expression of ARSs using the copper responsive promoter *Ptcu-1* [89]. The expectation is if they play a role in rhythmic CPC-3 activation, all time of constitutive expression of ARSs would increase uncharged tRNA levels at all times of day, which in turn would lead to high, arrhythmic, P-eIF2α levels. Alternatively, ARSs inhibitors can also be used to inhibit their function [178].

GCN1 controls GCN2 activity by transferring uncharged tRNA to GCN2 in *S. cerevisiae* [46]. Given that the levels of GCN1 cycle in *N. crassa* cells, GCN1 may rhythmically activate CPC-3. To determine if GCN1 rhythmic accumulation is necessary for cycling CPC-3 activation, constructs to constitutively express GCN1 under control of the copper responsive promoter *(Ptcu-1)* [89] are being generated. If GCN1 rhythms are necessary,

P-eIF2α levels would be expected to be arrhythmic. Physical interactions between CPC-3 and GCN1 should also be tested using co-IP. In addition to the interactions between GCN1 and GCN2, interaction of GCN1 and GCN2 with ribosomes are also essential for GCN2 activation [91]. A recent study showed GCN2 can be activated *in vitro* when bound to the ribosomal P-stalk [179]. In *N. crassa,* mass spec data of crude ribosome preparations identified CPC-3 as a ribosome-interacting protein, supporting the notion that CPC-3 is activated in similar manner. To validate CPC-3 interactions with the ribosome, and to test if this interaction is clock-controlled, polysomes isolated in WT and Δ*frq* cells over a circadian cycle could be examined by western blot for changes in CPC-3 levels. This will require using the tagged CPC-3::V5 strain or a CPC-3-specific antibody. As CPC-3 is highly activated during the day, the expectation is that we would observe high levels of CPC-3 interacting with polysomes during day as compared to night. For further validation, the conserved ribosome binding site sequence at C-terminal domain in CPC-3 [180] can be deleted, and determine if eIF2α phosphorylation is abolished in the resulting mutant.

GCN2 is an inert kinase that undergoes a conformational change after binding uncharged tRNAs, which leads to activation of kinase domain [45]. In *S. cerevisiae*, GCN2 activity is regulated through dephosphorylation of S577 by SIT4 phosphatase, a TOR pathway component, but the mechanism of how TOR activates GCN2 is unknown [127]. S577 is not conserved in mammalian GCN2 nor *N. crassa* CPC-3. However, CPC-3 mass spec data carried by Zhaolan Ding identified other possible phospho-sites S239, S356, T358, S360 S361, S864, S867, T874, S876 and T879. Of these, the autophosphorylation sites:

T874 and T879 are highly conserved between GCN2 and CPC-3 [124]. Experiments to examine the functional roles of these phospho-sites are ongoing and may provide further insight into the regulation of CPC-3 activity. In addition to CPC-3, night peaking clock-controlled PPEI phosphatase (SIT4 homolog) is required for rhythmic phosphorylation of eIF2α as PPEI deletion led to higher arrhythmic P-eIF2α levels (Zhaolan Ding, unpublished). It is possible that PPEI regulates CPC-3 activity by dephosphorylating the autophosphorylation site or other unknown sites that modulates CPC-3 activity, leading to constitutively active CPC-3 in $\Delta ppeI$. Alternatively, PPEI may directly dephosphorylates eIF2α similar to data in *S. cerevisiae* that suggests SIT4 and GCL7 directly dephosphorylate eIF2α [105]. Experiments are underway to explore these possibilities. Another interesting observation to follow up on is what else is controlled by rhythmic CPC-3 given that the rhythmic accumulation of CPC-3 is not required for P-eIF2α rhythmicity.

Similar to GCN2 activation, CPC-3 could also be activated by oxidative stress through the accumulation of reactive oxygen species (ROS). In *N. crassa*, ROS is generated rhythmically as a metabolic byproduct [181]. This suggests the possibility that rhythmic CPC-3 activation may be through cycling ROS levels. To test if P-eIF2α is induced on oxidative stress, preliminary experiments were carried out by growing WT cells in DD for 28 h followed by 10mm hydrogen peroxide (H_2O_2) treatment for 15 mins before harvest. P-eIF2α levels were induced in H_2O_2 treated vs untreated cells suggesting possible activation of CPC-3 through oxidative stress (data not shown). More follow up experiments examining the effect of oxidative stress at different times of day are required to conclude if ROS levels play a role in rhythmic CPC-3 activation. If time of day difference

in abolished in P-eIF2α level on oxidative treatment, the next step would be to examine P-eIF2α rhythms under arrhythmic ROS conditions. This could be accomplished in strains that are deleted for NADPH-1 oxidase *(Δnox-1)*, which abolishes ROS rhythms [181].

In addition to understanding mechanistic details of CPC-3 activation, we sought to determine the consequences of rhythmic CPC-3 activation and accumulation of P- eIF2α. Translational regulation depends not only on initiation and elongation factors, but also on mRNA features such as a highly structured 5' UTR, and the presence of specific motifs at the 5' and 3' UTRs [31, 182]. We performed ribosome profiling in parallel with RNA-seq to uncover possible mechanisms of regulation and identified specific subsets of mRNAs with T-rich, A-rich, IRE rich motifs and uORFs in the 5' UTR that are translationally regulated by the clock through eIF2α. Work is in progress to experimentally validate candidate genes, as well as to examine the functional role of these motif sequences.

Lastly, growth rate is significantly reduced in Δ*cpc-3* cells (**Chapter 2 and 3**). These data support the idea that rhythmic accumulation of P-eIF2α provides a growth advantage to the organism by partitioning most translation to the night when energy levels are high. This idea was validated by showing that growth rate is similarly reduced in *cpc-3$_c$* mutant cells that abolish the rhythm in P-eIF2α levels and in Δ*gcn1* cells that abolish eIF2α phosphorylation by CPC-3. It will be of interest in the future to determine if clock control of eIF2α is conserved in higher eukaryotes, and if links between energy metabolism and mRNA translation were maintained throughout evolution.

Translational regulation is critical for normal cell functions and eIF2α activity has been shown to be mis-regulated in different types of neuro-degenerative disorders, cancers and tumors making it one of the major target for chemotherapy [183, 184]. Links between the circadian clock and different disorders including cancer, tumors are well established [185]. Given the crucial role of eIF2α in translation, and its link with circadian clock and cancer, tumors, neurodegenerative disorders, the pathway for clock control of translation through eIF2α/GCN2 could be major target for chronotherapy, which could lead to more efficient treatment and helps to minimize toxicity by treating the target at specific times of day. Given that both translation and circadian clock mechanisms are conserved, understanding the mechanism of clock-control eIF2α activity in *N. crassa* will offer fundamental insights into translation control by the clock, and will provide a platform to extend these studies to mammalian cells.

REFERENCES

1. Panda, S., J.B. Hogenesch, and S.A. Kay., *Circadian rhythms from flies to human.* Nature, 2002. **417**(6886): p. 329-35.sss

2. Dunlap, J.C. and J.J. Loros., *The neurospora circadian system.* J Biol Rhythms, 2004. **19**(5): p. 414-24.

3. Kondo, T., et al., *Circadian clock mutants of cyanobacteria.* Science, 1994. **266**(5188): p. 1233-6.

4. de Paula, R.M., et al., *A connection between mapk pathways and circadian clocks.* cell cycle (georgetown, tex.), 2008. **7**(17): p. 2630-2634.

5. Green, C.B., J.S. Takahashi, and J. Bass., *The meter of metabolism.* Cell, 2008. **134**(5): p. 728-742.

6. Bell-Pedersen, D., et al., *Circadian rhythms from multiple oscillators: Lessons from diverse organisms.* Nature Reviews Genetics, 2005. **6**(7): p. 544-556.

7. Dunlap, J.C., *Molecular bases for circadian clocks.* Cell, 1999. **96**(2): p. 271-90.

8. Dunlap, J.C., et al., *Enabling a community to dissect an organism: overview of the Neurospora functional genomics project.* Adv Genet, 2007. **57**: p. 49-96.

9. Colot, H.V., et al., *A high-throughput gene knockout procedure for Neurospora reveals functions for multiple transcription factors.* Proc Natl Acad Sci U S A, 2006. **103**(27): p. 10352-10357.

10. McCluskey K., W.A., Plamann M, *The Fungal Genetics Stock Center: a repository for 50 years of fungal genetics research.* J Biosci, 2010. **35**(1): p. 119-26.

11. Cheng, P., et al., *Regulation of the Neurospora circadian clock by an RNA helicase.* Genes Dev, 2005. **19**(2): p. 234-41.

12. Froehlich, A.C., et al., *White Collar-1, a circadian blue light photoreceptor, binding to the frequency promoter.* Science, 2002. **297**(5582): p. 815-9.

13. Froehlich, A.C., J.J. Loros, and J.C. Dunlap., *Rhythmic binding of a WHITE COLLAR-containing complex to the frequency promoter is inhibited by FREQUENCY.* Proc Natl Acad Sci U S A, 2003. **100**(10): p. 5914-9.

14. Cheng, P., et al., *Coiled-coil domain-mediated FRQ-FRQ interaction is essential for its circadian clock function in Neurospora.* EMBO J, 2001. **20**(1-2): p. 101-8.

15. Cheng, P., Y. Yang, and Y. Liu., *Interlocked feedback loops contribute to the robustness of the Neurospora circadian clock.* Proc Natl Acad Sci U S A, 2001. **98**(13): p. 7408-13.

16. He, Q., et al., *CKI and CKII mediate the FREQUENCY-dependent phosphorylation of the WHITE COLLAR complex to close the Neurospora circadian negative feedback loop.* Genes Dev, 2006. **20**(18): p. 2552-65.

17. Schafmeier, T., et al., *Phosphorylation-dependent maturation of Neurospora circadian clock protein from a nuclear repressor toward a cytoplasmic activator.* Genes Dev, 2006. **20**(3): p. 297-306.

18. Heintzen, C. and Y. Liu., *The Neurospora crassa circadian clock.* Adv Genet, 2007. **58**: p. 25-66.

19. Liu, Y., J. Loros, and J.C. Dunlap., *Phosphorylation of the Neurospora clock protein FREQUENCY determines its degradation rate and strongly influences the*

period length of the circadian clock. Proc Natl Acad Sci U S A, 2000. **97**(1): p. 234-9.

20. Schafmeier, T., et al., *Transcriptional feedback of Neurospora circadian clock gene by phosphorylation-dependent inactivation of its transcription factor.* Cell, 2005. **122**(2): p. 235-46.

21. Hurley, J.M., et al., *Analysis of clock-regulated genes in Neurospora reveals widespread posttranscriptional control of metabolic potential.* Proc Natl Acad Sci U S A, 2014. **111**(48): p. 16995-7002.

22. Hurley, J.M., et al., *Circadian Proteomic Analysis Uncovers Mechanisms of Post-Transcriptional Regulation in Metabolic Pathways.* Cell Syst, 2018. **7**(6): p. 613-626 e5.

23. Fustin, J.M., et al., *RNA-methylation-dependent RNA processing controls the speed of the circadian clock.* Cell, 2013. **155**(4): p. 793-806.

24. Belanger, V., N. Picard, and N. Cermakian., *The circadian regulation of Presenilin-2 gene expression.* Chronobiol Int, 2006. **23**(4): p. 747-66.

25. Koike, N., et al., *Transcriptional architecture and chromatin landscape of the core circadian clock in mammals.* Science, 2012. **338**(6105): p. 349-54.

26. Baggs, J.E. and C.B. Green., *Nocturnin, a deadenylase in Xenopus laevis retina: a mechanism for posttranscriptional control of circadian-related mRNA.* Curr Biol, 2003. **13**(3): p. 189-98.

27. Lipton, J.O., et al., *The Circadian Protein BMAL1 Regulates Translation in Response to S6K1-Mediated Phosphorylation.* Cell, 2015. **161**(5): p. 1138-51.

28.	Robles, M.S., J. Cox, and M. Mann., *In-vivo quantitative proteomics reveals a key contribution of post-transcriptional mechanisms to the circadian regulation of liver metabolism.* PLoS Genet, 2014. **10**(1): p. e1004047.

29.	Mauvoisin, D., et al., *Circadian clock-dependent and -independent rhythmic proteomes implement distinct diurnal functions in mouse liver.* Proc Natl Acad Sci U S A, 2014. **111**(1): p. 167-72.

30.	Reddy, A.B., et al., *Circadian orchestration of the hepatic proteome.* Curr Biol, 2006. **16**(11): p. 1107-15.

31.	Hershey, J.W.B., N. Sonenberg, and M.B. Mathews., *Principles of translational control.* Cold Spring Harb Perspect Biol, 2018.

32.	Jouffe, C., et al., *The circadian clock coordinates ribosome biogenesis.* PLoS Biol, 2013. **11**(1): p. e1001455.

33.	Cao, R., et al., *Translational control of entrainment and synchrony of the suprachiasmatic circadian clock by mTOR/4E-BP1 signaling.* Neuron, 2013. **79**(4).

34.	Caster, S.Z., et al., *Circadian clock regulation of mRNA translation through eukaryotic elongation factor eEF-2.* Proc Natl Acad Sci U S A, 2016. **113**(34): p. 9605-10.

35.	Caster, S.Z., et al., *Circadian clock regulation of mRNA translation through eukaryotic elongation factor eEF-2.* Proceedings of the National Academy of Sciences of the United States of America, 2016. **113**(34): p. 9605-9610.

36.	Sonenberg, N. and T.E. Dever., *Eukaryotic translation initiation factors and regulators.* Curr Opin Struct Biol, 2003. **13**(1): p. 56-63.

37. Aitken, C.E. and J.R. Lorsch., *A mechanistic overview of translation initiation in eukaryotes.* Nat Struct Mol Biol, 2012. **19**(6): p. 568-76.

38. Sonenberg, N. and A.G. Hinnebusch., *Regulation of translation initiation in eukaryotes: mechanisms and biological targets.* Cell, 2009. **136**(4): p. 731-45.

39. Hinnebusch, A.G. and J.R. Lorsch., *The mechanism of eukaryotic translation initiation: new insights and challenges.* Cold Spring Harb Perspect Biol, 2012. **4**(10).

40. Han, A.P., et al., *Heme-regulated eIF2alpha kinase (HRI) is required for translational regulation and survival of erythroid precursors in iron deficiency.* EMBO J, 2001. **20**(23): p. 6909-18.

41. Hinnebusch, A.G., *Translational regulation of GCN4 and the general amino acid control of yeast.* Annu Rev Microbiol, 2005. **59**: p. 407-50.

42. Dey, M., et al., *Mechanistic link between PKR dimerization, autophosphorylation, and eIF2alpha substrate recognition.* Cell, 2005. **122**(6): p. 901-13.

43. Beatriz A.Castilho, R.S., Richard C.Silva, Rashmi Ramesh, Benjamin M.Himme, EvelynSattlegger., *Keeping the eIF2 alpha kinase Gcn2 in check.* BBA Molecular Cell Research, 2014. **1843**(9): p. 1948-1968.

44. Sattlegger, E., A.G. Hinnebusch, and I.B. Barthelmess., *cpc-3, the Neurospora crassa homologue of yeast GCN2, encodes a polypeptide with juxtaposed eIF2alpha kinase and histidyl-tRNA synthetase-related domains required for general amino acid control.* J Biol Chem, 1998. **273**(32): p. 20404-16.

45.   Dong, J., et al., *Uncharged tRNA activates GCN2 by displacing the protein kinase moiety from a bipartite tRNA-binding domain.* Mol Cell, 2000. **6**(2): p. 269-79.

46.   Marton, M.J., D. Crouch, and A.G. Hinnebusch., *GCN1, a translational activator of GCN4 in Saccharomyces cerevisiae, is required for phosphorylation of eukaryotic translation initiation factor 2 by protein kinase GCN2.* Mol Cell Biol, 1993. **13**(6): p. 3541-56.

47.   Vazquez de Aldana CR1, M.M., Hinnebusch AG., *GCN20, a novel ATP binding cassette protein, and GCN1 reside in a complex that mediates activation of the eIF-2 alpha kinase GCN2 in amino acid-starved cells.* EMBO J, 1995. **14**(13): p. 3184-99.

48.   Garcia-Barrio, M., et al., *Association of GCN1-GCN20 regulatory complex with the N-terminus of eIF2alpha kinase GCN2 is required for GCN2 activation.* EMBO J, 2000. **19**(8): p. 1887-99.

49.   Sattlegger, E., et al., *Gcn1 and actin binding to Yih1: implications for activation of the eIF2 kinase GCN2.* J Biol Chem, 2011. **286**(12): p. 10341-55.

50.   Bogorad, A.M., K.Y. Lin, and A. Marintchev., *Novel mechanisms of eIF2B action and regulation by eIF2alpha phosphorylation.* Nucleic Acids Res, 2017. **45**(20): p. 11962-11979.

51.   Hinnebusch, A.G., *Mechanism and regulation of initiator methionyl-tRNA binding to ribosomes.* 2000. 185-243.

52.   Zhang, P., et al., *The GCN2 eIF2alpha kinase is required for adaptation to amino acid deprivation in mice.* Mol Cell Biol, 2002. **22**(19): p. 6681-8.

53.   Hsieh, A.C., et al., *The translational landscape of mTOR signalling steers cancer initiation and metastasis.* Nature, 2012. **485**(7396): p. 55-61.

54.   Vattem, K.M. and R.C. Wek., *Reinitiation involving upstream ORFs regulates ATF4 mRNA translation in mammalian cells.* Proc Natl Acad Sci U S A, 2004. **101**(31): p. 11269-74.

55.   L Paluh, M.J.O., T L Legerton, and C Yanofsky., *The cross-pathway control gene of Neurospora crassa, cpc-1, encodes a protein similar to GCN4 of yeast and the DNA-binding domain of the oncogene v-jun-encoded protein.* PNAS, 1988. **85**(11): p. 3728-3732.

56.   Hinnebusch, A.G., I.P. Ivanov, and N. Sonenberg., *Translational control by 5'-untranslated regions of eukaryotic mRNAs.* Science, 2016. **352**(6292): p. 1413-6.

57.   Holcik, M., *Could the eIF2α-independent translation be the achilles heel of cancer?* Front Oncol., 2015. **5**.

58.   Trinh, M.A. and E. Klann., *Translational control by eif2α kinases in long-lasting synaptic plasticity and long-term memory.* Neurobiology of learning and memory, 2013. **105**: p. 93-99.

59.   Costa-Mattioli, M., et al., *Translational control of hippocampal synaptic plasticity and memory by the eIF2alpha kinase GCN2.* Nature, 2005. **436**(7054): p. 1166-73.

60.   Holcik, M. and N. Sonenberg., *Translational control in stress and apoptosis.* Nat Rev Mol Cell Biol, 2005. **6**(4): p. 318-27.

61.   Holcik, M., *Targeting translation for treatment of cancer--a novel role for IRES?* Curr Cancer Drug Targets, 2004. **4**(3): p. 299-311.

62. Trinh, M.A., et al., *Brain-specific Disruption of the eIF2α Kinase PERK Decreases ATF4 Expression and Impairs Behavioral Flexibility.* Cell Reports, 2012. **1**(6): p. 676-688.

63. Lee, K.H., et al., *Rhythmic interaction between Period1 mRNA and hnRNP Q leads to circadian time-dependent translation.* Mol Cell Biol, 2012. **32**(3): p. 717-28.

64. Janich, P., et al., *Ribosome profiling reveals the rhythmic liver translatome and circadian clock regulation by upstream open reading frames.* Genome Res, 2015. **25**(12): p. 1848-59.

65. Diernfellner, A.C., et al., *Molecular mechanism of temperature sensing by the circadian clock of Neurospora crassa.* Genes Dev, 2005. **19**(17): p. 1968-73.

66. Liu, Y., et al., *Thermally regulated translational control of FRQ mediates aspects of temperature responses in the neurospora circadian clock.* Cell, 1997. **89**(3): p. 477-86.

67. Dong J, Q.H., Garcia-Barrio M, Anderson J, Hinnebusch AG., *Uncharged tRNA activates gcn2 by displacing the protein kinase moiety from a bipartite trna-binding domain.* Molecular cell, 2000. **6**(2): p. 269-79.

68. Sharma, V.K., *Adaptive significance of circadian clocks.* Chronobiol Int, 2003. **20**(6): p. 901-19.

69. Menet, J.S., et al., *Nascent-Seq reveals novel features of mouse circadian transcriptional regulation.* Elife, 2012. **1**: p. e00011.

70. Partch, C.L., C.B. Green, and J.S. Takahashi., *Molecular architecture of the mammalian circadian clock.* Trends Cell Biol, 2014. **24**(2): p. 90-9.

71.   Vitalini, M.W., et al., *The rhythms of life: circadian output pathways in Neurospora.* J Biol Rhythms, 2006. **21**(6): p. 432-44.

72.   Vollmers, C., et al., *Circadian oscillations of protein-coding and regulatory RNAs in a highly dynamic mammalian liver epigenome.* Cell Metab, 2012. **16**(6): p. 833-45.

73.   Zhang, R., et al., *A circadian gene expression atlas in mammals: implications for biology and medicine.* Proc Natl Acad Sci U S A, 2014. **111**(45): p. 16219-24.

74.   Dever, T.E. and R. Green., *The elongation, termination, and recycling phases of translation in eukaryotes.* Cold Spring Harb Perspect Biol, 2012. **4**(7): p. a013706.

75.   Wei, J., et al., *The stringency of start codon selection in the filamentous fungus Neurospora crassa.* J Biol Chem, 2013. **288**(13): p. 9549-62.

76.   Hinnebusch, A.G., *Structural Insights into the Mechanism of Scanning and Start Codon Recognition in Eukaryotic Translation Initiation.* Trends Biochem Sci, 2017. **42**(8): p. 589-611.

77.   Garriz, A., et al., *A network of hydrophobic residues impeding helix alphaC rotation maintains latency of kinase Gcn2, which phosphorylates the alpha subunit of translation initiation factor 2.* Mol Cell Biol, 2009. **29**(6): p. 1592-607.

78.   Anda, S., R. Zach, and B. Grallert., *Activation of Gcn2 in response to different stresses.* PLoS One, 2017. **12**(8): p. e0182143.

79.   Wek, S.A., S. Zhu, and R.C. Wek., *The histidyl-tRNA synthetase-related sequence in the eIF-2 alpha protein kinase GCN2 interacts with tRNA and is*

required for activation in response to starvation for different amino acids. Mol Cell Biol, 1995. **15**(8): p. 4497-506.

80.   Lee SJ, S.M., Sattlegger E., *Gcn1 contacts the small ribosomal protein Rps10, which is required for full activation of the protein kinase Gcn2..* Biochem J., 2015. **466**(3): p. 547-59.

81.   Tian, C., et al., *Transcriptional profiling of cross pathway control in Neurospora crassa and comparative analysis of the Gcn4 and CPC1 regulons.* Eukaryot Cell, 2007. **6**(6): p. 1018-29.

82.   Advani, V.M. and P. Ivanov., *Translational control under stress: Reshaping the Translatome.* Bioessays, 2019. **41**(5): p. e1900009.

83.   Barthelmess, I.B. and J. Kolanus., *The range of amino acids whose limitation activates general amino-acid control in Neurospora crassa.* Genet Res, 1990. **55**(1): p. 7-12.

84.   Flint, H.J. and B.F. Kemp., *General control of arginine biosynthetic enzymes in Neurospora crassa.* J Gen Microbiol, 1981. **124**(1): p. 129-40.

85.   Hinnebusch, A.G., *Transcriptional and translational regulation of gene expression in the general control of amino-acid biosynthesis in Saccharomyces cerevisiae.* Prog Nucleic Acid Res Mol Biol, 1990. **38**: p. 195-240.

86.   Sachs, M.S., *General and cross-pathway controls of amino acid biosynthesis*, in *The Mycota: biochemsityr and molecular biology*, R.M.G.A. Brambl, Editor. 1996, Spinger-Verlag: Heidelberg, Germany. p. 315-345.

87.   Ivanov, I.P., et al., *Translation initiation from conserved non-aug codons provides additional layers of regulation and coding capacity.* MBio, 2017. **8**(3).

88. Belden, W.J., et al., *The band mutation in Neurospora crassa is a dominant allele of ras-1 implicating RAS signaling in circadian output.* Genes Dev, 2007. **21**(12): p. 1494-505.

89. Lamb, T.M., J. Vickery, and D. Bell-Pedersen., *Regulation of gene expression in Neurospora crassa with a copper responsive promoter.* G3 (Bethesda), 2013. **3**(12): p. 2273-80.

90. Wek SA, Z.S., Wek RC., *The histidyl-tRNA synthetase-related sequence in the eIF-2 alpha protein kinase GCN2 interacts with tRNA and is required for activation in response to starvation for different amino acids.* Mol Cell Biol, 1995. **15**(8): p. 4497-506.

91. Sattlegger, E. and A.G. Hinnebusch., *Separate domains in GCN1 for binding protein kinase GCN2 and ribosomes are required for GCN2 activation in amino acid-starved cells.* Embo j, 2000. **19**(23): p. 6622-33.

92. Qiu, H., et al., *Mutations that bypass tRNA binding activate the intrinsically defective kinase domain in GCN2.* Genes Dev, 2002. **16**(10): p. 1271-80.

93. Larsen, I.S.B., et al., *Multiple distinct O-Mannosylation pathways in eukaryotes.* Curr Opin Struct Biol, 2019. **56**: p. 171-178.

94. Bell-Pedersen, D., et al., *Circadian clock-controlled genes isolated from Neurospora crassa are late night- to early morning-specific.* Proc Natl Acad Sci U S A, 1996. **93**(23): p. 13096-101.

95. Sancar, C., et al., *Dawn- and dusk-phased circadian transcription rhythms coordinate anabolic and catabolic functions in Neurospora.* BMC Biol, 2015. **13**: p. 17.

96.   Baird, T.D. and R.C. Wek., *Eukaryotic initiation factor 2 phosphorylation and translational control in metabolism.* Adv Nutr, 2012. **3**(3): p. 307-21.

97.   Lu, P.D., H.P. Harding, and D. Ron., *Translation reinitiation at alternative open reading frames regulates gene expression in an integrated stress response.* J Cell Biol, 2004. **167**(1): p. 27-33.

98.   Park, S., et al., *Elongation factor 2 and fragile X mental retardation protein control the dynamic translation of Arc/Arg3.1 essential for mGluR-LTD.* Neuron, 2008. **59**(1): p. 70-83.

99.   Weatherill, D.B., et al., *Compartment-specific, differential regulation of eukaryotic elongation factor 2 and its kinase within Aplysia sensory neurons.* J Neurochem, 2011. **117**(5): p. 841-55.

100.   Zhu, S., A.Y. Sobolev, and R.C. Wek., *Histidyl-tRNA synthetase-related sequences in GCN2 protein kinase regulate in vitro phosphorylation of eIF-2.* J Biol Chem, 1996. **271**(40): p. 24989-94.

101.   Marton, M.J., et al., *Evidence that GCN1 and GCN20, translational regulators of GCN4, function on elongating ribosomes in activation of eIF2alpha kinase GCN2.* Mol Cell Biol, 1997. **17**(8): p. 4474-89.

102.   Ramirez, M., R.C. Wek, and A.G. Hinnebusch., *Ribosome association of GCN2 protein kinase, a translational activator of the GCN4 gene of Saccharomyces cerevisiae.* Mol Cell Biol, 1991. **11**(6): p. 3027-36.

103.   Fustin JM, K.S., Okamura H., *Circadian profiling of amino acids in the scn and cerebral cortex by laser capture microdissection-mass spectrometry.* J Biol Rhythms, 2017. **32**(6): p. 609-620.

104. Wek, R.C., et al., *Truncated protein phosphatase GLC7 restores translational activation of GCN4 expression in yeast mutants defective for the eIF-2 alpha kinase GCN2.* Mol Cell Biol, 1992. **12**(12): p. 5700-10.

105. Cherkasova, V., H. Qiu, and A.G. Hinnebusch., *Snf1 promotes phosphorylation of the α subunit of eukaryotic translation initiation factor 2 by activating gcn2 and inhibiting phosphatases glc7 and sit4.* Mol Cell Biol, 2010. **30**(12): p. 2862-73.

106. Visweswaraiah, J., et al., *Evidence that eukaryotic translation elongation factor 1A (eEF1A) binds the Gcn2 protein C terminus and inhibits Gcn2 activity.* J Biol Chem, 2011. **286**(42): p. 36568-79.

107. Yuan, W., et al., *General control nonderepressible 2 (gcn2) kinase inhibits target of rapamycin complex 1 in response to amino acid starvation in Saccharomyces cerevisiae.* J Biol Chem, 2017. **292**(7): p. 2660-2669.

108. Zhu, S. and R.C. Wek., *Ribosome-binding domain of eukaryotic initiation factor-2 kinase GCN2 facilitates translation control.* J Biol Chem, 1998. **273**(3): p. 1808-14.

109. Darnell, A.M., A.R. Subramaniam, and E.K. O'Shea., *Translational control through differential ribosome pausing during amino acid limitation in mammalian cells.* Mol Cell, 2018. **71**(2): p. 229-243 e11.

110. Rowland H. Davis, F.J.d.S., *Genetic and microbial research techniques for Neurospora crassa.* Methods Enzymol, 1970. **27A**: p. 79-143.

111. Bennett, L.D., et al., *Circadian activation of the Mitogen-Activated Protein Kinase MAK-1 facilitates rhythms in clock-controlled genes in Neurospora crassa.* Eukaryotic Cell, 2013. **12**(1): p. 59-69.

112. Gooch, V.D., et al., *Fully codon-optimized luciferase uncovers novel temperature characteristics of the Neurospora clock.* Eukaryot Cell, 2008. **7**(1): p. 28-37.

113. Lamb, T.M., J. Vickery, and D. Bell-Pedersen., *Regulation of Gene Expression in Neurospora crassa with a Copper Responsive Promoter.* G3: Genes|Genomes|Genetics, 2013. **3**(12): p. 2273-2280.

114. S., E.D.J.a.S.M., *A rapid and simple method for isolation of Neurospora crassa homokaryons using microconidia.* FUngal Genetics Newsletter, 1990. **37**: p. 17-18.

115. Pall, M.L., and J.P. Brunelli., *A series of six compact fungal transformation vectors containing polylinkers with multiple unique restriction sites.* Fungal Genetics Reports, 1993. **40**(22).

116. Larrondo, L.F., J.J. Loros, and J.C. Dunlap., *High-resolution spatiotemporal analysis of gene expression in real time: in vivo analysis of circadian rhythms in Neurospora crassa using a FREQUENCY-luciferase translational reporter.* Fungal Genet Biol, 2012. **49**(9): p. 681-3.

117. Lamb, T.M., et al., *Direct transcriptional control of a p38 MAPK pathway by the circadian clock in Neurospora crassa.* PLoS ONE, 2011. **6**(11): p. e27149.

118. Jones, C.A., S.E. Greer-Phillips, and K.A. Borkovich., *The response regulator RRG-1 functions upstream of a mitogen-activated protein kinase pathway impacting asexual development, Female Fertility, Osmotic Stress, and Fungicide Resistance in Neurospora crassa.* Molecular Biology of the Cell, 2007. **18**(6): p. 2123-2136.

119. Schneider, C.A., W.S. Rasband, and K.W. Eliceiri, *NIH Image to ImageJ: 25 years of Image Analysis.* Nature methods, 2012. **9**(7): p. 671-675.

120. Liu, H. and J.H. Naismith., *A simple and efficient expression and purification system using two newly constructed vectors.* Protein expression and purification, 2009. **63**(2): p. 102-111.

121. Zielinski, T., et al., *Strengths and limitations of period estimation methods for circadian data.* PLoS One, 2014. **9**(5).

122. Debra J. Skene, E.S., Namrata R. Chowdhury, Rajendra P. Gajula, Benita Middleton, Brieann C. Satterfield, Kenneth I. Porter, Hans P. A. Van Dongen, and Shobhan Gaddameedhi., *Separation of circadian- and behavior-driven metabolite rhythms in humans provides a window on peripheral oscillators and metabolism.* PNAS, 2018. **115**(30): p. 7825-7830.

123. Richard J. Wurtman, M.D., Christopher M. Rose, Chuan Chou, M.S., and Frances F. Larin, D.P.H., *daily rhythms in the concentrations of various amino acids in human plasma.* N Engl J Med, 1968. **279**: p. 171-175.

124. Romano PR, G.-B.M., Zhang X, Wang Q, Taylor DR, Zhang F, Herring C, Mathews MB, Qin J, Hinnebusch AG., *Autophosphorylation in the activation loop is required for full kinase activity in vivo of human and yeast eukaryotic initiation factor 2alpha kinases PKR and GCN2.* Mol Cell Biol, 1998. **18**(4): p. 2282-97

125. Narasimhan, J., K.A. Staschke, and R.C. Wek., *Dimerization is required for activation of eIF2 kinase Gcn2 in response to diverse environmental stress conditions.* J Biol Chem, 2004. **279**(22): p. 22820-32.

126. Padyana, A.K., et al., *Structural basis for autoinhibition and mutational activation of eukaryotic initiation factor 2alpha protein kinase GCN2.* J Biol Chem, 2005. **280**(32): p. 29289-99.

127. Garcia-Barrio, M., et al., *Serine 577 is phosphorylated and negatively affects the tRNA binding and eIF2alpha kinase activities of GCN2.* J Biol Chem, 2002. **277**(34): p. 30675-83.

128. Cherkasova, V.A. and A.G. Hinnebusch., *Translational control by TOR and TAP42 through dephosphorylation of eIF2alpha kinase GCN2.* Genes Dev, 2003. **17**(7): p. 859-72.

129. Sattlegger, E., et al., *YIH1 is an actin-binding protein that inhibits protein kinase GCN2 and impairs general amino acid control when overexpressed.* J Biol Chem, 2004. **279**(29): p. 29952-62.

130. Kruger, D., J. Koch, and I.B. Barthelmess., *cpc-2, a new locus involved in general control of amino acid synthetic enzymes in Neurospora crassa.* Curr Genet, 1990. **18**(3): p. 211-5.

131. Barthelmess, F.M.K.S.H.B.K.B., *The cpc-2 gene of Neurospora crassa encodes a protein entirely composed of WD-repeat segments that is involved in general amino acid control and female fertility.* MGG, 1995. **248**(2): p. 162-173.

132. Tarumoto, Y., J. Kanoh, and F. Ishikawa., *Receptor for activated C-kinase (RACK1) homolog Cpc2 facilitates the general amino acid control response through Gcn2 kinase in fission yeast.* J Biol Chem, 2013. **288**(26): p. 19260-8.

133. Schmit, J.C. and S. Brody., *Neurospora crassa conidial germination: role of endogenous amino acid pools.* J Bacteriol, 1975. **124**(1): p. 232-42.

134. Cigdem Sancar, G.S., Nati Ha, Francois Cesbron, Michael Brunner., *Dawn- and dusk-phased circadian transcription rhythms coordinate anabolic and catabolic functions in Neurospora.* BMC Biol, 2015. **13**(17).

135. Masamitsu Shimazu, T.S., Koichi Akiyama, Yoshinori Ohsumi and Yoshimi Kakinuma., *A Family of Basic Amino Acid Transporters of the Vacuolar Membrane from Saccharomyces cerevisiae.* The journal of Biochemistry, 2004. **280**: p. 4851-4857.

136. Cramer, C.L., L.E. Vaughn, and R.H. Davis., *Basic amino acids and inorganic polyphosphates in Neurospora crassa: independent regulation of vacuolar pools.* J Bacteriol, 1980. **142**(3): p. 945-52.

137. Simone Gallo, S.R., Nicola Manfrini, Elisa Pesce, Stefania Oliveto, Piera Calamita, Marilena Mancino, Elisa Maffioli, Monica Moro, Mariacristina Crosti, Valeria Berno, Mauro Bombaci, Gabriella Tedeschi, Stefano., *RACK1 specifically regulates translation through its binding to ribosomes.* Molecular and Cellular Biology, December 2018. **38**(23).

138. Ingolia, N.T., et al., *Genome-wide analysis in vivo of translation with nucleotide resolution using ribosome profiling.* Science, 2009. **324**(5924): p. 218-23.

139. Kim, D., B. Langmead, and S.L. Salzberg., *HISAT: a fast spliced aligner with low memory requirements.* Nat Methods, 2015. **12**(4): p. 357-60.

140. Xiao, Z., et al., *Genome-wide assessment of differential translations with ribosome profiling data.* Nat Commun, 2016. **7**: p. 11194.

141. Hannah De los Santos, E.J.C., Kristen P. Bennett, Jennifer M. Hurley., *Circadian rhythms in Neurospora exhibit biologically relevant driven and damped harmonic oscillations.* ACM-BCB, 2017.

142. Hughes, M.E., J.B. Hogenesch, and K. Kornacker., *JTK_CYCLE: an efficient nonparametric algorithm for detecting rhythmic components in genome-scale data sets.* J Biol Rhythms, 2010. **25**(5): p. 372-80.

143. Steffen Priebe, J.L., Daniela Albrecht, Reinhard Guthke, Axel A. Brakhage., *FungiFun: A web-based application for functional categorization of fungal genes and proteins.* Fungal Genetics and Biology, 2011. **48**(4): p. 353-358.

144. Berg JM, T.J., Stryer L., *Biochemistry.* 2002, W H Freeman: New York.

145. Rubio, C.A., et al., *Transcriptome-wide characterization of the eIF4A signature highlights plasticity in translation regulation.* Genome Biol, 2014. **15**(10): p. 476.

146. O, M., *Synthesis of the translational apparatus is regulated at the translational level.* Eur J Biochem, 2000. **267**(21): p. 6321-30.

147. Ulf Anderson Orom, F.C.N., Anders H. Lund., *MicroRNA-10a binds the 5'utr of ribosomal protein mrnas and enhances their translation.* Mol Cell, 2008. **30**(4): p. 460-471.

148. Philippe, L., et al., *La-related protein 1 (LARP1) repression of TOP mRNA translation is mediated through its cap-binding domain and controlled by an adjacent regulatory region.* Nucleic Acids Res, 2018. **46**(3): p. 1457-1469.

149. Atger, F., et al., *Circadian and feeding rhythms differentially affect rhythmic mRNA transcription and translation in mouse liver.* Proc Natl Acad Sci U S A, 2015. **112**(47): p. E6579-88.

150. Bailey, T.L. and C. Elkan., *Fitting a mixture model by expectation maximization to discover motifs in biopolymers.* Proc Int Conf Intell Syst Mol Biol, 1994. **2**: p. 28-36.

151. Xiao, Z., et al., *De novo annotation and characterization of the translatome with ribosome profiling data.* Nucleic Acids Res, 2018. **46**(10): p. e61.

152. Matthew S. Sachs, C.Y., *Developmental expression of genes involved in conidiation and amino acid biosynthesis in Neurospora crassa.* Developmental Biology, 1991. **148**(1): p. 117-128.

153. Hughes, M.E., et al., *Harmonics of circadian gene transcription in mammals.* PLoS Genet, 2009. **5**(4): p. e1000442.

154. Hughes, M.E., et al., *Guidelines for Genome-Scale Analysis of Biological Rhythms.* J Biol Rhythms, 2017. **32**(5): p. 380-393.

155. Haimov, O., et al., *Efficient and accurate translation initiation directed by TISU involves RPS3 and RPS10e binding and differential eukaryotic initiation factor 1A Regulation.* Mol Cell Biol, 2017. **37**(15).

156. Hyo-Jin Kim, H.-R.L., Ji-Young Seo, Hye Guk Ryu, Kyung-Ha Lee, Do-Yeon Kim & Kyong-Tai Kim., *Heterogeneous nuclear ribonucleoprotein A1 regulates rhythmic synthesis of mouse Nfil3 protein via IRES-mediated translation.* Scientific reports, 2017. **7**.

157. Baird, S.D., et al., *Searching for IRES.* RNA, 2006{Baird, 2006 #474}. **12**(10): p. 1755-85.

158. Mokrejs, M., et al., *IRESite: the database of experimentally verified IRES structures (www.iresite.org).* Nucleic Acids Res, 2006. **34**(Database issue): p. D125-30.

159. Muckenthaler, M.U., et al., *a red carpet for iron metabolism.* Cell, 2017. **168**(3): p. 344-361.

160. Grant, C.E., T.L. Bailey, and W.S. Noble., *FIMO: scanning for occurrences of a given motif.* Bioinformatics, 2011. **27**(7): p. 1017-8.

161. Li, S. and J.D. Lin., *Transcriptional control of circadian metabolic rhythms in the liver.* Diabetes Obes Metab, 2015. **17 Suppl 1**: p. 33-8.

162. Montal, E.D., et al., *PEPCK Coordinates the Regulation of Central Carbon Metabolism to Promote Cancer Cell Growth.* Mol Cell, 2015. **60**(4): p. 571-83.

163. Kalhan, S.C. and A. Ghosh., *Dietary iron, circadian clock, and hepatic gluconeogenesis.* Diabetes, 2015. **64**(4): p. 1091-3.

164. Caballero-Molada, M., et al., *The Gcn2-eIF2alpha pathway connects iron and amino acid homeostasis in Saccharomyces cerevisiae.* Biochem J, 2018. **475**(8): p. 1523-1534.

165. Jang, C., et al., *Ribosome profiling reveals an important role for translational control in circadian gene expression.* Genome Res, 2015. **25**(12): p. 1836-47.

166. Trapnell, C., et al., *Differential analysis of gene regulation at transcript resolution with RNA-seq.* Nat Biotechnol, 2013. **31**(1): p. 46-53.

167. Martin, M., *Cutadapt removes adapter sequences from high-throughput sequencing reads. , EMBnet.* 2011. p. 10-12.

168. Wingett SW, A.S. *FastQ Screen: A tool for multi-genome mapping and quality control.* . F100Res, 2018. **7**, DOI: 0.12688/f1000research.15931.2.

169. Bolger, A.M., M. Lohse, and B. Usadel, *Trimmomatic: a flexible trimmer for Illumina sequence data.* Bioinformatics, 2014. **30**(15): p. 2114-20.

170. Anders, S., P.T. Pyl, and W. Huber., *HTSeq--a Python framework to work with high-throughput sequencing data.* Bioinformatics, 2015. **31**(2): p. 166-9.

171. Rstudio, *RStudio: Integrated development environment for R (Version 0.96.122) [Computer software].* 2012: Boston MA.

172. Moreno, J.A., et al., *Sustained translational repression by eIF2alpha-P mediates prion neurodegeneration.* Nature, 2012. **485**(7399): p. 507-11.

173. Ma, T., et al., *Suppression of eIF2alpha kinases alleviates Alzheimer's disease-related plasticity and memory deficits.* Nat Neurosci, 2013. **16**(9): p. 1299-305.

174. McCamphill, P.K., et al., *Bidirectional regulation of eEF2 phosphorylation controls synaptic plasticity by decoding neuronal activity patterns.* J Neurosci, 2015. **35**(10): p. 4403-17.

175. Wurtman, R.J., et al., *Daily rhythms in the concentrations of various amino acids in human plasma.* N Engl J Med, 1968. **279**(4): p. 171-5.

176. Yulong Wei, J.R.S.a.X.X., *An improved estimation of tRNA expression to better elucidate the coevolution between tRNA abundance and codon usage in bacteria.* Sci Rep., 2019 feb 28. **9**.

177. Kohrer, C. and U.L. Rajbhandary., *The many applications of acid urea polyacrylamide gel electrophoresis to studies of tRNAs and aminoacyl-tRNA synthetases.* Methods, 2008. **44**(2): p. 129-38.

178.   Keller, T.L., et al., *Halofuginone and other febrifugine derivatives inhibit prolyl-tRNA synthetase.* Nat Chem Biol, 2012. **8**(3): p. 311-7.

179.   Inglis, A.J., et al., *Activation of GCN2 by the ribosomal P-stalk.* Proc Natl Acad Sci U S A, 2019. **116**(11): p. 4946-4954.

180.   Qiu H., G.-B.M.T., Hinnebusch A. G., *Dimerization by translation initiation factor 2 kinase GCN2 is mediated by interactions in the C-terminal ribosome-binding region and the protein kinase domain.* Mol. Cell Biol., 1998. **18**: p. 2697-2711.

181.   Gyongyosi, N. and K. Kaldi., *Interconnections of reactive oxygen species homeostasis and circadian rhythm in Neurospora crassa.* Antioxid Redox Signal, 2014. **20**(18): p. 3007-23.

182.   Kathrina Leppek, R.D.a.M.B., *Functional 5' UTR mRNA structures in eukaryotic translation regulation and how to find them.* Nature Reviews Molecular Cell Biology, 2018. **19**.

183.   Lobo, M.V., et al., *Levels, phosphorylation status and cellular localization of translational factor eIF2 in gastrointestinal carcinomas.* Histochem J, 2000. **32**(3): p. 139-50.

184.   Wang, S., et al., *Expression of the eukaryotic translation initiation factors 4E and 2alpha in non-Hodgkin's lymphomas.* Am J Pathol, 1999. **155**(1): p. 247-55.

185.   Fu, L. and N.M. Kettner., *The circadian clock in cancer development and therapy.* Prog Mol Biol Transl Sci, 2013. **119**: p. 221-82.
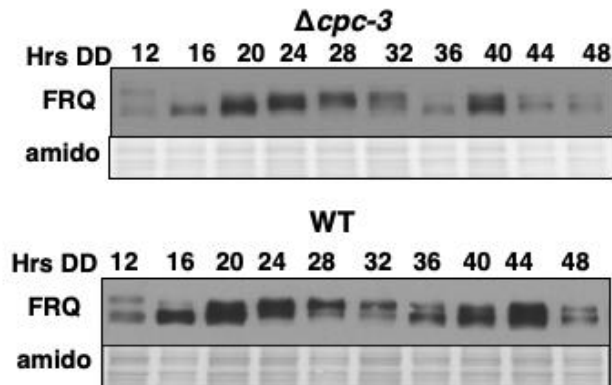
Figure A-1. FRQ rhythmicity in WT and Δ*cpc-3* cells. Western blot of protein extracted from WT and Δ*cpc-3* cells grown in DD, harvested every 4h over 2 days (Hrs DD), and probed with FRQ antibody. Amido stained protein is shown as a loading control.
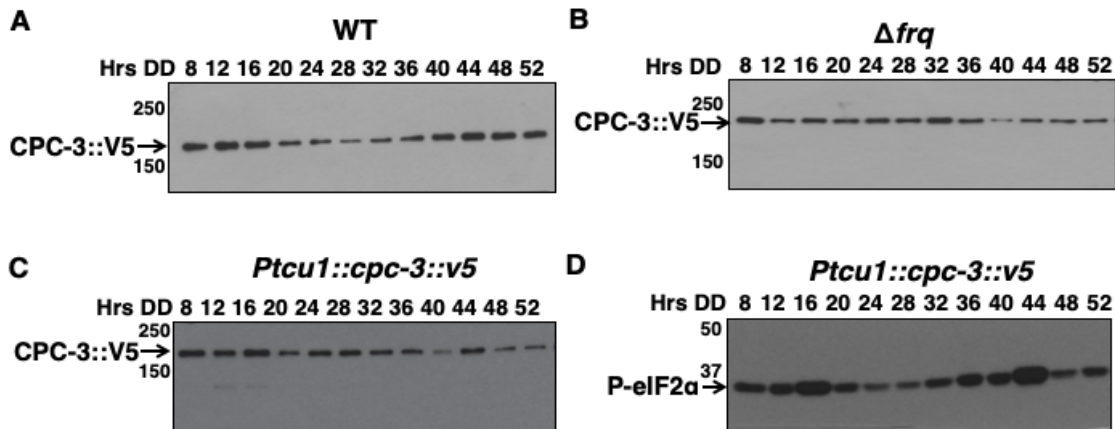
Figure A-2. Expression of CPC-3::V5 . Full gels for western blots shown in **Figure 3** and labeled as in **Figure S1**. The anti-V5 antibody detected a protein of ~180 KDa, matching the predicted size of CPC-3::V5. Protein extracted from (A) WT, (B) Δ*frq*, or (C&D) *Ptcu1::cpc-3::v5* cells grown in DD, harvested every 4 h over 2 days (Hrs DD), and probed with (A-C) V5 or (D) P-eIF2α antibody.
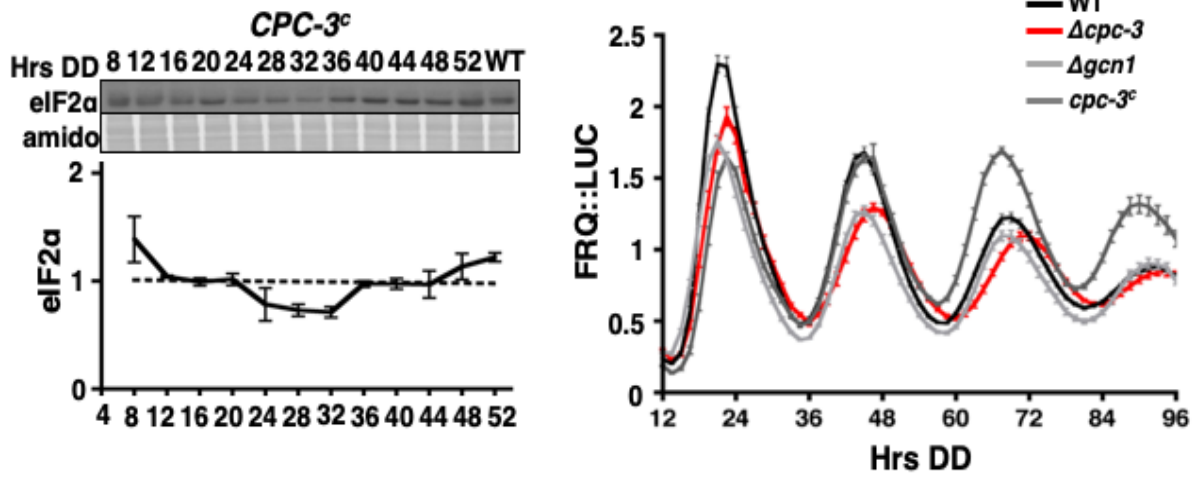
Figure A-3. Total eIF2α and FRQ::LUC levels in *cpc-3c, WT, Δgcn1, Δcpc-3*. A) Western blot of protein extracted from *cpc-3c* and probed with total eIF2α antibody. Amido black stained proteins are shown as a loading control. (B) Plot of relative luciferase activity from FRQ::LUC translational fusion protein in the indicated strains grown in DD and assayed every 1.5 h (Hrs DD).

Table B-1: Amino acid quantification (nm/10ul) from WT cells

	12	16	20	24	28	32	36	40	44	48
ASP	2.473855	1.84569	1.684045	3.425135	2.358265	2.24879	1.51321	0.972305	0.888395	1.24575
GLU	10.02669	9.70809	9.129955	12.840555	9.43045	9.77296	14.18471	10.07495	9.916985	7.9168
ASN	6.99237	5.81009	5.69008	9.22491	7.01746	7.43749	7.24423	5.131125	4.593985	6.299595
SER	4.087145	3.54333	3.54819	4.18394	3.26331	3.41918	4.92327	4.08692	4.2385	3.3303
GLN	40.13031	38.18554	35.87969	50.56383	41.08943	40.603125	36.213935	28.973665	25.29247	31.323265
HIS	5.25737	4.608225	4.2294	6.36691	4.71348	4.76207	6.011135	4.07846	3.875205	4.845495
GLY	9.514605	9.478755	9.36126	8.895305	7.859655	8.602705	14.42091	11.828905	10.455265	12.6182
THR	3.090975	3.382135	3.38524	2.32473	2.367285	2.50916	6.885175	4.805645	4.159915	5.693345
ALA	119.238045	122.23635	121.73452	106.124825	90.352305	98.107045	171.744305	140.002975	150.347455	119.00669
ARG	7.47215	7.235485	6.385055	11.01001	7.83293	7.778235	8.889285	6.659495	6.61142	7.627455
TYR	0.438425	0.420115	0.419905	0.60076	0.49248	0.475935	0.770115	0.57338	0.4955	0.621665
VAL	3.666355	3.9039	3.933075	4.101165	3.6905	3.981535	7.84366	5.633115	6.028985	5.86767
MET	1.418625	1.234525	1.1303	1.709285	1.279375	1.33188	1.56642	1.10327	1.11703	1.133975
TRP	0.20045	0.175095	0.172345	0.28317	0.212105	0.242365	0.23446	0.18908	0.18029	0.20544
PHE	0.582355	0.51786	0.513185	0.79174	0.582685	0.59641	0.82344	0.61165	0.522165	0.55098
ILE	0.823405	0.846335	0.8235	1.013465	0.75064	0.78586	1.611455	1.070455	0.944235	1.103415
LEU	1.20564	1.175835	1.147585	1.71083	1.219805	1.253005	2.169845	1.49463	1.30602	1.5663
LYS	4.313135	4.08111	3.68247	5.11203	3.946755	4.11331	6.95866	4.63409	4.72235	5.287345
PRO	2.450355	2.76723	2.471795	2.383545	2.00912	2.275745	4.969905	3.79507	3.788505	3.99327

Table B-2: Amino acid quantification (nm/10ul) from Δ*frq* cells

	12	16	20	24	28	32	36	40	44	48
ASP	1.392445	1.678345	1.19439	1.749495	1.485005	2.104435	1.02187	0.83799	0.93354	1.054035
GLU	12.059635	11.894805	10.30601	8.796885	7.739665	9.252445	11.798785	11.92537	12.90518	8.777275
ASN	6.736465	7.317905	5.564285	6.921165	6.10566	6.908965	6.490095	5.515075	4.964155	5.46915
SER	4.670805	4.62742	4.085725	3.79366	3.08882	3.133785	4.913545	5.05788	5.091165	3.616715
GLN	48.399025	49.278455	36.881985	41.578345	34.95861	37.937505	31.86149	26.317615	28.2185	29.154405
HIS	6.12696	6.16838	4.942305	5.658775	5.196985	4.38679	5.35866	4.856335	5.088135	5.060335
GLY	11.934075	13.149335	12.133345	10.15377	9.90136	7.36513	16.888935	14.56568	13.353675	13.69193
THR	4.471515	4.96759	4.662275	2.96152	4.17063	2.341475	7.17221	6.010165	5.13291	5.85169
ALA	164.919135	167.86845	151.473565	116.42282	116.14967	93.61461	192.977435	182.49292	183.161325	135.12018
ARG	9.072505	8.98586	6.920885	8.528625	8.399585	7.63602	9.555725	9.57302	9.90846	8.094725
TYR	0.51309	0.51873	0.49377	0.46569	0.447675	0.42587	0.932155	0.756705	0.60939	0.7188
VAL	6.109045	5.927485	5.68448	4.548345	5.09655	3.73376	7.94311	7.61688	7.416535	6.80337
MET	1.57884	1.459635	1.235135	1.243625	1.0766	0.824485	1.275955	1.21866	1.28003	1.007
TRP	0.22012	0.20511	0.179455	0.224055	0.19746	0.22151	0.32222	0.243555	0.193975	0.24951
PHE	0.664915	0.660895	0.57002	0.620335	0.54965	0.56923	0.897555	0.75945	0.64576	0.628935
ILE	1.108095	1.161545	1.07319	0.878685	0.95602	0.74965	1.696105	1.43505	1.235455	1.28647
LEU	1.50432	1.55286	1.3659	1.33349	1.358985	1.169385	2.18804	1.828365	1.56928	1.658495
LYS	4.611255	4.67381	3.826085	3.78709	3.611775	3.397845	6.033755	5.54179	5.94659	5.618955
PRO	2.866755	3.118135	2.96033	2.031475	2.167295	2.00279	4.87035	4.373365	4.5172	4.057175

Table C-1: List of translationally clock-controlled genes dependent on CPC-3

Gene	Symbol	Name	
NCU00443	nup-3	ran-specific GTPase-activating protein 1	
NCU00604	0	hypothetical protein	
NCU01435	stk-1	serine/threonine-protein kinase bur-1	
NCU01623	0	hypothetical protein	
NCU01796	0	hypothetical protein	
NCU01851	0	hypothetical protein	
NCU02076	eif4E	eukaryotic translation initiation factor 4E	
NCU02078	pbd-2	hypothetical protein	
NCU02079	div-6	cyclin-dependent kinase regulatory subunit	
NCU02354	pbd-1	RSC complex subunit	
NCU02602	0	hypothetical protein	
NCU02727	0	glycine cleavage system T protein	
NCU03072	0	hypothetical protein	
NCU03275	0	hypothetical protein	
NCU03315	0	hypothetical protein	
NCU03546	0	hypothetical protein	
NCU03824	0	hypothetical protein	
NCU04116	0	DUF618 domain-containing protein	
NCU04149	0	mitochondrial GTPase	
NCU04284	0	hypothetical protein	
NCU04602	0	hypothetical protein	
NCU04609	0	hypothetical protein	
NCU04672	0	MatE family transporter	
NCU04902	trm-5	sodium-hydrogen antiporter	
NCU04949	0	hypothetical protein	
NCU05102	0	hypothetical protein	
NCU05159	ce5-2	acetylxylan esterase	
NCU05251	0	DNA-directed RNA polymerase I polypeptide	
NCU05627	0	high affinity glucose transporter ght1	
NCU05733	acr-2	acriflavine sensitivity control protein acr-2	
NCU06118	0	hypothetical protein	
NCU06206	0	hypothetical protein	
NCU06617	0	myosin regulatory light chain cdc4	
NCU06731	0	hypothetical protein	
NCU07041	0	ribosomal RNA assembly protein mis3	
NCU07266	dph-5	diphthine synthase	

Table C-1 continued

NCU07384	mic-23	mitochondrial thiamine pyrophosphate carrier 1	
NCU07445	0	hypothetical protein	
NCU07934	0	hypothetical protein	
NCU08397	0	hypothetical protein	
NCU08412	0	endo-beta-1,4-mannanase	
NCU08851	0	hypothetical protein	
NCU09208	0	transcription factor SPT8	
NCU09267	0	copper radical oxidase	
NCU09315	nuc-1	nuclease-l	
NCU09523	0	hypothetical protein	
NCU09644	uvs-3	ultraviolet sensitive-3	
NCU09860	0	telomere silencing protein Zds1	
NCU09873	acu-6	phosphoenolpyruvate carboxykinase	
NCU10006	0	hypothetical protein	
NCU11088	dnr-4	MGMT family protein	
NCU16019		group I intron endonuclease	
NCU16323		hypothetical protein	
NCU16402		hypothetical protein	
NCU16634		hypothetical protein	
NCU16651	fol-2	folate-2	
NCU16688		hypothetical protein	
NCU16690		hypothetical protein	
NCU16993		hypothetical protein	
NCU17116		hypothetical protein	
NCU00092	0	rRNA-processing protein efg-1	
NCU00133	ctc-1	FACT complex subunit pob-3	
NCU00310	0	hypothetical protein	
NCU00773	0	hypothetical protein	
NCU01595	0	SOF1	
NCU02796	0	PHD finger domain-containing protein	
NCU03630	0	hypothetical protein	
NCU03991	0	sterol O-acyltransferase 1	
NCU04518	0	hypothetical protein	
NCU04617	0	hypothetical protein	
NCU05137	ncw-1	non-anchored cell wall protein-1	
NCU05543	0	hypothetical protein	
NCU05635	0	hypothetical protein	
NCU06685	0	protein kinase	
NCU07839	drh-1	ATP-dependent RNA helicase dbp-2	
NCU07984	0	chromosome segregation protein	
NCU10927	0	signal recognition particle protein	

Table C-1 continued

NCU11357		0	cell cycle control protein	
NCU01032		0	hypothetical protein	
NCU02243		0	hypothetical protein	
NCU03552		0	hypothetical protein	
NCU06276		0	hypothetical protein	
NCU06664		0	recombination hotspot-binding protein	
NCU07268		0	hypothetical protein	
NCU07314		0	CinY protein	
NCU08055	zip-1		b-ZIP transcription factor IDI4	
NCU16867			hypothetical protein	
NCU17031			hypothetical protein	
NCU01855		0	hypothetical protein	
NCU02804	mrp-31		mitochondrial 60S ribosomal protein L25	
NCU11209		0	vacuolar protein sorting-associated protein Vps28	
NCU01560		0	hypothetical protein	
NCU02404		0	RNP domain-containing protein	
NCU02627		0	hypothetical protein	
NCU04072		0	catechol dioxygenase	
NCU05033		0	hypothetical protein	
NCU06533		0	hypothetical protein	
NCU06987		0	hypothetical protein	
NCU07731		0	hypothetical protein	
NCU07939		0	syntaxin	
NCU00060		0	WW domain-containing protein	
NCU01098		0	hypothetical protein	
NCU02691		0	hypothetical protein	
NCU03928		0	hypothetical protein	
NCU05294		0	C6 finger domain-containing protein	
NCU05559		0	hypothetical protein	
NCU05893		0	AT DNA binding protein	
NCU06316		0	hypothetical protein	
NCU06573	cea-9		chlorogenic acid esterase	
NCU06791		0	hypothetical protein	
NCU06959		0	hypothetical protein	
NCU06975		0	hypothetical protein	
NCU08161	rhc-1		histone chaperone RTT106	
NCU09296		0	hypothetical protein	
NCU09901		0	hypothetical protein	
NCU01570		0	hypothetical protein	
NCU01754	adh-1		alcohol dehydrogenase I	
NCU01945		0	IMP-specific 5'-nucleotidase 1	

Table C-1 continued

NCU02438		0	dihydrolipoamide succinyltransferase	
NCU02942		0	hypothetical protein	
NCU03809		0	hypothetical protein	
NCU04062	pex20		peroxisome biogenesis factor 20	
NCU04644		0	hypothetical protein	
NCU04778		0	carbonic anhydrase	
NCU05454	glp-2		glycerol-3-phosphate dehydrogenase	
NCU05974	gh16-7		cell wall glucanosyltransferase Mwg1	
NCU06586		0	AN1 zinc finger protein	
NCU06614		0	hypothetical protein	
NCU06729	gna-2		guanine nucleotide-binding protein alpha-2	
NCU06863	hH1		histone H1	
NCU07734		0	zinc finger protein gcs1	
NCU10014		0	hypothetical protein	
NCU00398		0	hypothetical protein	
NCU02035		0	helix-hairpin-helix domain-containing protein	
NCU05971		0	xaa-Pro dipeptidase	
NCU06559		0	3-hydroxyisobutyrate dehydrogenase	
NCU07569		0	hypothetical protein	
NCU17319	rRNA		rRNA	
NCU00005		0	hypothetical protein	
NCU02271		0	YagE family protein	
NCU03053		0	hypothetical protein	
NCU05016		0	hypothetical protein	
NCU06680		0	hypothetical protein	
NCU08841		0	hypothetical protein	
NCU09247		0	hypothetical protein	
NCU09366	pcb-6		proteasome component C5	
NCU14163			hypothetical protein	
NCU00023		0	ferric reductase	
NCU00472	cdc37		CDC37	
NCU01061		0	dienelactone hydrolase	
NCU01403		0	GPI anchored protein	
NCU01427	al-3		albino-3	
NCU01433	ppt-1		phosphoprotein phosphatase-1	
NCU01752	ncw-2		non-anchored cell wall protein-2	
NCU02132		0	hypothetical protein	
NCU02164		0	hypothetical protein	
NCU02374	rpn-9		proteasome regulatory particle subunit	
NCU02416		0	Phospholipid:diacylglycerol acyltransferase	
NCU02598		0	hypothetical protein	

Table C-1 continued

NCU03024		0	GARP complex subunit Vps53	
NCU03028		0	deubiquitination-protection protein dph1	
NCU03086		0	HpcH/HpaI aldolase/citrate lyase family protein	
NCU03320	ada-4		all development altered-4	
NCU03495		0	protein phosphatase 2c	
NCU03848		0	hypothetical protein	
NCU04303	asn-1		asparagine synthetase 2	
NCU04909		0	hypothetical protein	
NCU05404		0	endoglucanase	
NCU05410	arg-5		acetylornithine aminotransferase	
NCU05757		0	nitrilase	
NCU05789	gh16-6		secreted glucosidase	
NCU06207	erg-10		C-5 sterol desaturase	
NCU06779	alg-11		alpha-1,2-mannosyltransferase alg11	
NCU06874		0	HMG box-containing protein	
NCU07066	mus-44		mating-type switching protein swi10	
NCU07072	gt35-1		galactose-1-phosphate uridylyltransferase	
NCU07352		0	hypothetical protein	
NCU07414	djc-4		hypothetical protein similar to protein mitochondrial targeting protein Mas5	
NCU07476		0	hypothetical protein	
NCU07497		0	hypothetical protein	
NCU08886		0	amidohydrolase	
NCU09087		0	hypothetical protein	
NCU09133	acw-7		hypothetical protein	
NCU12130		0	hypothetical protein	
NCU14077			hypothetical protein	
NCU16606			hypothetical protein	
NCU01542		0	hypothetical protein	
NCU01615		0	hypothetical protein	
NCU01873		0	hypothetical protein	
NCU05667	acw-3		anchored cell wall protein-3	
NCU00606		0	short-chain alcohol dehydrogenase	
NCU01116	gsl-10		ceramide glucosyltransferase	
NCU04460	gpu-1		galactose-1-phosphate uridylyltransferase	
NCU05391		0	hypothetical protein	
NCU06862		0	hypothetical protein	
NCU07288		0	hypothetical protein	
NCU08072	gh16-10		cell wall glucanase	
NCU08948		0	NIF domain-containing protein	
NCU09659		0	5'-nucleotidase	
NCU00050		0	pyruvate dehydrogenase X component	

Table C-1 continued

NCU00051		0	hypothetical protein
NCU00195		0	MFS transporter
NCU00463	kyn-2		kynureninase
NCU00676		0	F1-ATP synthase assembly protein
NCU01195	am-1		amination-deficient
NCU01610		0	hypothetical protein
NCU01666	ilv-4		acetolactate synthase small subunit
NCU01801		0	hypothetical protein
NCU01938		0	hypothetical protein
NCU02010	leu-4		2-isopropylmalate synthase
NCU02480		0	short-chain dehydrogenase/reductase
NCU02502		0	S-adenosyl-methionine-sterol-C
NCU02799		0	hypothetical protein
NCU03010	lys-3		L-aminoadipate-semialdehyde dehydrogenase large subunit
NCU03297	ccp-1		cytochrome c peroxidase
NCU03347	nic-4		kynurenine-oxoglutarate transaminase 1
NCU03608	ilv-2		ketol-acid reductoisomerase
NCU03883	vtc-1		vacuolar transporter chaperone 1
NCU04074	nuo30.4		NADH:ubiquinone oxidoreductase 30.4
NCU04622		0	hypothetical protein
NCU04771		0	fructosyl-amino acid oxidase
NCU05045		0	MFS monocarboxylate transporter
NCU05095		0	phenylalanyl-tRNA synthetase subunit alpha
NCU05511		0	cytidine/deoxycytidylate deaminase
NCU05550		0	hypothetical protein
NCU05754		0	hypothetical protein
NCU06251		0	KH domain RNA-binding protein
NCU06259	vsp-6		sorting nexin-41
NCU06821		0	CRO1 protein
NCU06914		0	histidyl-tRNA synthetase
NCU07078		0	hypothetical protein
NCU07165		0	mannose-6-phosphate isomerase
NCU07386	mrp-1		Fe superoxide dismutase
NCU07564		0	siderophore iron transporter mirC
NCU07784		0	SAM binding domain-containing protein
NCU07982	als		acetolactate synthase
NCU08185		0	hypothetical protein
NCU08281		0	hypothetical protein
NCU08648		0	nuclease PA3
NCU08763		0	hypothetical protein
NCU08855		0	hypothetical protein

Table C-1 continued

NCU08888		0	phenylalanyl-tRNA synthetase subunit beta
NCU08935		0	peroxisomal-coenzyme A synthetase
NCU09306		0	hypothetical protein
NCU09533		0	NAD binding Rossmann fold oxidoreductase
NCU10029		0	peptide methionine sulfoxide reductase msrA
NCU10101		0	hypothetical protein
NCU10232		0	hypothetical protein
NCU16673			hypothetical protein
NCU17260			hypothetical protein
NCU00121		0	CLC channel protein
NCU00132		0	hypothetical protein
NCU00234		0	hypothetical protein
NCU00260		0	oxidoreductase
NCU00277		0	hypothetical protein
NCU00545		0	hypothetical protein
NCU00714		0	heat shock protein STI1
NCU00768		0	mRNA binding post-transcriptional regulator
NCU00837		0	6-phosphogluconate dehydrogenase
NCU00903		0	hypothetical protein
NCU01412	pro-3		gamma-glutamyl phosphate reductase
NCU01738	preg		phosphatase regulation
NCU01751		0	ATP-binding cassette protein
NCU01841	dash-3		hypothetical protein
NCU01899		0	hypothetical protein
NCU02126		0	isovaleryl-CoA dehydrogenase
NCU02190		0	oxysterol binding protein
NCU02240	gh61-1		endoglucanase II
NCU02399		0	hypothetical protein
NCU02592		0	chitin synthase activator
NCU02623		0	mitochondrial hypoxia responsive domain-containing protein
NCU02730		0	hypothetical protein
NCU02775		0	hypothetical protein
NCU03111		0	hypothetical protein
NCU03362	gsl-16		steroid alpha reductase
NCU03451		0	hypothetical protein
NCU03514		0	hypothetical protein
NCU03624		0	hypothetical protein
NCU03813	fdh		formate dehydrogenase
NCU03815	nap-1		large neutral amino acids transporter small subunit 2
NCU03944		0	WD repeat containing protein 2
NCU03998		0	adaptor protein complex 3 Mu3A

Table C-1 continued

NCU04044	nuo51	NADH2 dehydrogenase flavoprotein 1	
NCU04192	0	vacuolar aspartyl aminopeptidase Lap4	
NCU04579	ilv-1	dihydroxy-acid dehydratase	
NCU04780	0	VEG136 protein	
NCU05198	aap-21	general amino acid permease	
NCU05226	0	ABC transporter	
NCU05558	0	3-ketoacyl-CoA thiolase	
NCU05623	tim17	translocase of mitochondrial inner membrane 17	
NCU05841	0	UMTA	
NCU05958	0	hypothetical protein	
NCU06026	qa-Y	quinate-Y	
NCU06110	0	thiazole biosynthetic enzyme	
NCU06175	pex3	peroxisomal membrane protein	
NCU06187	ad-4	adenylosuccinate lyase	
NCU06380	trm-42	zinc transporter YKE4	
NCU06395	0	hypothetical protein	
NCU06406	0	hypothetical protein	
NCU06424	0	aminomethyl transferase	
NCU06440	pca-4	proteasome component PRE6	
NCU06856	0	ubiquitin fusion degradation protein	
NCU06930	0	hypothetical protein	
NCU07241	0	hypothetical protein	
NCU07242	0	short-chain dehydrogenase/oxidoreductase	
NCU07405	0	hypothetical protein	
NCU07572	0	hypothetical protein	
NCU07823	scy	scytalone dehydratase	
NCU08137	0	hypothetical protein	
NCU08319	0	developmental regulator flbA	
NCU08330	0	hypothetical protein	
NCU09000	0	fyv-10	
NCU09155	39913	hypothetical protein	
NCU09388	0	hypothetical protein	
NCU09532	0	L-threo-3-deoxy-hexulosonate aldolase	
NCU09676	0	hypothetical protein	
NCU09729	0	hypothetical protein	
NCU09746	nit-9	gephyrin	
NCU09773	0	oligopeptide transporter	
NCU09795	0	hypothetical protein	
NCU09885	0	acyl-CoA dehydrogenase	
NCU09910	0	hypothetical protein	
NCU09912	0	MFS transporter	

Table C-1 continued

NCU14019			Hypothetical protein	
NCU14110			Hypothetical protein	
NCU14119			Hypothetical protein	
NCU15834			Hypothetical protein	
NCU16009			Hypothetical protein	
NCU16222			Hypothetical protein	
NCU16682			PXA domain-containing protein	
NCU16972			Hypothetical protein	
NCU00244	gt8-1		glycosyl transferase	
NCU00552	al-1		albino-1	
NCU01227	tca-8		succinyl-CoA ligase alpha-chain	
NCU01559		0	hypothetical protein	
NCU02682		0	hypothetical protein	
NCU02932		0	hypothetical protein	
NCU03497	trm-51		plasma membrane iron permease	
NCU04336	mrp-28		60S ribosomal protein L19	
NCU04913		0	hypothetical protein	
NCU05308		0	Zn(II)2Cys6 transcription factor	
NCU05345		0	zearalenone lactonase	
NCU05564	pex31		peroxisomal membrane protein PEX31	
NCU05960	gt76-1		GPI mannosyltransferase 2	
NCU06211	tca-16		malate dehydrogenase	
NCU06443		0	hypothetical protein	
NCU08166		0	hypothetical protein	
NCU08701		0	hypothetical protein	
NCU08857		0	hypothetical protein	
NCU09376		0	hypothetical protein	
NCU09739	fld		hypothetical protein	
NCU09974		0	fungal specific transcription factor domain-containing protein	
NCU11240		0	hypothetical protein	
NCU16549			Thermotolerance protein Dti	
NCU00187		0	carboxyvinyl-carboxyphosphonate phosphorylmutase	
NCU00536		0	homoserine O-acetyltransferase	
NCU00792		0	branched-chain-amino-acid aminotransferase	
NCU01374		0	CutC family protein	
NCU01652		0	O-acetylhomoserine	
NCU01843	cpn-3		T-complex protein 1 subunit gamma	
NCU03425	thr-2		threonine synthase	
NCU04013	ylo-1		yellow-1	
NCU04768		0	electron transfer flavoprotein-ubiquinone oxidoreductase	
NCU05050		0	2-hydroxyacid dehydrogenase	

Table C-1 continued

NCU06576		0	hypothetical protein
NCU06971		0	transcriptional activator xlnR
NCU07153		0	glutamate carboxypeptidase
NCU08512	hsf-1		hypothetical protein
NCU08652		0	hypothetical protein
NCU08868	tgl-3		hypothetical protein
NCU09656		0	carboxymethylenebutenolidase
NCU09727		0	NADPH-dependent FMN/FAD containing oxidoreductase
NCU00257		0	dynactin Arp1 p62 subunit RO2
NCU01162	gh72-1		glycolipid-anchored surface protein 5
NCU01563		0	RNA polymerase II holoenzyme cyclin-like subunit
NCU05422		0	vacuolar protein sorting protein
NCU06349		0	hypothetical protein
NCU09689		0	hypothetical protein
NCU09888		0	hypothetical protein
NCU16725			Potassium Ion channel Yvc1
NCU00129		0	AMP-binding domain-containing protein
NCU00267		0	hypothetical protein
NCU00438		0	adenosine deaminase
NCU00774		0	hypothetical protein
NCU00877		0	hypothetical protein
NCU00936		0	succinate semialdehyde dehydrogenase
NCU01291		0	hypothetical protein
NCU01305		0	rhomboid family membrane protein
NCU01349		0	hypothetical protein
NCU01704		0	NADP:D-xylose dehydrogenase
NCU02594		0	hypothetical protein
NCU02712		0	acetate kinase
NCU02887		0	voltage-gated potassium channel beta-2 subunit
NCU03489	col-21		hypothetical protein
NCU04143		0	protein kinase
NCU04207		0	mechanosensitive ion channel family protein
NCU04578	spr-2		ATP-dependent Clp protease proteolytic subunit 1
NCU04692		0	hypothetical protein
NCU04748		0	hypothetical protein
NCU05069		0	FAD dependent oxidoreductase
NCU05094		0	short chain dehydrogenase/reductase
NCU06173		0	hypothetical protein
NCU06264	mus-53		mutagen sensitive-53
NCU06407	vad-3		zinc finger transcription factor 1
NCU06518		0	NADH-cytochrome b5 reductase 2

Table C-1 continued

NCU06530		0	palmitoyl-protein thioesterase
NCU06656	acu-15		transcriptional activator protein acu-15
NCU06967		0	hypothetical protein
NCU07008	cao-1		carotenoid oxygenase-1
NCU07032		0	hypothetical protein
NCU07073		0	hypothetical protein
NCU07474		0	ergot alkaloid biosynthetic protein A
NCU07723		0	norsolorinic acid reductase
NCU07967		0	hypothetical protein
NCU07977		0	hypothetical protein
NCU08194		0	hypothetical protein
NCU08803		0	general amidase GmdA
NCU09049		0	hypothetical protein
NCU09775	gh54-1		alpha-N-arabinofuranosidase
NCU09821		0	oxidoreductase
NCU11128		0	hypothetical protein
NCU16011			hypothetical protein
NCU16023			hypothetical protein
NCU16026			hypothetical protein
NCU16223			hypothetical protein
NCU17069			hypothetical protein
NCU01565		0	hypothetical protein
NCU02378		0	integral membrane protein
NCU02590		0	hypothetical protein
NCU02806	dnr-1		14-3-3 family protein 7
NCU03910		0	microsomal cytochrome b5
NCU04142	hsp80		heat shock protein 80
NCU05609		0	hypothetical protein
NCU05850		0	rubredoxin-NAD(+) reductase
NCU05919		0	hypothetical protein
NCU06129		0	hypothetical protein
NCU06436		0	hypothetical protein
NCU06460		0	acid phosphatase
NCU07959		0	hypothetical protein
NCU08155		0	hypothetical protein
NCU08998		0	4-aminobutyrate aminotransferase
NCU09719		0	hypothetical protein
NCU09800		0	taurine dioxygenase
NCU11288		0	xaa-Pro dipeptidase
NCU17275			hypothetical protein
NCU01840		0	hypothetical protein

Table C-1 continued

NCU02017	ada-2	CBF/NF-Y family transcription factor	
NCU02297	0	hypothetical protein	
NCU02314	0	hypothetical protein	
NCU02398	0	hypothetical protein	
NCU02849	0	hypothetical protein	
NCU03323	0	hypothetical protein	
NCU03903	0	lipase/esterase	
NCU04306	0	methionine aminopeptidase 2B	
NCU04601	0	hypothetical protein	
NCU04741	dash-7	hypothetical protein	
NCU06414	0	hypothetical protein	
NCU08726	fl	fluffy	
NCU10430	0	SNF7 family protein	
NCU14023		hypothetical protein	
NCU00801	0	MFS lactose permease	
NCU01069	amph-1	amphiphysin-like lipid raft protein	
NCU16311		hypothetical protein	
NCU01807	0	hypothetical protein	
NCU04623	gh35-2	beta-galactosidase	
NCU06066	0	hypothetical protein	
NCU07167	0	isoflavone reductase	
NCU07834	0	MYB DNA-binding domain-containing protein	
NCU08282	0	hypothetical protein	
NCU09307	0	hypothetical protein	
NCU15294	tRNA(his-8)	tRNA-his	
NCU16460		hypothetical protein	
NCU00100	0	hypothetical protein	
NCU00223	0	bZIP transcription factor	
NCU00834	0	hypothetical protein	
NCU01073	0	hypothetical protein	
NCU01218	0	hypothetical protein	
NCU01472	0	hypothetical protein	
NCU02618	pex13	peroxisomal membrane protein	
NCU02784	0	hypothetical protein	
NCU03007	msp-21	pre-mRNA-splicing factor slt-11	
NCU03342	0	hypothetical protein	
NCU03462	0	leucine Rich Repeat domain-containing protein	
NCU03649	0	hypothetical protein	
NCU03652	0	SNF2 family helicase/ATPase	
NCU03915	0	hypothetical protein	
NCU04015	0	vacuolar protein sorting-associated protein 27	

Table C-1 continued

NCU04690		0	hypothetical protein
NCU04755		0	protein kinase domain-containing protein ppk32
NCU05394		0	MFS transporter
NCU05427		0	ATP-dependent Clp protease
NCU05862		0	hypothetical protein
NCU05903		0	hypothetical protein
NCU06890		0	hypothetical protein
NCU07684		0	hypothetical protein
NCU08413		0	hypothetical protein
NCU08601		0	hypothetical protein
NCU08697		0	hypothetical protein
NCU09188		0	hypothetical protein
NCU09653		0	YhhN family protein
NCU09707	cpn-8		hypothetical protein
NCU10015		0	methanesulfonate monooxygenase
NCU10091		0	hypothetical protein
NCU15832			hypothetical protein
NCU16025			ATPase subunit 6
NCU16659			hypothetical protein
NCU16819			hypothetical protein
NCU17048			hypothetical protein
NCU17284			hypothetical protein
NCU00405		0	glycyl-tRNA synthetase 1
NCU00732	cyp450-1		trichothecene C-15 hydroxylase
NCU01954	msp-14		pre-mRNA-splicing factor cwc-24
NCU05049		0	hypothetical protein
NCU07210		0	hypothetical protein
NCU09381		0	RWD domain-containing protein
NCU17277			hypothetical protein
NCU00520		0	oxidoreductase
NCU03397		0	hypothetical protein
NCU04640	eif2-beta		eukaryotic translation initiation factor 2 beta subunit
NCU04670		0	hypothetical protein
NCU07695		0	hypothetical protein
NCU07844		0	hypothetical protein
NCU07928		0	hypothetical protein
NCU16001			NADH dehydrogenase subunit 2
NCU00055		0	catechol 1,2-dioxygenase 1
NCU01202		0	hypothetical protein
NCU01361		0	hypothetical protein
NCU01786		0	ribose-phosphate pyrophosphokinase II

Table C-1 continued

NCU02249	hat-5	histone acetyltransferase	
NCU02706	sna-2	protein transporter GOS1	
NCU02983	0	hypothetical protein	
NCU03799	msp-24	pre-mRNA splicing factor prp45	
NCU04278	0	hypothetical protein	
NCU04557	0	hypothetical protein	
NCU04887	gt71-1	hypothetical protein	
NCU05966	0	DNA repair protein	
NCU05999	0	CaaX farnesyltransferase beta subunit Ram1	
NCU06780	0	tRNA (uracil-5-)-methyltransferase	
NCU07335	0	hypothetical protein	
NCU07379	0	bZIP-type transcription factor	
NCU07389	ham-9	SAM and PH domain-containing protein	
NCU07496	set-7	hypothetical protein	
NCU08332	hex-1	hexagonal-1	
NCU08595	0	ribosome biogenesis protein	
NCU09092	0	hypothetical protein	
NCU09547	0	U4/U6.U5 tri-snRNP-associated protein 2	
NCU09867	0	hypothetical protein	
NCU10142	0	hypothetical protein	
NCU10352	snr-6	U6 snRNA-associated Sm-like protein LSm6	
NCU10788	0	hypothetical protein	
NCU11248	0	oligosaccharyltransferase subunit ribophorin II	
NCU14092		hypothetical protein	
NCU16347		hypothetical protein	
NCU17135		hypothetical protein	

Table C-2: Clock-controlled CPC-3 dependent genes with predicted Iron Responsive Element

Known IRE	Gene	p-value	Matched Sequence
YRCACCCR	NCU16460	8.13E-06	CGCACCCG
YRCACCCR	NCU04913	3.78E-05	CACACCCG
YRCACCCR	NCU02271	3.78E-05	TGCACCCG
YRCACCCR	NCU07967	3.78E-05	CGCACCCA
YRCACCCR	NCU07572	7.40E-05	CACACCCA
YRCACCCR	NCU11209	7.40E-05	CACACCCA
YRCACCCR	NCU02784	7.40E-05	TGCACCCA
YRCACCCR	NCU09873	7.40E-05	TACACCCG

Table C-2 continued

YRCACCCR	NCU08155	7.40E-05	TGCACCCA
YRCACCCR	NCU01412	7.40E-05	TGCACCCA
YRCACCCR	NCU00936	7.40E-05	CACACCCA
YRCACCCR	NCU07414	7.40E-05	CACACCCA
YRCACCCR	NCU08137	7.40E-05	CACACCCA

**Table C-3: Clock-controlled CPC-3 dependent genes
with predicted uORFs**

Locus	Symbol	Name	
NCU00277	0	hypothetical protein	
NCU00774	0	hypothetical protein	
NCU00801	0	MFS lactose permease	
NCU01162	gh72-1	glycolipid-anchored surface protein 5	
NCU01291	0	hypothetical protein	
NCU01305	0	rhomboid family membrane protein	
NCU01349	0	hypothetical protein	
NCU01361	0	hypothetical protein	
NCU01435	stk-1	serine/threonine-protein kinase bur-1	
NCU01542	0	hypothetical protein	
NCU01565	0	hypothetical protein	
NCU01652	0	O-acetylhomoserine	
NCU01754	adh-1	alcohol dehydrogenase I	
NCU01786	0	ribose-phosphate pyrophosphokinase II	
NCU01796	0	hypothetical protein	
NCU01807	0	hypothetical protein	
NCU02010	leu-4	2-isopropylmalate synthase	
NCU02240	gh61-1	endoglucanase II	
NCU02243	0	hypothetical protein	
NCU02378	0	integral membrane protein	
NCU02398	0	hypothetical protein	
NCU02502	0	S-adenosyl-methionine-sterol-C	
NCU02590	0	hypothetical protein	
NCU02627	0	hypothetical protein	
NCU02730	0	hypothetical protein	
NCU02887	0	voltage-gated potassium channel beta-2 subunit	
NCU03297	ccp-1	cytochrome c peroxidase	

Table C-3 continued

NCU03495		0	protein phosphatase 2c
NCU03514		0	hypothetical protein
NCU03813	fdh		formate dehydrogenase
NCU03915		0	hypothetical protein
NCU03928		0	hypothetical protein
NCU04013	ylo-1		yellow-1
NCU04062	pex20		peroxisome biogenesis factor 20
NCU04072		0	catechol dioxygenase
NCU04116		0	DUF618 domain-containing protein
NCU04207		0	mechanosensitive ion channel family protein
NCU04518		0	hypothetical protein
NCU04601		0	hypothetical protein
NCU04672		0	MatE family transporter
NCU05045		0	MFS monocarboxylate transporter
NCU05159	ce5-2		acetylxylan esterase
NCU05511		0	cytidine/deoxycytidylate deaminase
NCU05559		0	hypothetical protein
NCU05564	pex31		peroxisomal membrane protein PEX31
NCU05627		0	high affinity glucose transporter ght1
NCU06207	erg-10		C-5 sterol desaturase
NCU06251		0	KH domain RNA-binding protein
NCU06407	vad-3		zinc finger transcription factor 1
NCU06460		0	acid phosphatase
NCU06518		0	NADH-cytochrome b5 reductase 2
NCU06664		0	recombination hotspot-binding protein
NCU06779	alg-11		alpha-1,2-mannosyltransferase alg11
NCU06874		0	HMG box-containing protein
NCU06930		0	hypothetical protein
NCU06987		0	hypothetical protein
NCU07241		0	hypothetical protein
NCU07268		0	hypothetical protein
NCU07288		0	hypothetical protein
NCU07572		0	hypothetical protein
NCU07695		0	hypothetical protein
NCU07784		0	SAM binding domain-containing protein
NCU07823	scy		scytalone dehydratase
NCU07959		0	hypothetical protein
NCU08055	zip-1		b-ZIP transcription factor IDI4
NCU08319		0	developmental regulator flbA

Table C-3 continued

NCU08701	0	hypothetical protein
NCU08855	0	hypothetical protein
NCU08868	tgl-3	hypothetical protein
NCU09087	0	hypothetical protein
NCU09155	0	hypothetical protein
NCU09296	0	hypothetical protein
NCU09307	0	hypothetical protein
NCU09676	0	hypothetical protein
NCU09860	0	telomere silencing protein Zds1
NCU09910	0	hypothetical protein
NCU10014	0	hypothetical protein
NCU12130	0	hypothetical protein
NCU16460	0	hypothetical protein
NCU16549	0	hypothetical protein
NCU17275	0	hypothetical protein